

1-1-2016

Unraveling The Molecular Mechanisms Of Aposematic Pigmentation In *Oncopeltus Fasciatus*

Jin Liu

Wayne State University,

Follow this and additional works at: https://digitalcommons.wayne.edu/oa_dissertations

 Part of the [Biology Commons](#)

Recommended Citation

Liu, Jin, "Unraveling The Molecular Mechanisms Of Aposematic Pigmentation In *Oncopeltus Fasciatus*" (2016). *Wayne State University Dissertations*. 1554.

https://digitalcommons.wayne.edu/oa_dissertations/1554

This Open Access Dissertation is brought to you for free and open access by DigitalCommons@WayneState. It has been accepted for inclusion in Wayne State University Dissertations by an authorized administrator of DigitalCommons@WayneState.

**UNRAVELING THE MOLECULAR MECHANISMS OF APOSEMATIC
PIGMENTATION IN ONCOPELTUS FASCIATUS**

by

JIN LIU

DISSERTATION

Submitted to the Graduate School

of Wayne State University

Detroit, Michigan

in partial fulfillment of the requirements

for the degree of

DOCTOR OF PHILOSOPHY

2016

MAJOR: BIOLOGICAL SCIENCES

Approved By:

Advisor

Date

© COPYRIGHTED BY

JIN LIU

2016

All Rights Reserved

DEDICATION

This work is dedicated to my parents Longjiang Liu and Fuchun Che for their support throughout my graduate training.

ACKNOWLEDGEMENTS

First I would like to thank my advisor Dr. Aleksandar Popadić for his mentoring and support throughout my graduate training. I would also like to thank my doctoral committee members Dr. Mark VanBerkum, Dr. William Branford and Dr. Patricia Wittkopp for their valuable advice and assistance throughout the progress of this work.

I would like to thank my former lab colleague Thomas Lemonds for his support and contribution to my work. I also thank former lab members Dr. Steve Hrycaj, Dr. Nataliya Turchyn, and Dr. Victor Medved for their help of my work in the lab.

I would like to express my gratitude to the staff members of the Biological Sciences department for all of their assistance with the administrative requirements for my doctoral degree.

TABLE OF CONTENTS

Dedication	ii
Acknowledgements	iii
List of Tables.....	vii
List of Figures.....	viii
Chapter 1 INTRODUCTION	1
Chapter 2 THE GENETIC CONTROL OF APOSEMATIC BLACK PIGMENTATION IN HEMIMETABOLOUS INSECTS: INSIGHTS FROM ONCOPELTUS FASCIATUS	11
Abstract	11
Introduction.....	12
Materials and Methods	15
Results	18
Discussion	26
Chapter 3 A PATHWAY ANALYSIS OF MELANIN PATTERNING IN A HEMIMETABOLOUS INSECT.....	30
Abstract	30
Introduction.....	31
Materials and Methods	34
Results	39
Discussion	53
Chapter 4 PIGMENTATION PATHWAYS UNDERLYING ORANGE COLORATION IN INSECTS.....	61
Introduction.....	61
Materials and Methods	63
Results	67

Discussion	81
Appendix A <i>TH</i> , <i>DDC</i> , <i>ebony</i> and <i>yellow</i> contribute to the black color patterns in 5th nymphs of <i>Oncopeltus</i>	89
Appendix B <i>ebony</i> RNAi altered the color patterns of the lateral bristles the abdominal segments of <i>Oncopeltus</i> adults.....	91
Appendix C Among the ommochrome and pteridine genes, only <i>Punch</i> affects the color patterns of the hindwings	92
Appendix D <i>apterous-a</i> (<i>ap-a</i>) RNAi caused defects in the forewings of <i>Oncopeltus</i> adults.....	93
Appendix E <i>silver</i> (<i>svr</i>) RNAi resulted inflated wings in <i>Oncopeltus</i> adults	94
Appendix F <i>achaete-scute homolog</i> (<i>ASH</i>) is responsible for bristle development of <i>Oncopeltus</i> adults	95
Appendix G <i>homothorax</i> (<i>hth</i>) is expressed in the body and proximal regions of the appendages in <i>Gryllus bimaculatus</i> embryos	96
Appendix H <i>dachshund</i> (<i>dac</i>) is primarily expressed in the middle regions of the developing legs in <i>Gryllus bimaculatus</i> embryos	97
Appendix I <i>Delta</i> (<i>DI</i>) is expressed at boundaries between segments of appendages in <i>Gryllus bimaculatus</i> embryos	98
Appendix J <i>Sex comb reduced</i> (<i>Scr</i>) is expressed in the labial and T1 segments of <i>Tenodera sinensis</i> embryos	99
Appendix K Depletion of <i>Scr</i> did not alter the expression pattern of Antennapedia (<i>Antp</i>) in <i>Periplaneta americana</i> embryos	100
References.....	101
Abstract.....	115
Autobiographical Statement	118

LIST OF TABLES

Table 3.1 Primers for RT-PCR and the lengths of the obtained cDNA fragments of relevant genes	35
Table 4.1 Primers for RT-PCR and the lengths of the obtained cDNA fragments of <i>Oncopeltus</i> genes.....	64

LIST OF FIGURES

Figure 1.1 A summary of the melanin pathway in insects	3
Figure 1.2 The hypothetical ommochrome pathway and pteridine pathway in <i>Drosophila</i>	5
Figure 2.1 The summary consensus view of melanin biosynthesis pathway in <i>Drosophila</i>	15
Figure 2.2 Phylogenetic relationships between <i>Tribolium</i> and <i>Oncopeltus</i> melanin pathway genes.....	16
Figure 2.3 RT-PCR analysis of <i>TH</i> , <i>DDC</i> , <i>laccase 2 (lac2)</i> , and <i>tyrosinase (Tyr)</i> mRNA in 5 th nymphs of <i>Oncopeltus</i>	17
Figure 2.4 Functions of <i>TH</i> , <i>DDC</i> , and <i>lac2</i> in <i>Oncopeltus</i> adults	19
Figure 2.5 The <i>Oncopeltus tyrosinase (tyr)</i> RNAi phenotype	21
Figure 2.6 Black patterning of <i>Oncopeltus</i> wings is vein dependent	23
Figure 2.7 Pre-mature <i>Oncopeltus</i> wings can develop black pigmentation with exogenously supplied melanin precursors	25
Figure 2.8 In wild type, bristles on the <i>Oncopeltus</i> forewing attain black pigmentation well before the melanization of a wing tissue	29
Figure 3.1 Phylogenetic analysis of <i>Drosophila melanogaster</i> and <i>Oncopeltus fasciatus</i> melanin pathway genes.....	36
Figure 3.2 Phylogenetic analysis of <i>yellow</i> gene family.....	36
Figure 3.3 RT-PCR analysis of <i>ebony</i> , <i>black</i> , <i>aaNAT</i> , <i>tan</i> , <i>yellow</i> , and <i>Ubx</i> mRNA in <i>Oncopeltus</i> 5 th nymphs	37
Figure 3.4 RT-PCR analysis of <i>black</i> mRNA in isolated body regions of <i>Oncopeltus</i> 5 th nymphs at Day8 of development	39
Figure 3.5 Functions of <i>ebony</i> , <i>black</i> , <i>tan</i> , and <i>yellow</i> in different body regions of <i>Oncopeltus</i> adults	41
Figure 3.6 The comparison of black intensity in isolated body regions of wild type, <i>tan</i> RNAi and <i>yellow</i> RNAi adults.....	45
Figure 3.7 Phenotype of <i>aaNAT</i> RNAi in black coloration of <i>Oncopeltus</i> body	46

Figure 3.8 Functions of <i>ebony</i> , <i>black</i> , <i>aaNAT</i> , <i>yellow</i> , and <i>tan</i> in the FW and HW of <i>Oncopeltus</i> adults	49
Figure 3.9 <i>in situ</i> hybridization of <i>ebony</i> and <i>aaNAT</i> in developing wild-type and <i>Ubx</i> RNAi <i>Oncopeltus</i> wings.....	51
Figure 3.10 RT-PCR analyses of <i>black</i> , <i>yellow</i> , and <i>tan</i> mRNA in the developing wings of <i>Oncopeltus</i> throughout the entire 5 th nymphal stage	53
Figure 3.11 Three proposed modes of insect melanin patterning, as illustrated by pigmentation in <i>Oncopeltus</i>	60
Figure 4.1 Phylogenetic analysis of ommochrome and pteridine pathway genes in <i>Drosophila melanogaster</i> and <i>Oncopeltus fasciatus</i>	65
Figure 4.2 RT-PCR analysis of RNAi depletion of targeted genes in 5th nymphs of <i>Oncopeltus</i>	66
Figure 4.3 RT-PCR analysis of embryonic RNAi against <i>vermilion</i> (<i>v</i>) and <i>Punch</i> (<i>Pu</i>) in <i>Oncopeltus</i>	67
Figure 4.4 Functions of ommochrome and pteridine genes in the coloration of adult eyes in <i>Oncopeltus</i>	70
Figure 4.5 <i>brown</i> RNAi does not reduce the eye coloration or the orange coloration in the body and forewing	71
Figure 4.6 Functions of ommochrome and pteridine genes in the orange coloration of adult forewings	73
Figure 4.7 The magnified views of the orange subregions surrounding the medial veins of the forewing	74
Figure 4.8 Effects of RNAi against <i>eya</i> in the eyes and forewings of <i>Oncopeltus</i> adults	75
Figure 4.9 Functions of ommochrome and pteridine genes in the orange body coloration of <i>Oncopeltus</i> adults	78
Figure 4.10 The remaining exoskeleton of the 5th nymphs after molting into Adults	79
Figure 4.11 Functions of <i>vermilion</i> and <i>Punch</i> in the eye and body coloration during early developmental stages	80
Figure 4.12 Summary of the contributions by the pteridine, melanin, and ommochrome pathways to the adult color patterns of <i>Oncopeltus</i>	86

Figure 4.13 The three proposed types of insect coloration..... 88

CHAPTER 1 INTRODUCTION

The central focus of evolutionary developmental studies is the effects of changes in genes and gene regulation on developmental pathways underlying differences of morphological traits (Massey and Wittkopp, 2016). By using a synergistic strategy that combines molecular, evolutionary and developmental experimental approaches, it is now possible to study in detail the molecular mechanisms regulating the evolution of specific morphological trait(s). In this regard, insect coloration represents a premier model, featuring both the nearly unlimited diversity among species and relatively simple modes of regulation (Wittkopp et al., 2003). As insect pigmentation plays critical roles in visual communication, it also affects individual's survival and reproduction (Kronforst et al., 2012; Wittkopp and Beldade, 2009). It is also essential for a wide range of physiological processes such as thermotolerance, photoprotection, and desiccation resistance (Wittkopp and Beldade, 2009). Variation in coloration encompasses the extraordinary differences in the usage of colors, ranging from brown (in flour beetle, *Tribolium castaneum*) to green (in pea aphid, *Acyrtosiphon pisum*) to red (in red dragonfly, *Sympetrum fonscolombii*). In addition, other than these inter-specific variations, coloration can also vary between populations, between species, between individuals within the same population, as well as within the same individual (Wittkopp and Beldade, 2009). Such diversity in pigmentation has enabled insects to successfully adapt to a wide variety of environments. Analyzing the molecular mechanisms underlying insect pigmentation has provided emerging insights into diverse branches of biology, including ecology, development, evolution, genetics, and physiology (Nijhout, 1991; Wittkopp and Beldade, 2009).

Current understanding of insect pigmentation is to a large degree built upon studies on *Drosophila melanogaster* (Wittkopp and Beldade, 2009; Wittkopp et al., 2003). The body pigments in this species, including black, brown and yellow, are all produced by the melanin pathway (Wittkopp et al., 2003; Wright, 1987). The characterization of genes within the pathway can be traced to now classical genetic experiments, such as observations of color defective phenotypes in the *ebony* locus (Bridges and Morgan, 1923). Over the course of the next 50 years, these observations were followed by analysis and interpretation of the enzymatic function of the *ebony* gene (Hodgetts and Konopka, 1973; Jacobs and Brubaker, 1963; Walter et al., 1996; Wright, 1987). As a matter of fact, *ebony* was only fully characterized by the beginning of the 21st century (True et al., 1999; Wittkopp et al., 2002). Other melanin genes were characterized in a similar way, as documented in several reviews (Kronforst et al., 2012; Massey and Wittkopp, 2016; Wittkopp and Beldade, 2009; Wittkopp et al., 2003; Wright, 1987), and these can be credited with providing the means for complete characterization of the melanin pathway in *Drosophila*. As illustrated in Fig. 1.1, the melanin pathway starts with the conversion of tyrosine to DOPA (dihydroxyphenylalanine), which is catalyzed by tyrosine hydroxylase (TH). DOPA can either be directly utilized to synthesize the black DOPA melanin, or transformed to dopamine by DOPA decarboxylase (DDC). Dopamine serves as the direct precursor of the black/brown dopamine melanin. The conversions from DOPA and dopamine to the dark melanin require the promoting role of the *yellow* gene. Alternatively, dopamine can also be converted to two other major catecholamine metabolites, NBAD (N- β -alanyldopamine) or NADA (N-acetyldopamine). The conversion of NBAD is processed

via binding β -alanine to dopamine. This process requires the functions of Ebony (catalyzes the binding reaction) and Black (synthesizes β -alanine). This binding reaction can be reversed by Tan, which in turn promotes the synthesis of dark dopamine melanin. In addition to NBAD, dopamine can also be converted to NADA, catalyzed by arylalkylamine-N-acetyltransferase (AANAT), which can be further utilized to synthesize colorless sclerotin. All of these catecholamine metabolites, including DOPA, dopamine, NBAD and NADA, must be converted to their relevant quinones, which are then used to synthesize the pigments and incorporate into the cuticle. This process requires the functions of Phenol Oxidases (PO) (Arakane et al., 2005). These genes described above compose the core part of the melanin pathway, which is essential for the generation of the diversity in coloration between and within *Drosophila* species (Wittkopp et al., 2003; Wright, 1987).

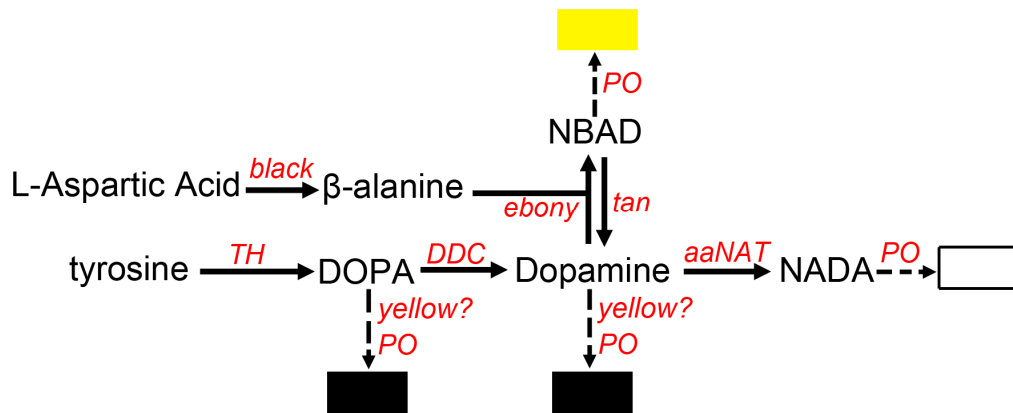


Fig. 1.1. A summary of the melanin pathway in insects, redrawn from Wright (1987). Dashed lines represent the multi-step biochemical reactions within the conversions from precursors (DOPA, dopamine, NBAD, and NADA) to the final pigments (Liu et al., 2016).

Functional studies in *Tribolium*, *Bombyx*, *Monochamus* and *Apis*, as well as expressional studies in lepidopterans have also found the presence of melanin pathway genes in the dark coloration of these species (Arakane et al., 2010; Arakane et al.,

2009; Arakane et al., 2005; Barbera et al., 2013; Elias-Neto et al., 2010; Ferguson et al., 2011a; Ferguson and Jiggins, 2009; Ferguson et al., 2011b; Futahashi et al., 2010; Futahashi and Fujiwara, 2005; Gorman and Arakane, 2010; Hines et al., 2012; Niu et al., 2008; Zhan et al., 2010). These findings suggest that the pigmentation role of the melanin pathway is conserved among holometabolous insects. In contrast, few studies have analyzed the pigmentation roles of melanin pathway in hemimetabolous insects (Futahashi et al., 2011). Due to such lack of knowledge, how the melanin pathway originated and how it evolved from basal insects are still currently unclear.

In addition to the melanin pathway, previous studies have found two other essential pigmentation mechanisms in *Drosophila melanogaster*: ommochrome and pteridine (Linzen, 1974; Summers et al., 1982; Ziegler, 1961). These two pathways are utilized exclusively for eye coloration in this species: the ommochrome pathway provides brown coloration, whereas the pteridine pathway contributes to red coloration (Fig. 1.2). Mutations in essential ommochrome genes result in red eye color, whereas mutations of pteridine genes cause brown eye phenotype (Summers et al., 1982).

The ommochrome pathway starts with the conversion from tryptophan to formyl kynurenine, catalyzed by tryptophan oxidase (encoded by gene *vermillion*) (Fig. 1.2). Then formyl kynurenine is processed by several enzymes, including kynurenine formamidase and kynurenine 3-hydroxylase (encoded by gene *cinnabar*), into 3-hydroxy kynurenine (3-OHK). 3-OHK is a precursor of ommochrome pigments: xanthommatin and dihydroxanthommatin. The conversions from 3-OHK to final pigments are still yet to be determined. Unlike the melanin pathway, which incorporates pigments directly into the non-cellular cuticle, the ommochrome coloration is established in granules

contained inside the tissue cells. The assembly of granules requires the functions of a heterodimer formed by two ATP-binding-cassette transporters (ABC transporters), encoded by genes *scarlet* and *white*, respectively (Ewart and Howells, 1998). Mutation in these two transporter genes result in the loss of ommochrome coloration, which is thought to be caused by the failure in assembling granules (Ewart et al., 1994; Ewart and Howells, 1998). However, the underlying mechanisms, especially the biochemical reactions of taking place inside the granules, remain largely unknown so far.

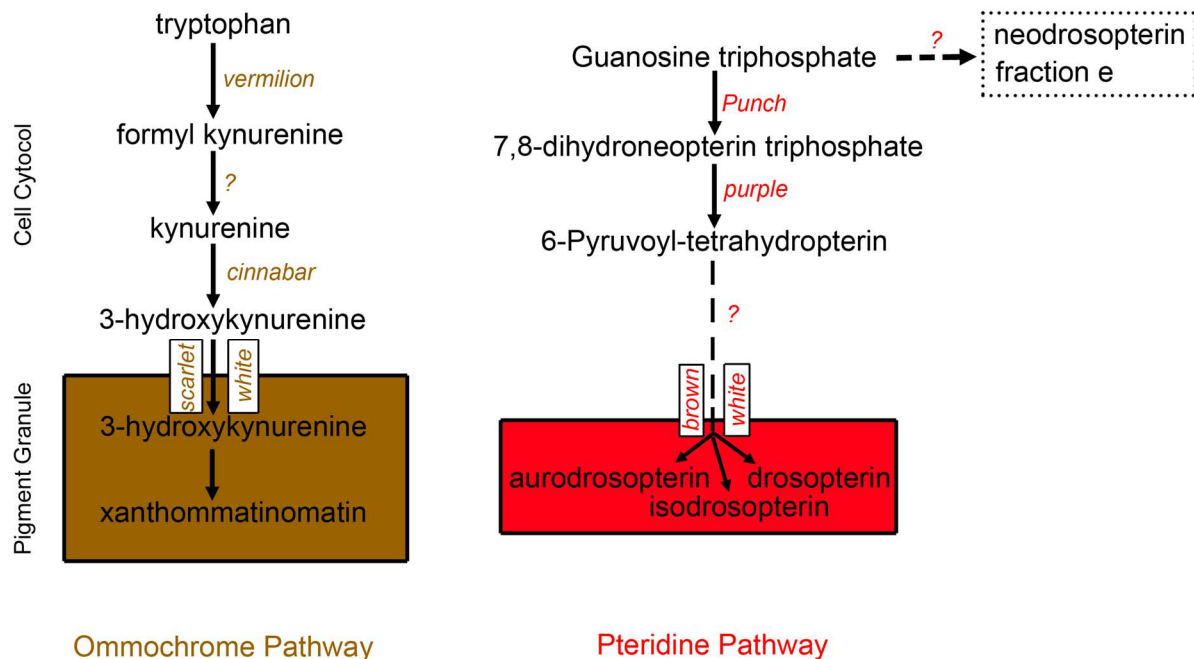


Fig. 1.2. The hypothetical ommochrome pathway and pteridine pathway in *Drosophila* (Ewart and Howells, 1998; Kim et al., 2013; Reed and Nagy, 2005) (Left) The ommochrome pigment is originated from tryptophan. This precursor is converted to 3-hydroxykynurenine (3-OHK) by a series of enzymes, including the ones encoded by genes *vermilion* and *cinnabar*. 3-OHK is then transported into granules by *Scarlet* and *White* to produce final establishment of ommochrome coloration in the granules. (Right) The pteridine pathway is initialized from the conversion of GTP to 7,8-dihydroneopterin triphosphate (H₂-NTP), by GTP cyclohydrolase I (encoded by gene *Punch*). This substrate might serve as the precursor for multiple pteridine pigments. Final establishment of pteridine coloration also requires the assembly of granules, where *White* and *Brown* serve as the transporters.

In non-*Drosophila* species, biochemical and expression studies have detected the presence of ommochrome pathway in other body regions. Its pigmentation role has been found associated with the orange patterns in the wings of butterflies *Papilio* and *Heliconius*, as well as the red/orange coloration in the abdomen of red dragonflies (Futahashi et al., 2012; Nijhout, 1997; Reed and Nagy, 2005). In contrast, functional analyses have only been performed in grasshoppers and beetles (*Tribolium*), where ommochrome pathway has been shown to contribute to the eye coloration exclusively (Dong and Friedrich, 2005; Grubbs et al., 2015; Lorenzen et al., 2002). Taken together, if and to what degree the ommochrome pathway can be involved in coloration other than the eyes, remains generally unknown.

In addition to ommochrome, the pteridine pigments were also revealed to contribute to eye color in *Drosophila* (Ziegler and Harmsen, 1970). The pteridine pathway starts with the conversion from guanosine-50-triphosphate (GTP) to 7,8-dihydroneopterin triphosphate (H2-NTP), catalyzed by GTP cyclohydrolase I (encoded by gene *Punch*). H2-NTP is then involved in branches of conversions that lead to various pteridine pigments (Fig. 1.2). A total of five different pteridine pigments have been found in *Drosophila*: Drosopterin, Aurodrosopterin, neodrosopterin, isodrosopterin, and fraction e (Kim et al., 2013). How these pigments are produced, though, still remains largely unknown. Only a small portion of the synthesizing mechanisms of drosopterin, isodrosopterin and aurodrosopterin has been characterized, including the conversion from H2-NTP to 6-pyruvoyl by the activity of tetrahydropterin synthase gene (encoded by gene *purple*) (Kim et al., 2013). The establishment of pteridine coloration also requires the input from the heterodimer formed by ABC transporters. This

heterodimer is formed by the products of *brown* and *white* genes (Dreesen et al., 1988; Ewart and Howells, 1998). Note that *white* is shared between the ommochrome and pteridine granules. Mutations in the *white* gene cause failure in production of both pigments, resulting in white-eye phenotype in *Drosophila* (Ewart et al., 1994; Ewart and Howells, 1998; Summers et al., 1982). In non-dipteran insects, the information on the pteridine pathway is very limited, with only a handful of studies in *Bombyx* and plerid butterflies providing a molecular insight (Kato et al., 2006; Morehouse et al., 2007). Overall, among the three major pigmentation mechanisms, the contribution of the pteridine pathway to insect coloration remains least understood.

Although melanin, ommochrome and pteridine have long been recognized as the major components of insect coloration, these pigments have been traditionally studied in isolation from one another (Kato et al., 2006). And yet, many insects utilize multiple pigment pathways to establish their overall color patterns. For this reason, it is critical to gain an insight into how different pathways are coordinated in a single species. Such research has only been initiated recently in *Bombyx* (Kato et al., 2006), where it has been reported that changes in pteridine pathway may in turn alter the melanin and ommochrome production. In addition, the genetically tractable model systems such as *Drosophila* and *Tribolium* have a rather limited color palette, whereas species with rich coloration (such as *Heliconius* butterflies) generally lack the ability to perform functional studies. As a result, whether or not the insight from model systems can be applied to species with complex color patterns is yet to be determined. Furthermore, most of the primarily studied species, including flies, beetles, and lepidopterans, belong to holometabolous groups, which establish coloration only once at larval stage and/or once

at adult stage. In contrast, the coloration of hemimetabolous insects is re-established multiple times during nymphal and adult stages, is poorly understood. Therefore, building a hemimetabolous model system is critical for determining the degree of conservation in pigmentation mechanisms between holometabolous and hemimetabolous species.

To bridge the above gaps in the current understanding of insect coloration, we utilized a hemimetabolous species *Oncopeltus fasciatus* (milkweed bug) as a new model for studying the evolution and divergence of insect pigmentation. *Oncopeltus* is very well suited for such a purpose, as functional experiments (via RNAi) are highly effective in this species. Furthermore, it has striking orange/black aposematic coloration that serves as a warning signal in “advertising” its distastefulness to predators (Berenbaum and Miliczky, 1984; Sexton et al., 1966). Hence, by characterizing the pigmentation pathways underlying orange/black color patterns in *Oncopeltus*, we will also gain general insights into the genetic regulation of aposematic coloration in insects. In this dissertation, we performed comprehensive analyses on all three pigmentation pathways: melanin, ommochrome, and pteridine. In Chapter 2, we analyzed the fundamental enzymes in the melanin pathway, including TH, DDC and Lac2. The results obtained show that the black coloration of *Oncopeltus* comes solely from the melanin pathway, whereas other pathways generate the orange coloration. We also investigated the color patterning in adult wings, which showed that the wing color patterns are generated via a two-step process: 1) the relevant enzymes must be pre-located and activated on the pre-eclosion wings; 2) after eclosion, the melanin precursors are distributed to the mature wings through the veins, allowing the enzymes

to catalyze the synthetic reactions to produce final pigments. In Chapter 3, we determined the functions of modifier genes within the melanin pathway that can either suppress (*ebony*, *black* and *aaNAT*) or promote (*yellow* and *tan*) melanin formation. The results showed that unlike in the model species, where these modifier genes are essential for color patterns throughout every body region, their pigmentation roles in *Oncopeltus* are exhibited in a region-specific manner. This finding provides a novel insight into the strategy of black patterning in insect coloration where different parts of the melanin pathway are employed in distinct body regions. In Chapter 4, we performed functional analyses on the ommochrome genes (*vermillion*, *cinnabar* and *scarlet*) and pteridine genes (*Punch*, *purple*, *white* and *brown*) to determine their pigmentation roles in *Oncopeltus*. We found that although both pathways contribute to the eye color, they are employed at different developmental stages. In addition, the pigmentation function of the pteridine pathway extends into the orange coloration in the wings and other body regions. These pteridine pigments, together with the melanin products in the cuticle, form a two-layer overlay that generates the final orange/black patterns in *Oncopeltus* adults. This multi-layer concept can be generally applied to a wide range of species, and provides a working framework for future pigmentation studies of multi-colored insects.

Overall, the work described here has now established *Oncopeltus* as a new model for studies of insect coloration. For the first time, all of the three main pigmentation pathways have been functionally studied in a single species, laying out a foundation for future work on the upstream regulatory mechanisms. Furthermore, the generated insights provided new concepts that can be applied to any study with a focus

on insect pigmentation. First, we had demonstrated that a single pathway can be divided into different branches that are utilized in region-specific and/or developmental stage-specific ways. While other studies have primarily focused on the inter- or intra-species perspectives, our findings provide a first insight into how such diversity can be generated during ontogenesis in a single individual. Second, although the functions of the single genes within a synthesis pathway are conserved among species, we found that the assembly of the pathway itself (such as number of involved genes and position of specific reactions, etc.) can be modified through evolution. For example, while the pteridine pathway did not originally encompass *brown* (as evidenced by results in *Oncopeltus*), this gene has been subsequently recruited in more derived species such as *Drosophila*. Lastly, our data have shown how different synthesis pathways are coordinated together to generate a particular color pattern within a specific body region. This finding highlights the necessity of combinatorial analyses involving multiple mechanisms when studying the molecular basis of coloration divergence. Taken together, the present studies not only provided new insights into insect pigmentation, but also addressed fundamental evo-devo questions, which in turn, can further our understanding of evolution and divergence of morphological traits in nature.

CHAPTER 2 THE GENETIC CONTROL OF APOSEMATIC BLACK PIGMENTATION IN HEMIMETABOLOUS INSECTS: INSIGHTS FROM ONCOPELTUS FASCIATUS

The contents of this chapter have been published in *Evolution & Development*.

Liu, J., Lemonds, T. R. and Popadic, A. (2014). The genetic control of aposematic black pigmentation in hemimetabolous insects: insights from *Oncopeltus fasciatus*. *Evol Dev* 16, 270-277.

Abstract

Variations in body pigmentation, encompassing both the range of specific colors as well as the spatial arrangement of those colors, are among the most noticeable and lineage-specific insect features. However, the genetic mechanisms responsible for generating this diversity are still limited to several model species that are primarily holometabolous insects. To address this lack of knowledge, we utilize *Oncopeltus fasciatus*, an aposematic hemimetabolous insect, as a new model to study insect pigmentation. First, to determine the genetic regulation of black pigment production in *Oncopeltus*, we perform an RNAi analysis on three core genes involved in the melanin pathway, *tyrosine hydroxylase (TH)*, *dopa decarboxylase (DDC)*, and *laccase 2 (lac2)*. The black pigmentation is affected in all instances, showing that the black pigments in this species are derived from the melanin pathway. The results of the *DDC* RNAi are particularly informative because they reveal that it is Dopamine melanin, not DOPA melanin, which is the predominant component of black pigments in *Oncopeltus*. Second, we test whether pigmentation follows a two-step model where the spatial pre-mapping of enzymatic activity is followed by vein-dependent transportation of melanin substances. We confirm the existence of the first step by observing that premature wings develop black pigmentation when exposed to melanin precursors. In addition, we

provide evidence for the second step by showing that wing melanin patterning is disrupted when vein transportation is halted. These findings bring novel insights from a hemimetabolous species and establish a framework for subsequent studies on the mechanisms of pigment production and patterning responsible for variations in insect coloration.

Introduction

Pigmentation is one of the most conspicuous and variable features of insect diversity, playing essential functions in a variety of behavioral, physiological, and reproductive processes (Nijhout, 1991). Although highly diverse, variations in insect pigmentation are generated through a common mechanism that encompasses both pigment patterning and pigment production (Wittkopp and Beldade, 2009). Because most of the available genetic information was generated from the studies in model species such as *Drosophila*, which not only have a limited color spectrum but also undergo a more derived holometabolous development, it is unclear whether this mechanism is broadly applicable to other insect lineages.

Pigment patterning is determined by regulatory factors, which directly or indirectly control the spatial distribution of enzymes involved in pigment biosynthesis (Wittkopp and Beldade, 2009). In *Drosophila*, wing patterning follows a two-step model, described by True et al. (1999). First, the enzymes are pre-patterned prior to the initialization of wing pigmentation. Then, in newly molted adults, the precursors are transported through the wing veins and gradually diffuse out into the wing tissue, allowing the pre-patterned enzymes to oxidize the precursors forming dark brown or black patterns. At present, the role of vein transport in pigment patterning is still not fully understood due

to a limited number of studies that provided conflicting results. As previously reported, the disruption of this transport in *Drosophila* and the swallowtail butterfly *Papilio*, by either genetic or surgical means, resulted in abnormal color patterns in the wing regions associated with the affected veins (Koch and Nijhout, 2002; True et al., 1999). However, in the brush-footed butterfly *Heliconius*, mutants with severe vein deficiency do not display significant alteration in wing coloration, suggesting that wing patterning may be vein independent in this species (Reed and Gilbert, 2004). Such contradictory findings make it hard to generalize whether the two-step model is also applicable to other insect species.

Most of our insight into pigment production comes from *Drosophila*. In this species, all body and wing pigments are produced by the melanin pathway (Riedel et al., 2011; True et al., 2005; Wittkopp et al., 2003; Wittkopp et al., 2002; Wright, 1987). As illustrated in Fig. 2.1, the first step of the melanin pathway is the conversion of tyrosine to DOPA (dihydroxyphenylalanine) by tyrosine hydroxylase (TH). DOPA can either be directly utilized to synthesis black DOPA melanin, or converted to Dopamine, which is catalyzed by DOPA decarboxylase (DDC). Dopamine, in turn, can be converted into two other major catecholamine metabolites, NBAD (N- β -alanyldopamine) or NADA (N-acetyldopamine). Finally, Phenol Oxidases (PO) change these products to their relative quinones, which are then converted to Dopamine melanin (brown/black pigment), NBAD sclerotin (yellow), or NADA sclerotin (colorless), respectively. Additional functional data from *Tribolium*, *Apis*, and *Monochamus* (Arakane et al., 2009; Arakane et al., 2005; Elias-Neto et al., 2010; Gorman and Arakane, 2010; Niu et al., 2008; Roseland, 1987), in combination with recent expression

studies suggest that the melanin pathway might also be involved in pigmentation in other holometabolous groups (Ferguson et al., 2011b; Futahashi et al., 2010; Futahashi and Fujiwara, 2005; Shirataki et al., 2010; Yu et al., 2011). However, much less genetic data has been reported in hemimetabolous insects except a functional report showing that *laccase 2 (lac2)*, a phenol oxidase, is involved in cuticular pigmentation in stinkbug species (Futahashi et al., 2011).

Our understanding of the molecular mechanism of aposematism, which is one of the most successful anti-predator adaptations in insects, remains extremely limited. Model species such as *Drosophila* or *Tribolium*, in which genetic tools are readily available, do not display any striking coloration. In contrast, in traditional aposematic model insects such as *Heliconius*, a functional approach is not yet feasible. To fill in this gap we utilized *Oncopeltus fasciatus* (milkweed bug) as a new model for studying the evolution and divergence of insect pigmentation in a more basal insect group. *Oncopeltus* is ideally suited for such a purpose being a hemimetabolous species in which functional experiments (via RNAi application) are highly effective. Furthermore, its orange/black aposematic coloration is relatively simple, allowing for an easy and direct molecular analysis of specific warning patterns.

In the first half of this study, we tested the role of the melanin pathway in the black pigmentation in *Oncopeltus*. We performed an RNAi analysis to examine the functions of three essential enzymes in this pathway: *TH*, *DDC*, and *lac2* (Arakane et al., 2005; Elias-Neto et al., 2010; Futahashi et al., 2011; Niu et al., 2008; Wright, 1987). Our results establish that in *Oncopeltus* black coloration is produced via the melanin pathway, with Dopamine as the predominant contributor to the black pigmentation.

Also, we tested if the *Drosophila* two-step wing melanin patterning model is applicable to *Oncopeltus*. Our results show that both the pre-mapping of melanization enzymes as well as the vein-dependent elaboration exist in this species. Overall, these observations suggest that the production of black pigmentation, as well as the two-step wing patterning model may be general mechanisms that are used across all insect lineages.

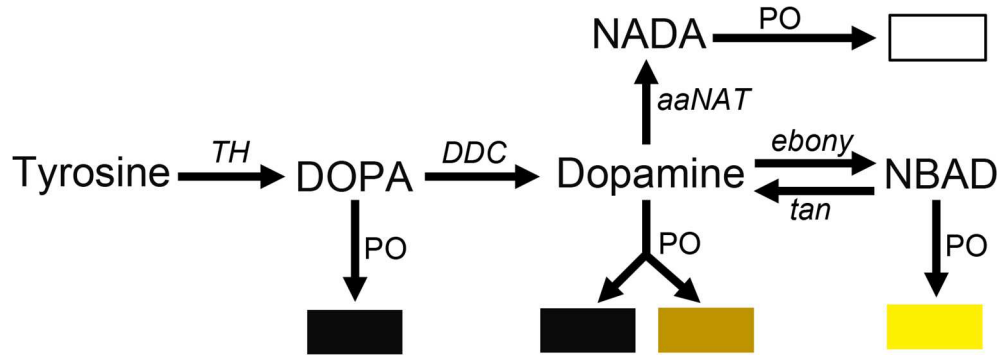


Figure 2.1. The summary consensus view of melanin biosynthesis pathway in *Drosophila* (Wittkopp et al., 2003; Wright, 1987).

Materials and Methods

Cloning and Sequence Analysis of cDNA Fragments

The total RNA extraction, production of cDNA, RT-PCR, and cloning were performed as described previously by Li and Popadic (Li and Popadic, 2004). Two rounds of nested-PCR were utilized to obtain the cDNA fragments of *TH*, *DDC*, and *lac2*. For details on primers and PCR conditions, please refer to Liu et al.(2014).. Identities of these *Oncopeltus* genes were confirmed by a phylogenetic analysis (Fig. 2.2).

RNA interference (RNAi)

For details on RNAi injections, please refer to Liu et al (2014).

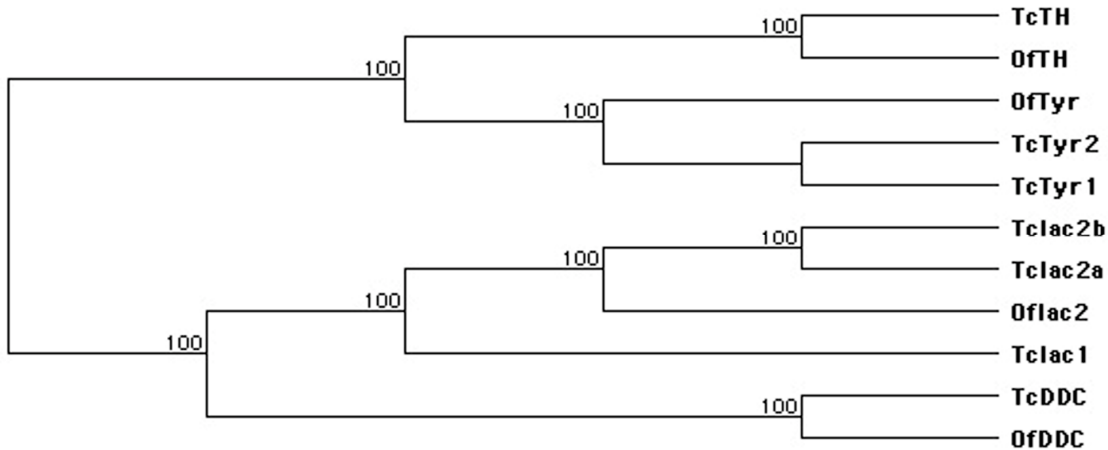


Figure 2.2. Phylogenetic relationships between *Tribolium* and *Oncopeltus* melanin pathway genes. Phylogeny was inferred using Neighbor Joining method based on amino acid sequences. Branch support values are bootstrap percentages from 500 replicates.

RT-PCR Analysis

Independent RT-PCR analyses were performed to determine the efficiency of our RNAi approach (Fig. 2.3). For details on preparation of total RNA, cDNA, as well as primers and PCR conditions, please refer to Liu et al (2014).

In Vitro Induction of Wing Pigmentation

This assay was performed following the approach described by Walter et al. (1996). The wing tissues were dissected from late 5th nymphs and fixed for 30 min with freshly made 4% formaldehyde in PBS (140 mM NaCl, 2mM KCl, 1.4mM KH₂PO₄, 8.1mM Na₂HPO₄, pH 7.5) containing 10% sucrose. This was followed by two washes in PBS+10% sucrose. After these washes, one forewing and hindwing from the same individual were incubated in a fresh solution of PBS+10% sucrose containing either 5mM L-DOPA or 5mM Dopamine (SIGMA). As a control, the other set of wings from

the same individual were incubated in the same buffer but without the added precursors.

Vein Cutting

Within one hour after molting, the subcostal and radial-medial veins of forewings and the radial and medial veins of hindwings were cut using scissors. The wings were then left attached to the body for 3-4 hours or 24 hours, after which they were removed for observation.

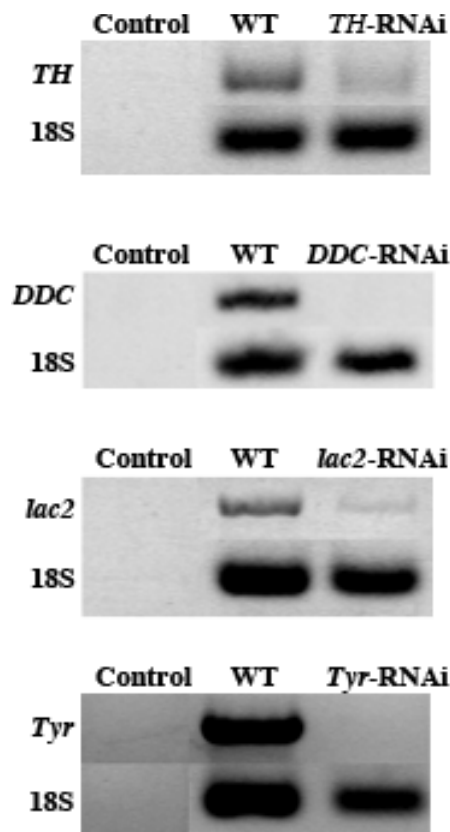


Fig. 2.3. RT-PCR analysis of *TH*, *DDC*, *laccase 2 (lac2)*, and *tyrosinase (Tyr)* mRNA in 5th nymphs of *Oncopeltus*. Only trace levels of each gene transcripts were detected in RNAi individuals compared to wild types.

Results

Functions of tyrosine hydroxylase (*TH*), dopa decarboxylase (*DDC*) and *laccase 2 (lac2)* in production of black pigmentation in *Oncopeltus*

The body and wings of *Oncopeltus* display alternating black and orange coloration (Fig. 2.4A1-A2). The head is characterized by a V-shaped orange stripe flanked by black pigmentation on its dorsal surface (Fig. 2.4A3). The dorsal plates of the thoracic segments are primarily black, with the exception of the lateral edge on the prothorax (T1) and the posterior tip of the mesothorax (T2) that are orange (Fig. 2.4A4). From the lateral side, the thoracic plates are almost completely black (Fig. 2.4A5). In contrast, the abdomen is mainly orange with several rectangular black patches on the ventral side (Fig. 2.4A6). In order to examine whether the melanin pathway is involved and to what degree it is generating the black wing and body pigmentation in *Oncopeltus*, we performed a functional analysis (via RNAi) on the core enzymes in the pathway.

First, we studied the role of *TH*, the enzyme catalyzing the initial step of the entire melanin pathway. Of the 44 injected bugs, 32 survived to adulthood and the most representative phenotype is illustrated in Fig. 2.4B. The *TH* RNAi adults display a complete absence of black pigmentation (Fig. 2.4B1). Specifically, the distinct black patterns that are present in WT are now completely lost in both pairs of wings (Fig. 2.4B2), head (Fig. 2.4B3), thorax (Fig. 2.4B4-B5), and abdomen (Fig. 2.4B6). These results establish that all of the black pigmentation in *Oncopeltus* is generated solely from the melanin pathway.

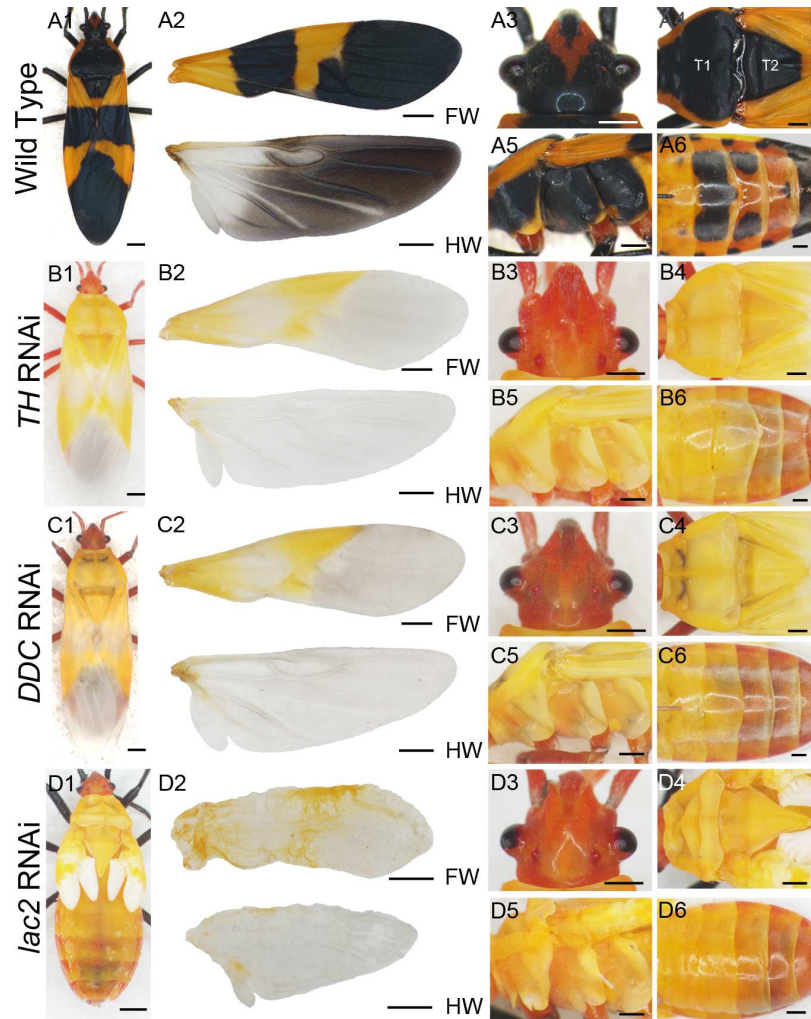


Fig 2.4. Functions of *TH*, *DDC*, and *lac2* in *Oncopeltus* adults. (A1-A6) Wild type *Oncopeltus* shows alternating black-orange patterning. The distinct black patterns are established in the wings (A2), head (A3), dorsal thorax (A4), lateral thorax (A5), and ventral abdomen (A6). (B1-B6) *TH* RNAi adults show a complete loss of black pigmentation in the whole body. (C1-C6) *DDC* RNAi adults display a significant reduction of black coloration. (D1-D6) *lac2* RNAi adults show that black pigmentation is abolished. The black legs and antennae are the residuals of un-removed exoskeleton. Scale bars: 1mm (A1, A2, B1, B2, C1, C2, D1, D2); 500 μ m (A3-A7, B3-B7, C3-C7, D3-D7). Abbreviations: FW, forewing; HW, hindwing; T1, prothorax; T2, mesothorax.

Since DOPA and Dopamine are believed to be the two direct precursors of black melanin (Walter et al., 1991; Wright, 1987), we examined their individual contributions in *Oncopeltus*. As described in Fig. 2.1, *DDC* converts DOPA to Dopamine, hence knocking down this enzyme should cause the irreversible loss of Dopamine.

Consequently, any black coloration observed in *DDC* RNAi adults is solely produced by DOPA. As shown in Fig. 2.4C1-C6, *DDC* RNAi individuals display a severe reduction in black coloration, which encompasses the whole body. This was observed in all of the 33 surviving adults. Such result shows that Dopamine is the main contributor to black pigmentation in *Oncopeltus*, whereas the remaining grayish coloration can be attributed to DOPA.

The above observations confirm that the melanin precursors contribute to black pigments in *Oncopeltus*. However, these precursors still need to be oxidized into quinones, which are in turn incorporated into the cuticle matrix (Andersen, 2010). The *lac2* gene, a phenol oxidase, was reported to be critical in completing the cuticular melanization process in several insect species (Arakane et al., 2005; Elias-Neto et al., 2010; Futahashi et al., 2011; Niu et al., 2008; Tomoyasu et al., 2009). To determine its function in *Oncopeltus*, we performed *lac2* RNAi experiments (Fig. 2.4D1-D6). Out of 32 injected individuals, 19 survived into adults. While 14 of them could not molt completely, they could still live for 2-3 days allowing us to remove most of the residuals of exoskeleton to analyze the body and wing pigmentation (Fig. 2.4D1). These individuals display an absence of black pigmentation across the whole body (Fig. 2.4D2-D6), confirming that *lac2* is essential for melanization in this species as well. Tyrosinase (TYR), another phenol oxidase present in insects, is also believed to be involved in the melanization process (Andersen, 2010). To test the role of this additional phenol oxidase in *Oncopeltus* body melanization, we performed RNAi experiments. Our results showed identical black pigmentation patterns as observed in wild type (Fig. 2.5),

indicating that it is *lac2*, and not TYR, which is the essential phenol oxidase that governs cuticular melanization in this species.

In addition to significantly affecting black pigmentation in RNAi adults, the depletion of *TH*, *DDC*, or *lac2* (confirmed by our RT-PCR control, as shown in Fig. 2.3) also causes a slight reduction on the overall orange pigmentation (Fig. 2.4B1-D6). These observations suggest that the melanin pathway also plays a minor role in the orange pigmentation in *Oncopeltus*.



Fig. 2.5. The *Oncopeltus tyrosinase* (*tyr*) RNAi phenotype. *Tyr* RNAi adults (B) have no significant changes in black pigmentation, compared to WT (A).

Wing black pigment patterning requires vein transportation in *Oncopeltus*

Previous conflicting reports make it unclear if the wing veins are essential in the wing melanization process (True et al., 1999). To determine the role of veins in wing melanization in *Oncopeltus*, we first determined the dynamics of attaining black pigmentation in freshly molted wild type adults. An hour after eclosion has occurred, these appendages still lack black coloration (Fig. 2.6A). In contrast, the characteristic orange pattern on the forewings is already present at this stage. The beginning of wing darkening starts three to four hours post eclosion (Fig. 2.6C1), when both pairs of wings

begin to turn grey. The darkening of tissue continues to increase and wings obtain an intense black color within 24 hours (Fig. 2.6C2). From this stage on, the final black pigmentation levels are reached and wing coloration becomes permanent.

Wing pigment patterning was previously shown to be vein-dependent in *Drosophila* (True et al., 1999), but not in *Heliconius* (Reed and Gilbert, 2004). To determine which of the two mechanisms is present in *Oncopeltus* we interrupted the vein transportation by performing surgical cuts on freshly eclosed wings (corresponding to stage depicted in Fig. 2.6A). The subcostal and radial-medial veins of forewings and the radial and medial veins of hindwings were severed (arrowheads in Fig. 2.6B). The effects of surgery become noticeable within three hours, with the affected regions localized in the anterior half of each wing (dotted areas in Fig. 2.6D1). In forewings, there are two significantly lighter grey regions: a smaller one immediately adjacent to the cut and a larger one encompassing the distal half (compare Fig. 2.6C1 vs. Fig. 2.6D1). In a similar fashion, there is a complete loss of grey coloration in the distal region of hindwings delineated by the radial and medial veins. By the 24 hours mark, these affected regions in both forewing and hindwing do become darker – but they never reach the levels of black pigmentation in the unaffected, posterior wing regions (compare dotted areas in Fig. 2.6D2 to regions immediately posterior to them). These observations show that the vein transportation is critical for completing melanin patterning in *Oncopeltus* wings.

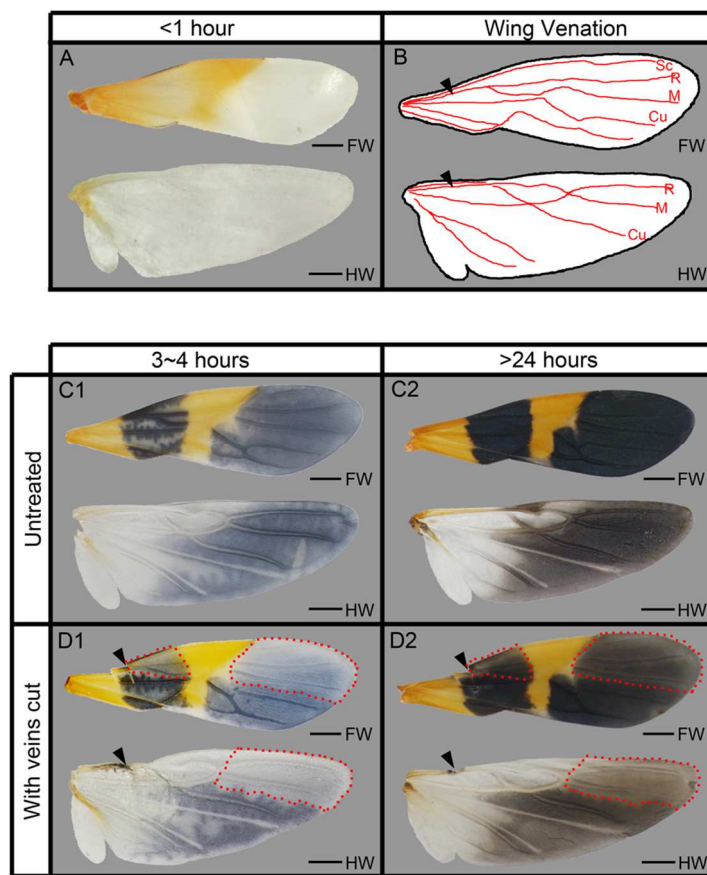


Fig 2.6. Black patterning of *Oncopeltus* wings is vein dependent. (A) Freshly molted adults have an alternating orange-white forewing and colorless hindwing. (B) The basic outline of veins, with cut sites represented by black arrowheads. The names of the veins are originated from Nivedita (1982). (C1-C2) The appearance of untreated wings 3-4 hr and 24 hr after molting, respectively. (D1-D2) Forewing with subcostal and radial-medial veins and hindwing with radial and medial veins surgically cut have black patterns disrupted in the subregions distal to the cutting sites (dotted areas). Such disruptions cannot be completely rescued even after 24 hrs, indicating that the black patterning process of *Oncopeltus* wings requires vein transportation. Scale bars: 1mm. Abbreviations: FW, forewing; HW, hindwing; Sc, subcostal; R, radial; M, medial; Cu, cubital.

Premature *Oncopeltus* wings can develop black pigmentation *in vitro* by supplying melanin precursors

According to (True et al., 1999), prior to the eclosion of wings, the enzymes for black pigmentation are pre-localized in immature wings. In order to determine if such a process is also present in *Oncopeltus*, we performed an *in vitro* induction of wing

pigmentation. Wings were dissected from late 5th nymphs and incubated in DOPA or Dopamine. As shown in Figs. 2.7A, B1, and B2, wings incubated in buffer alone did not develop any black pigmentation, whereas incubation with either precursor (DOPA or Dopamine) resulted in black pigmentation albeit with different levels of intensity. Wings exposed to DOPA (Fig. 2.7B1) were significantly lighter than the wings incubated with Dopamine (Fig. 2.7B2), which is consistent with our *DDC* RNAi observation (Fig. 2.7D1-D6).

The incubation of *TH* RNAi or *DDC* RNAi wings showed similar levels of melanization when compared to wild type wings (Fig 2.7C1-D2). On the other hand, the wings from *lac2* RNAi 5th nymphs failed in producing black pigmentation under exposure to either of these two melanin precursors (Fig. 2.7E1-E2). These observations suggest that the “production genes”, such as *lac2* are essential to oxidize the precursors and need to be pre-localized in premature wings before eclosion in *Oncopeltus*. While the “precursor enzymes” such as TH and DDC may also be pre-localized, the present data does not provide for a definitive answer in that regard. Together with the previously shown vein-dependent elaboration of melanin substances, these experiments suggest the presence of a two-step wing melanin patterning model in *Oncopeltus*.

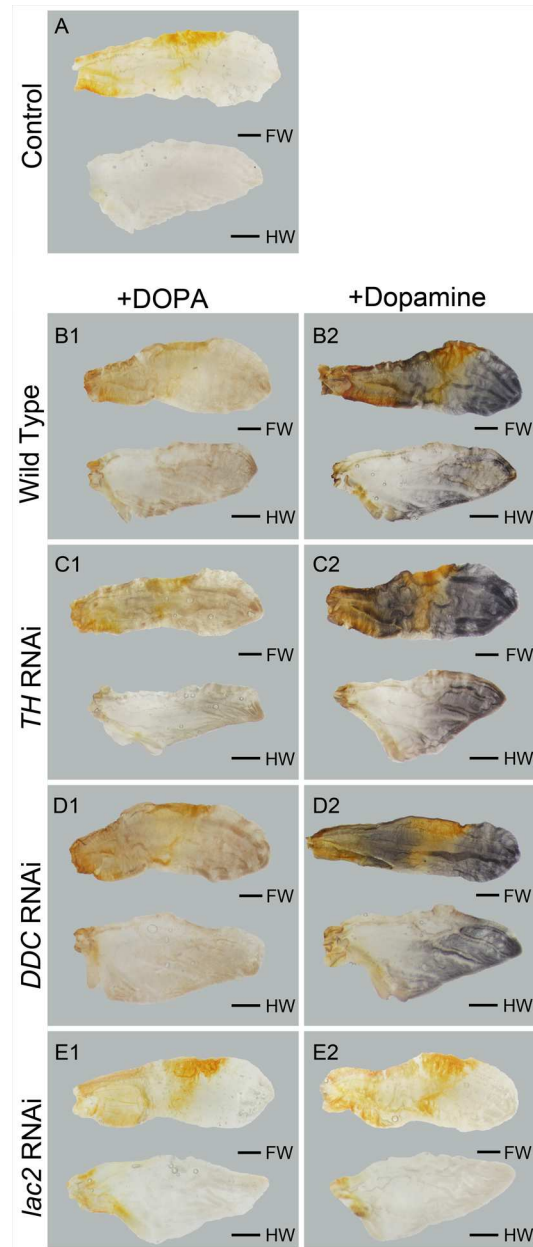


Fig 2.7. Pre-mature *Oncopeltus* wings can develop black pigmentation with exogenously supplied melanin precursors. All wings were dissected from late 5th nymphs. (A) Wings incubated in buffer without melanin precursors were used as a background control. (B1) Wings incubated in DOPA develop a low level of black pigment. (B2) Wings incubated in Dopamine develop a much stronger black pigmentation than the ones incubated in DOPA. (C1-D2) Similar results can be observed in *TH* RNAi and *DDC* RNAi wings. (E1, E2) *lac2* RNAi wings failed to generate any black pigment when incubated with DOPA or Dopamine. Scale bars: 500 μ m. Abbreviations: FW, forewing; HW, hindwing.

Discussion

Black pigment is produced via melanin pathway in *Oncopeltus*

Functional studies in *Drosophila* and *Tribolium* (True et al., 1999; True et al., 2005; Wittkopp et al., 2003; Wittkopp et al., 2002; Wright, 1987), suggest that the core part of the melanin pathway may be conserved among holometabolous insect species. In both species TH triggers the transformation of tyrosine to DOPA and DDC transforms DOPA into Dopamine, whereas PO is required for the conversion of melanin precursors to cuticular melanins. Our RNAi experiments in *Oncopeltus* show that the depletion of *TH*, *DDC*, and *lac2* causes the loss of black pigmentation, indicating the pivotal roles of these genes in *Oncopeltus* melanization (Fig. 2.4). In addition, our observations that *TH* RNAi and *DDC* RNAi wings developed black melanin through *in vitro* incubation with melanin precursors whereas *lac2* RNAi wings did not, further support the different positions of these three genes in the melanin pathway. That is, *TH* and *DDC* are “precursor enzymes” that produce substrates for subsequent melanization reactions, whereas *lac2* belongs to “production enzymes” that act on the precursors. Taken together, our findings imply that the basic components of melanin production in insects may have a single common origin.

In spite of the overall progress in understanding the melanization across different insects, the identity of the main precursor of black melanin remains an unresolved issue (Gibert et al., 2007). In the original studies of black pigmentation in *Drosophila*, *DDC* mutants were shown to generate only a low intensity of black pigment (gray), leading to the proposal that Dopamine melanin is the main component of black melanin (Walter et al., 1996; Wright, 1987). However, the follow-up analyses emphasized that the

contribution of DOPA to black melanin should be equally important as Dopamine (Wittkopp et al., 2003; Wittkopp et al., 2002). Of these two possibilities, our *DDC* RNAi study follows the original one, which showed that the contribution of DOPA to black pigment is quite limited and it is Dopamine that generates the majority of black pigments in *Oncopeltus*. While the latter results seem to swing the pendulum toward Dopamine as the main precursor, it will be important to confirm the generality of this insight through the sampling of additional hemimetabolous lineages.

The above discussion mainly focuses on the relationship between the melanin pathway and black pigment production. However, this pathway accounts only for a portion of the extraordinary range of colors that are present in insects. In classically studied aposematic species such as *Precis* and *Heliconius*, the warning colorations are thought to be produced independently from the melanin pathway (Ferguson and Jiggins, 2009; Nijhout, 1997; Reed and Nagy, 2005). Our observations in *Oncopeltus*, showing that *TH*, *DDC*, or *lac2* RNAi cause a very subtle reduction in orange coloration (Fig. 2.4), indicate that the melanin pathway plays only a minor role in orange pigmentation. Since the majority of orange color is still present in these RNAi individuals, the bulk of this pigment is generated by other pigmentation pathways. One possible component might be ommochrome, as reported in butterflies (Ferguson and Jiggins, 2009; Nijhout, 1997; Reed and Nagy, 2005) and red dragonflies (Futahashi et al., 2012). Another candidate is carotenoid, as indirectly suggested by studies in the pea aphid, *Acyrtosiphon pisum* (Moran and Jarvik, 2010; Novakova and Moran, 2012). However, these studies were only able to correlate either of the two proposed candidates to orange/red regions of the insect body without providing direct functional data showing a

causal effect. Thus, a follow up step in further developing *Oncopeltus* as a model for aposematic coloration would be to utilize the RNAi approach to determine the origin of residual orange pigments. This would significantly expand our overall understanding of the diversity of insect pigmentation and the genetic mechanisms responsible.

Wing melanin patterning in *Oncopeltus* is processed via a two-step model

Our current understanding of the mechanism regulating insect wing pigment patterning is restricted to *Drosophila*, on which the proposed two-step model is based (True et al., 1999). The first step involves the early pre-patterning of melanin enzyme activity. The second step is the vein-dependent transportation of melanin substances. In our study, the existence of the first step in *Oncopeltus* is supported by the fact that pre-mature wings can develop black pigmentation when melanin precursors are provided exogenously (Fig. 2.7). Confirmation of the second step is provided by our observations from the vein-cutting assay, showing that the melanization in areas of the wing downstream of the cut locations is affected by the physical damages to the veins (Fig. 2.6). When combined with insights from *Drosophila*, our results indicate that the two-step model may be shared between holometabolous and hemimetabolous species.

The previous studies in *Drosophila* and *Heliconius* provided conflicting views on the actual significance of vein transportation in wing melanization (Reed and Gilbert, 2004; True et al., 1999). As illustrated in Fig. 2.6, the vein cutting assay clearly confirms that vein transportation is required for melanin patterning in *Oncopeltus* wings. We also observe that on pre-melanized *Oncopeltus* wings, black bristles are already present (Fig. 2.8). A similar result was reported in *Drosophila* vein mutants (True et al., 1999), suggesting not only that bristle and wing tissue melanization are separated – but

also that the former process is generated by a vein-independent mechanism. The presence of such a mechanism in *Heliconius* could provide for an alternative explanation of the situation observed in this species, in which vein deficiency did not seem to affect melanin patterns. Assuming that the black wing coloration in butterflies is comprised solely of black scales (Janssen et al., 2001), which are reported to be modified bristles (Galant et al., 1998), then such observations may result from bristle melanization. Therefore, two different processes might co-exist during the wing melanin patterning in insects: bristle melanization, which is vein transportation independent and wing tissue melanization, which requires vein transportation.

ACKNOWLEDGEMENTS

We thank Jim Marden for help with cloning of the orthologues gene fragments in *Oncopeltus* and Patricia Wittkopp for helpful comments on the manuscript. This work was supported in part by NIH grant GM071927 to A.P. and WSU Rumble Fellowship to J. L.



Fig. 2.8. In wild type, bristles on the *Oncopeltus* forewing attain black pigmentation well before the melanization of a wing tissue. (A) Pre-melanized forewing of *Oncopeltus*. (B) Magnified image of the box in A.

CHAPTER 3 A PATHWAY ANALYSIS OF MELANIN PATTERNING IN A HEMIMETABOLOUS INSECT

The contents of this Chapter has been published in Genetics

Jin Liu¹, Thomas R. Lemonds¹, James H. Marden² and Aleksandar Popadić^{1*}

¹Wayne State University, Biological Sciences Department, Detroit, USA

²Pennsylvania State University, Department of Biology, University Park, USA

Abstract

Diversity in insect pigmentation, encompassing a wide range of colors and spatial patterns, is among the most noticeable features distinguishing species, individuals, and body regions within individuals. In holometabolous species, a significant portion of such diversity can be attributed to the melanin synthesis genes, but this has not been formally assessed in more basal insect lineages. Here we provide a comprehensive analysis of how a set of melanin genes (*ebony*, *black*, *aaNAT*, *yellow*, and *tan*) contributes to the pigmentation pattern in a hemipteran, *Oncopeltus fasciatus*. For all five genes, RNAi depletion caused alteration of black patterning in a region-specific fashion. Furthermore, the presence of distinct non-black regions in fore- and hindwings coincides with the expression of *ebony* and *aaNAT* in these appendages. These findings suggest that the region-specific phenotypes arise from regional employment of various combinations of the melanin genes. Based on this insight, we suggest that melanin genes are utilized in two distinct ways: a “painting” mode, using predominantly melanin promoting factors in areas that generally lack black coloration, and alternatively, an “erasing” mode, utilizing mainly melanin suppressing factors in regions where black is the dominant pigment. Different combinations of these strategies may account for the vast diversity of melanin patterns observed in insects.

Introduction

Pigment patterns are among the most striking and variable features of insect morphology. An extraordinary diversity in coloration distinguishes species, populations within species, individuals within populations, and different body regions (Wittkopp and Beldade, 2009). Most insights into the mechanisms underlying such diversity have come from studies on melanization in *Drosophila* (Wittkopp and Beldade, 2009; Wittkopp et al., 2003). Melanization is the pigmentation process wherein precursors (catecholamines) are converted into pigment molecules that are incorporated into the cuticle (Wittkopp and Beldade, 2009). These studies have helped identify a network of melanin genes and their roles in body color patterning (Wittkopp and Beldade, 2009; Wittkopp et al., 2003; Wright, 1987). The core part of this proposed pathway is shown in Fig. 1.1. The pathway begins with the conversion of tyrosine to DOPA (dihydroxyphenylalanine). DOPA can then be utilized in two different manners: to produce DOPA melanin (black) or be converted to dopamine, another precursor of black melanin. In the conversions from DOPA/dopamine to black melanin, the *yellow* gene is thought to play an essential role promoting these processes. However, it is still unclear whether *yellow* plays a role in producing DOPA melanin, or dopamine melanin, or both (question marks in Fig. 1.1). Alternatively, production of dopamine melanin can be suppressed by converting dopamine to NBAD (N-β-alanyldopamine) or NADA (N-acetyldopamine). The NBAD branch contains three main genes: *ebony*, *black*, and *tan*. Black catalyzes the production of β-alanine, which binds to dopamine by the activity of Ebony, thus forming NBAD, the precursor of yellow sclerotin. It is also possible to convert NBAD back to dopamine by the activity of Tan. The dopamine produced under

such circumstance is then converted to dopamine melanin thus promoting dark coloration (True et al., 2005; Wittkopp et al., 2002). In *Heliconius*, Tan has also been recognized as an additional factor that promotes dark melanization (Ferguson et al., 2011b). The NADA branch relies on the function of arylalkylamine-N-acetyltransferase (AANAT), which converts dopamine to NADA, the precursor of colorless sclerotin. These five genes, including three melanin suppressing (*ebony*, *black*, and *aaNAT*) and two promoting (*tan* and *yellow*) factors, are thought to be the main genes in the mechanism responsible for producing different melanin patterns (Wittkopp and Beldade, 2009; Wittkopp et al., 2003; Wright, 1987).

Assays in *Drosophila* have provided functional evidence associating *ebony*, *yellow*, and *tan* to body and wing pigmentation (Gompel et al., 2005; Jeong et al., 2008; True et al., 2005; Walter et al., 1996; Wittkopp et al., 2002). In addition, functional studies in *Tribolium* have also reported the essential involvement of *ebony*, *black*, and *yellow* (Arakane et al., 2010; Arakane et al., 2009; Tomoyasu et al., 2009), whereas the pigmented phenotype of *aaNAT* was reported only in *Bombyx* (Osanai-Futahashi et al., 2012; Zhan et al., 2010). A systematic functional profile of these melanin genes is lacking in any of the more basal hemimetabolous insect lineages. In this mode of development, the embryo hatches as a miniature adult that undergoes a succession of molts, with melanization occurring at each stage. Thus, as a complement to the studies already performed in holometabolous insects, it is important to begin evaluating the roles of melanization genes in the pigmentation of hemimetabolous species. This also establishes a foundation for understanding the evolution of the melanin pathway in insects.

Accordingly, we performed the first systematic functional analysis of *ebony*, *black*, *tan*, *yellow*, and *aaNAT* in a hemimetabolous species, the milkweed bug *Oncopeltus fasciatus*. This insect is well suited for the study of pigmentation since it features striking aposematic black/orange warning colorations and color patterns that are distinct in different body regions. The black coloration has been recently confirmed to be produced via the melanin pathway, whereas the majority of the orange coloration comes from another source (Liu et al., 2014). The RNAi approach in *Oncopeltus* is also highly efficient and generates phenotypes displaying systemic responses (Angelini and Kaufman, 2005; Liu and Kaufman, 2004a, b, 2005). This allows for the functional analysis of pigmentation genes at a whole-body scale, as was highlighted by a previous study (Liu et al., 2014). The depletion of master synthesis genes (*tyrosine hydroxylase* and *dopa decarboxylase*, which initialize the melanin pathway; Fig. 1.1) caused great reduction in black coloration throughout the whole body (Liu et al., 2014). In the present study, RNAi knockdowns of the five melanin genes establish regional pigmented phenotypes. More specifically, the phenotypes observed in the abdomen and hindwings of RNAi adults are different from those in the head, thorax, and forewings. These observations were unexpected because RNAi depletion of *ebony*, *black*, or *aaNAT* in holometabolous species (*Tribolium* and *Bombyx*) caused alterations of color patterns over the entire body (Arakane et al., 2010; Jeong et al., 2008; Osanai-Futahashi et al., 2012; Tomoyasu et al., 2009; True et al., 2005; Wittkopp et al., 2002; Zhan et al., 2010). Results presented here from *Oncopeltus* suggest that different melanin genes are utilized to form black patterns in distinct body regions. This finding provides novel insights regarding how pigment diversity is created in different body

regions by mechanisms that could be general to other insects with complex color patterns, including other aposematic species whose color patterns play critical roles in interspecies communication.

Materials and Methods

Cloning and Sequence Analysis of cDNA Fragments

Extraction of total RNA from embryos of *Oncopeltus fasciatus*, as well as the follow-up cDNA generation, nested RT-PCR, and cloning were carried out according to Liu et al. (Liu et al., 2014) and Li and Popadić (Li and Popadic, 2004). Multiple reactions of nested-PCR were performed to amplify the gene fragments. The primers used for PCR cloning, as well as the lengths of obtained cDNA fragments are listed in Table 3.1. All of these cDNA fragments cover the majority of the coding region of each gene. The orthologies of these *Oncopeltus* genes were confirmed by phylogenetic analysis (Fig. 3.1&3.2). In the case of *Oncopeltus Ubx*, a previously described clone was used (Medved et al., 2015).

RNA interference (RNAi)

For all genes in this assay, double stranded RNA (dsRNA) was generated using the entire cDNA fragment to ensure the specificity of RNAi depletion. For details of dsRNA injections, please refer to Liu et al (2016).

RT-PCR Analysis

Independent RT-PCR analysis were performed to determine the efficiency of our RNAi approach (Fig. 3.3). The procedures of total RNA extraction and cDNA synthesis

were carried out following Liu et al. (2014). Primers used for RT-PCR are listed in Table

3.1.

	Primers for PCR cloning	Primers for RT-PCR	Length of fragment	Corresponding AA residues of <i>Dm</i> orthologs
<i>Of-ebony</i>	Forward: 5' ACGACCGCAACTCTCAAAC 3' 5' TCACCAGCTCTTCTCGTTGA 3' Reverse: 5' TGCTGAGTTAGAGGGCTGGT 3' 5' TGCCAGTAAAGCCTCTGGAT 3'	Forward: 5' CTTCTCCCGACCTCATTCTG 3' Reverse: 5' GGTCACAGGGCATCTAAAA 3'	2333 bp	135~822 (out of 879aa)
<i>Of-black</i>	Forward: 5' GGTGCAGCGTCTTCTCTAC 3' 5' GGCCGGTACTGACTCTGT 3' Reverse: 5' AGAAGTTGGGTGTCCTTG 3' 5' TTGTCCTTCACGCATCATC 3'	Forward: 5' GGCCGGTACTGACTCTGT 3' Reverse: 5' TTGTCCTTCACGCATCATC 3'	1160 bp	147~532 (out of 575aa)
<i>Of-yellow</i>	Forward: 5' ATTCGCCTGGAAGTATGTGG 3' 5' GGACAAAGGTGTCCCGAGTA 3' Reverse: 5' GAGAATTCTGGCAGCTGAGG 3' 5' ATCGGCAACCTGTGGTAGAG 3'	Forward: 5' AGTCCAGAAACCCCTCT 3' Reverse: 5' ATCGGCAACCTGTGGTAGAG 3'	1062 bp	80~408 (out of 541aa)
<i>Of-tan</i>	Forward: 5' CGTCCGTTCTTACTTCTCG 3' Reverse: 5' CCTGGCATTGCAGTTGAATA 3'	Forward: 5' GGACATTCTACCAGCCCAA 3' Reverse: 5' CAATCGATCTCCAGCCTGAT 3'	1338 bp	6~386 (out of 387aa)
<i>Of-aaNAT</i>	Forward: 5' TGGGCGAAAGAGAGAATGAC 3' 5' CCAGGAAGACGTGGAAAGAG 3' Reverse: 5' GTGCAGACTTTGCAGTGTGG 3' 5' TCGGTCTTCCATCATTGTCA 3'	Forward: 5' CCAGGAAGACGTGGAAAGAG 3' Reverse: 5' CAAGGCTGTAGATGCTGTGG 3'	554 bp	30~206 (out of 240aa)

Table 3.1. Primers for RT-PCR and the lengths of the obtained cDNA fragments of relevant genes. Abbreviations: *Of*, *Oncopeltus fasciatus*; *Dm*, *Drosophila melanogaster*

Method: Neighbor Joining; Bootstrap (500 reps); tie breaking = Systematic
 Distance: Poisson-correction
 Gaps distributed proportionally

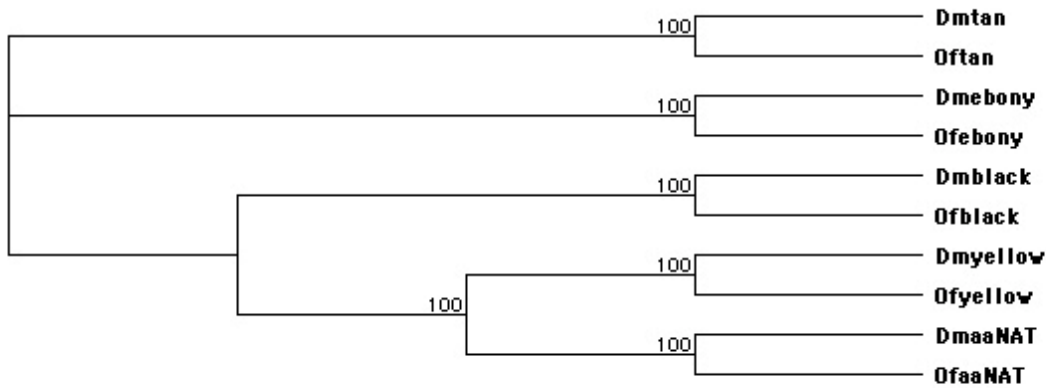


Fig. 3.1. Phylogenetic analysis of *Drosophila melanogaster* and *Oncopeltus fasciatus* melanin pathway genes. Phylogeny was inferred using the Neighbor-Joining method based on amino acid sequences. Branch support values are bootstrap percentages from 500 replicates.

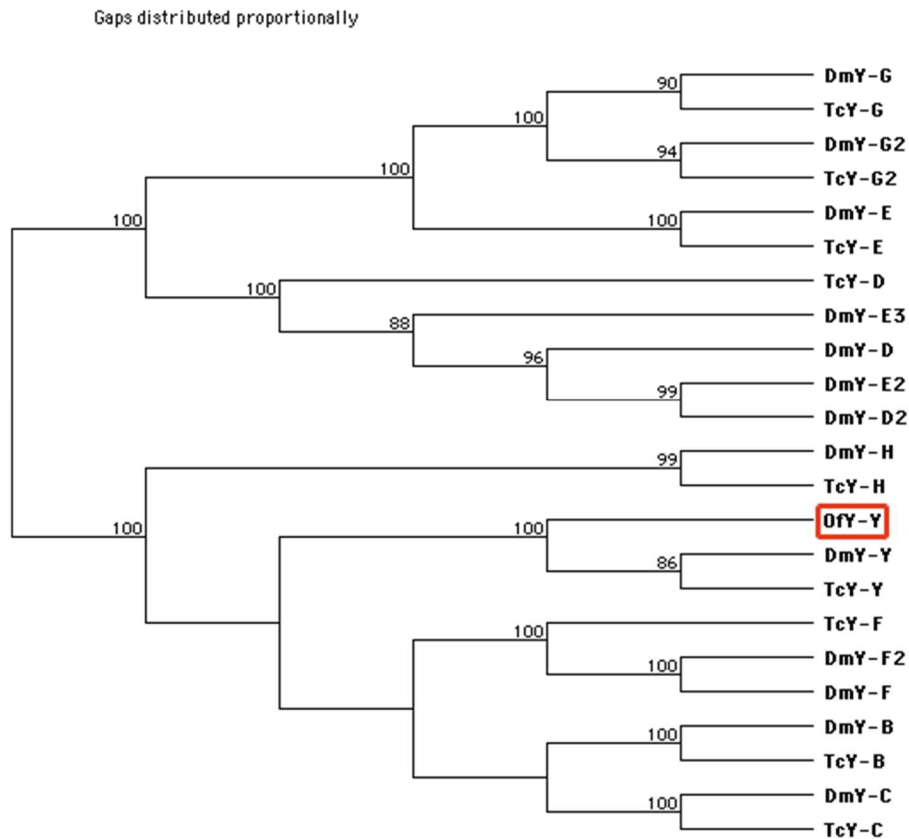


Fig. 3.2. Phylogenetic analysis of *yellow* gene family. *Oncopeltus* Yellow (OfY-Y) is orthologous to Yellow protein in *Drosophila melanogaster* (DmY-Y) and *Tribolium castaneum* (TcY-Y). Phylogeny was inferred using the Neighbor-Joining method based upon amino acid sequences. Branch support values are bootstrap percentages from 500 replicates.

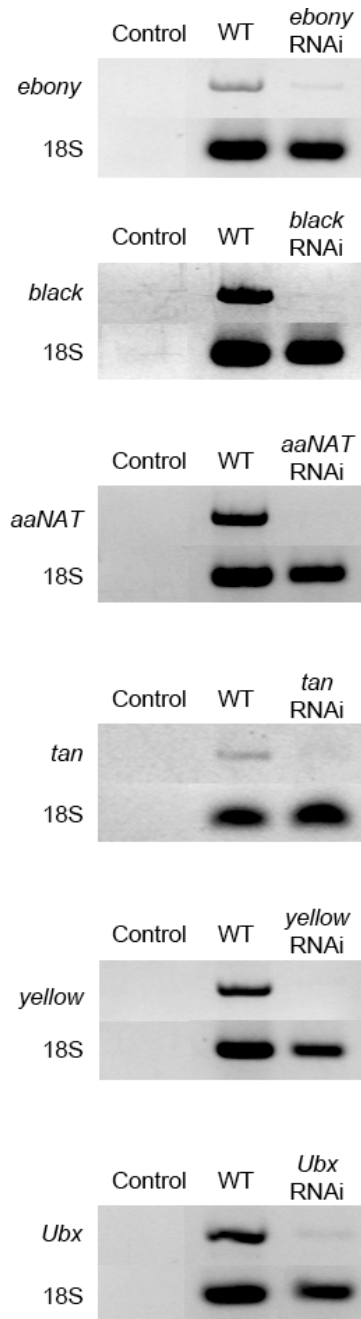


Fig. 3.3. RT-PCR analysis of *ebony*, *black*, *aaNAT*, *tan*, *yellow*, and *Ubx* mRNA in *Oncopeltus* 5th nymphs. Only trace levels of individual gene transcripts were detected in RNAi individuals when compared to wild types.

In addition, to determine if the systemic depletion was consistent throughout the body, we performed RT-PCR analyses on isolated body regions of *black* RNAi individuals that showed the greatest contrast in pigmented phenotypes between the abdomen and anterior body regions (Fig. 3.4). Two wild type or *black* RNAi 5th nymphs (day 8 of development) were utilized. The epidermis of head, thorax, FW, HW, and abdomen were dissected and separated. Each regional sample was used for total RNA extraction and cDNA synthesis following Liu et al. (2014).

Image Processing

Microscopy images were obtained using a SZX16 Microscope (Olympus) and DP72 camera (Olympus). To minimize the possible variation in captured images, the background and all of the microscope and camera settings were standardized: the images under a particular magnification were taken under the same light condition, aperture, exposure time, and white balance.

In addition, to quantify the changes in black intensity observed in *yellow* and *tan* RNAi adults, we measured the mean grayscales (at a scale of 0~255) of the black subregions using ImageJ in separate microscopy images of the head, thorax, FW, HW and ventral abdomen. The measurements were carried from 10 individuals of wild type, *yellow* RNAi, or *tan* RNAi *Oncopeltus* adults. The grayscale values were converted to brightness level as grayscale value/255 x 100. The converted brightness levels from these three groups were then compared to each other using group t-tests (the level of significance was 0.05). As a control, the same measurements and analyses were also applied to the orange subregions in the dorsal abdomens.

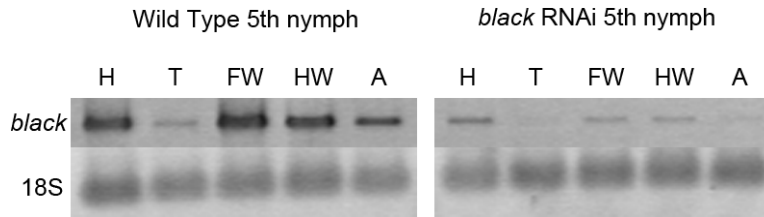


Fig. 3.4. RT-PCR analysis of *black* mRNA in isolated body regions of *Oncopeltus* 5th nymphs at Day8 of development. There is a significant reduction in *black* transcript in every body region in *black* RNAi individuals compared to wild type 5th nymphs. Abbreviations: H, head; T, thorax; FW, forewing; HW, hindwing; A, abdomen.

***In situ* hybridization**

The digoxigenin-labeled antisense RNA probes of *ebony* and *aaNAT* were synthesized as described in Li and Popadić (Li and Popadic, 2004). For each gene, both sense and antisense probes were used. The formation of wing tissue is completed at day 5 of the 5th nymphal stage, after which the cuticle starts forming, which in turn restricts the use of post-embryonic *in situ* hybridization analysis. Before day 5, the wing tissue is not completely formed and cannot be fixed intact. After day 6, the cuticle prevents the riboprobes from penetrating into the wing tissue. Therefore, in this assay, the wings were dissected from wild type and *Ubx*-RNAi 5th nymphs that were exactly 5~6 days old. 16-22 wings were analyzed in each group, and the shown images represent the consensus expression patterns. The *in situ* hybridization was modified from Tomoyasu et al. (2009). Details will be provided upon request.

Results

The functions of melanin genes on black patterns of body pigmentation in *Oncopeltus*

The *Oncopeltus* body has warning coloration consisting of alternating black and orange subregions and patches (Fig. 3.5A1). The dorsal head features a V-shaped

orange stripe flanked by black pigmentation covering the rest of the head (Fig. 3.5A2). Dorsal plates of the thoracic segments are primarily black, with the exception of orange at lateral edges on the prothorax (T1) and posterior tip of the mesothorax (T2; asterisks, Fig. 3.5A3). In contrast, the majority of the abdomen is orange with the exception of two rectangular black patches on the ventral side of A3-A4 segments (Fig. 3.5A4) and two small spots on the dorsal A1 segment (white arrows, Fig. 3.5A5).

To examine the role of the melanin pathway in *Oncopeltus* color patterning, we cloned five putative core melanin genes: *ebony*, *black*, *tan*, *yellow*, and *aaNAT*. Phylogenetic analyses confirmed that the obtained clones are indeed *Drosophila* orthologs (Fig. 3.1&3.2). To test the efficiency of RNAi we performed RT-PCR analyses for each gene, which showed that in all instances, the relevant transcription level was significantly reduced throughout the body, including the epidermis (Fig. 3.3). These levels of depletion are consistent with previous RNAi analyses in *Oncopeltus* showing changes in coloration encompassing the entire body (Liu et al., 2014). These findings, combined with an additional RT-PCR result showing a significant reduction in the level of *black* transcripts in all body regions (Fig. 3.4), support the conclusion that observed phenotypes resulted from a systemic response.

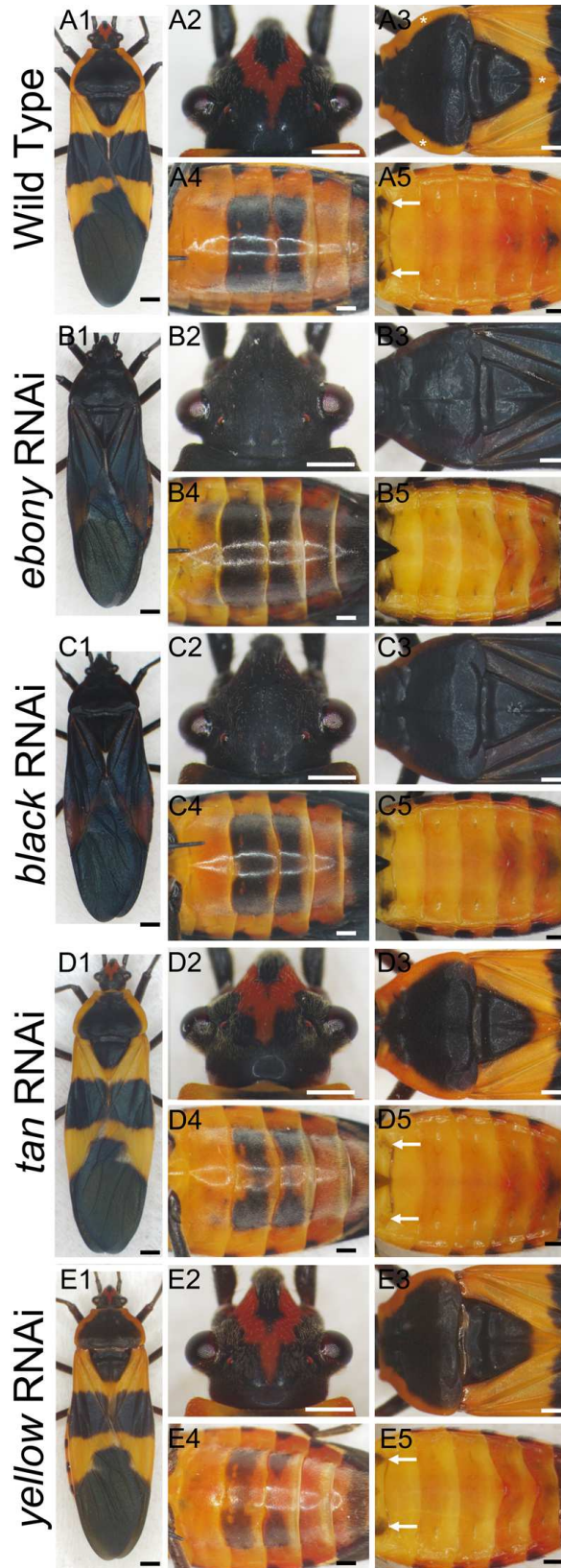


Fig. 3.5. Functions of *ebony*, *black*, *tan*, and *yellow* in different body regions of *Oncopeltus* adults. (A1-A5) Wild type *Oncopeltus* shows alternating black-orange patterning. Black pigmentation is present in the head (A2), thorax (A3), ventral abdomen (A4), and dorsal abdomen (A5). (B1-B5) The *ebony* RNAi adult phenotypes show the expansion of black pigment in the head (B2) and thorax (B3), whereas such an expansion is only moderate in the ventral abdomen (B4) and barely noticeable in dorsal abdomen (B5). (C1-C5) The *black* RNAi adults show a phenotype similar to the *ebony* RNAi individuals described above. (D1-D5) The *tan* RNAi adult phenotypes show a differential defect of black pigment across the body. The defect of black is subtle in the head (D2) and thorax (D3), while it is quite significant in ventral abdomen (D4). Also, on the dorsal A1 segment, the two black patches are lost (arrows, D5). (E1-E5) The *yellow* RNAi adults show varying levels of reduction in black pigment between body regions. Reduction is moderate in the head (E2) and thorax (E3), whereas quite significant in ventral abdomen (E4). The two black patches on the dorsal A1 segment are also significantly reduced (arrows, E5). Scale bars are: 1mm (A1, B1, C1, D1, and E1); 500 μ m (A2-A5, B2-B5, C2-C5, D2-D5, and E2-E5).

Studies in *Drosophila* and *Tribolium* have shown that *ebony* plays the central role in suppressing black pigmentation (Fig. 1.1). Upon the loss of function of *ebony*, a global darkening of body pigmentation was observed in both species (Takahashi et al., 2007; Tomoyasu et al., 2009; Wittkopp et al., 2002). Based upon these observations, we expected *ebony* RNAi *Oncopeltus* adults to exhibit black coloration throughout the body. Among 11 *ebony* RNAi adults, all but one exhibited a significant expansion of black melanization in the anterior body regions. As illustrated in Figs. 3.5B1-B3, all non-black anterior subregions, including the orange V-shape stripe on the head, the lateral edges on T1, and the posterior tip on T2 became black. However, in these 10 individuals, the expansion of black pigmentation was only moderate in posterior body regions. The A3 black rectangle expanded anteriorly into the A2 segment, whereas the A4 rectangle expanded posteriorly into A5 and A6 segments (Fig. 3.5B4). The remainder of the ventral abdomen and the non-black pigmented dorsal abdomen were generally unaltered (Fig. 3.5B5). Therefore, the different outcomes observed between anterior and posterior body regions suggested that while *ebony* was critical for non-

black patches in the head and thorax, it played only a minor role in the majority of non-black regions in the abdomen.

Ebony is the core enzyme in the conversion of dopamine to NBAD, catalyzing the binding of β -alanine to dopamine (Fig. 1.1). Therefore, the synthesis of β -alanine, which is catalyzed by the product of the *black* gene, is also critical for the NBAD branch (Arakane et al., 2009; Wright, 1987). Among 20 *black* RNAi adults, 18 showed an expansion of black coloration in the head and thorax that covered the original orange pigmentation (Figs. 3.5C1-C3). In the ventral abdomen, the effects were highly consistent between these 18 individuals, showing little of the melanin expansion that was observed in *ebony* knockdowns (compare Figs. 3.5C4 vs. B4). The dorsal abdomen and the majority of the non-black portions of the ventral abdomen also remained unchanged (Fig. 3.5C4&C5). These observations showed that *black* was required for the non-black patches in the anterior body regions, but not for the abdomen. Combined with *ebony* RNAi insights, these results establish that suppression of melanin by the NBAD branch is utilized differently between the anterior and posterior body regions of *Oncopeltus*.

While the above results focus on the mechanism that creates non-black subregions, it is equally important to understand the complementary process – the generation of black areas across the insect body. Studies in *Drosophila* have shown that, other than TH (tyrosine hydroxylase) and DDC (dopa decarboxylase) enzymes required for production of DOPA and dopamine, additional promoting enzymes are required for melanization (Jeong et al., 2008; True et al., 2005; Wittkopp et al., 2002; Wright, 1987). One of the essential enzymes is Tan, which counteracts Ebony in the

NBAD branch (Fig. 1.1), thus promoting melanin production (Jeong et al., 2008; True et al., 2005). Functional analyses on *tan* have been reported only in *Drosophila*, which showed that its loss causes a global reduction of melanin patterns (Jeong et al., 2008; True et al., 2005). Out of 37 *tan* RNAi *Oncopeltus* adults, 34 exhibited a consistent phenotype (Fig. 3.5D1). Black patterns in the head and thorax were generally unaltered (Fig. 3.5D2&D3). In contrast, the melanin patterns showed noticeable changes in the abdomen (Figs. 3.5D4 & D5). In particular, the two black spots on the dorsal A1 segment were significantly reduced (arrows in Fig. 3.5D5). The same trend was also observed in the ventral A3-A4, exhibiting a reduction in the middle portion of each black rectangle (Fig. 3.5D4). In 3 individuals the degree of reduction was more pronounced, with either the left or right half of the A4 rectangle disappearing completely. It is worth noting that the intensity of black coloration within the remaining A3 and A4 rectangles was not significantly different compared to wild type (Fig. 3.6; $P > 0.05$). These observations suggest that *tan* is required for proper patterning of black pigmentation in the *Oncopeltus* abdomen, but not for its intensity. Such role of *tan* in abdominal melanin patterning is consistent with previous studies of *Drosophila* species (Jeong et al., 2008; True et al., 2005).

As shown above, the depletions of *ebony*, *black* and *tan* did not affect the majority of the non-black subregions in the abdomen. These observations suggest that the NBAD branch of the melanin pathway is not involved in the generation of these subregions. Another possible candidate is *arylalkylamine N-acetyltransferase (aaNAT)*, which is the core gene in the NADA branch of the melanin pathway (Fig. 1.1). Studies in *Drosophila* have shown that *aaNAT* is responsible for converting dopamine to NADA

as a way of depleting melanin and creating colorless sclerotin (Brodbeck et al., 1998; Hintermann et al., 1995; Wright, 1987). Consistent with this, the depletion of *aaNAT* causes an increase of melanization across the body in *Bombyx* (Zhan et al., 2010). In order to determine if this mechanism can also explain the non-black subregions in the abdomen of *Oncopeltus*, we depleted *aaNAT* in 5th nymphs. The consequent adults, however, showed no effect in color patterns in the head, thorax, or abdomen (Fig. 3.7). This observation indicates that the NADA branch of the melanin pathway is not required for black patterns in these body regions.

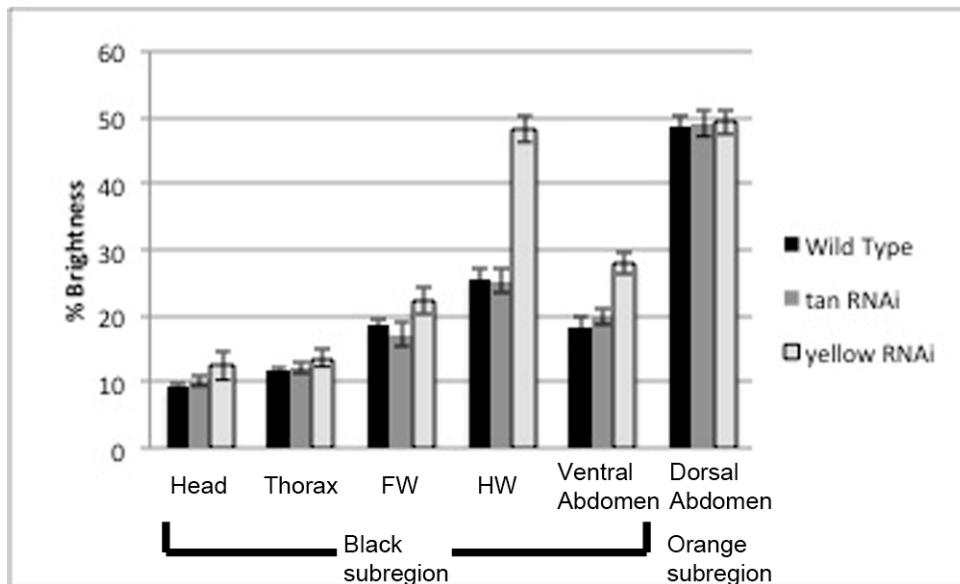


Fig. 3.6. The comparison of black intensity in isolated body regions of wild type, *tan* RNAi and *yellow* RNAi adults. The levels of black in the melanized subregions in the head, thorax, forewing, hindwing, and ventral abdomen are shown in average percent brightness. The error bars are showing the 95% confidence intervals. The depletion of *tan* did not show significant changes in the black intensity in all body regions ($P > 0.05$). The black intensity in *yellow* RNAi is significantly different from that in wild type in all body regions ($P < 0.05$). The amount of reduction in black is most significant in the hindwing and ventral abdomen, whereas it is moderate in the head, thorax, and forewing. In both *tan* RNAi and *yellow* RNAi adults, the brightness of the orange subregions of the dorsal abdomen are not significantly different from those in the wild type ($P > 0.05$). Abbreviations: FW, forewing; HW, hindwing.

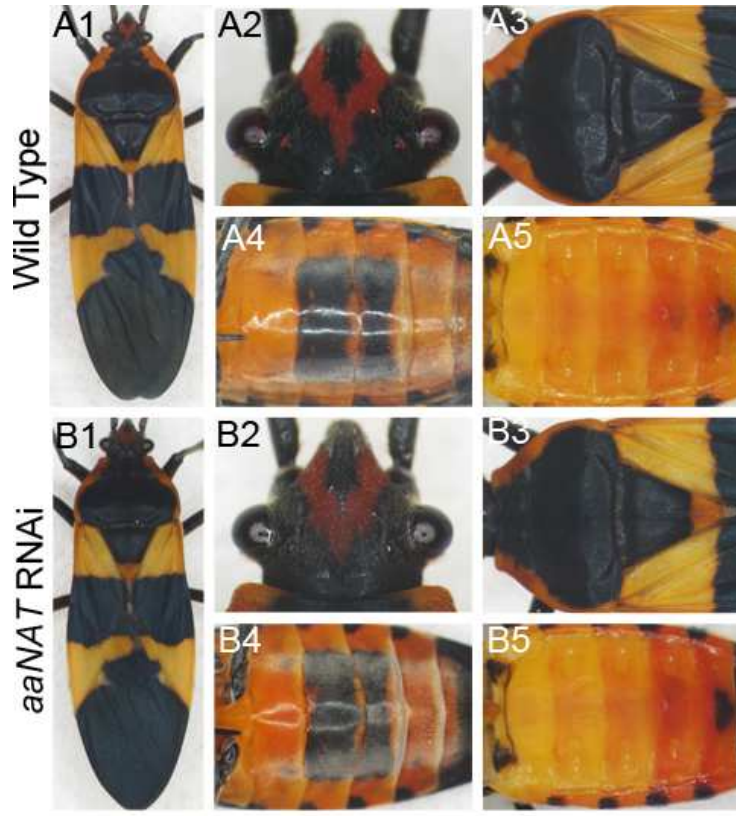


Fig. 3.7. Phenotype of *aaNAT* RNAi in black coloration of *Oncopeltus* body. (A1-A5) Wild type fully-melanized *Oncopeltus* adults establish black pigmentation in the head (A2), thorax (A3), ventral abdomen (A4), and dorsal abdomen (A5). (B1-B5) *aaNAT* RNAi adults showed similar black coloration as wild type, which can be observed in the head (B2), thorax (B3), ventral abdomen (B4) and dorsal abdomen (B5).

In addition to the above four genes within the NBAD and NADA branches, we also tested the function of *yellow*, another important gene that promotes melanin production (Arakane et al., 2010; Jeong et al., 2008; Tomoyasu et al., 2009; Wittkopp et al., 2002; Wright, 1987). Although this gene is not within the NBAD branch, its depletion in *Drosophila* causes a severe reduction of melanization across the whole body (Jeong et al., 2008; Wittkopp et al., 2002). Among the 38 *yellow* RNAi adults, 32 displayed a significant reduction in the intensity of black pigments (Fig. 3.6, $P < 0.05$) in ventral A3 and A4 rectangles (Fig. 3.5E4 & E5). In addition, in 30 out of 32 individuals, a reduction in the middle portions of the A3 and A4 rectangles was also observed (Fig. 3.5E4).

These pigmented phenotypes in the abdomen are similar to those reported in *Drosophila melanogaster* (Jeong et al., 2008; Wittkopp et al., 2002). While abdomens showed an increase in average brightness of 51%, the reduction in black intensity in the head and thorax was more moderate (Fig. 3.5E1-E3), with an increase in average brightness of 28% and 15%, respectively (Fig. 3.6). These findings indicate that *yellow* was involved in regulating both the extent of melanin patterns and their intensity in the abdomen, but had much less effect in thorax and abdomen. Based on results from *yellow* and *tan* RNAi results, we speculate that these “melanin promoting factors” may be critical for the melanin patterns in the posterior body regions.

Distinct black patterns between the forewing (FW) and hindwing (HW) are generated by different branches of the melanin pathway in *Oncopeltus*

The forewing (FW) and hindwing (HW) in *Oncopeltus* also have distinct melanin patterns. The FW has an alternating black and orange pattern (Fig. 3.8A1) whereas the HW is colorless at the proximal end and black throughout the distal region (Fig. 3.8A2). To determine if the NBAD branch regulates the melanin patterns in both pairs of wings, we examined the wings of *ebony* and *black* RNAi adults. In both instances, black pigmentation greatly expanded into the orange subregions on the FW (Fig. 3.8B1&C1). However, the depletion of either gene generated no noticeable changes in color patterns in the HW (Fig 3.8B2&C2). These observations indicate that the NBAD branch was required for repressing melanization in the non-melanized areas on the FW, whereas similar non-melanized regions on the hindwings used a different mechanism.

Candidate genes responsible for suppressing melanization in the proximal HW include the NADA branch of the melanin pathway (Fig. 1.1). Since *aaNAT*, the core

gene within this branch, is reported to be responsible for converting dopamine to colorless NADA sclerotin in *Drosophila* (Brodbeck et al., 1998; Hintermann et al., 1995; Wright, 1987), it is possible that such a mechanism can also generate the colorless pattern in the HW of *Oncopeltus*. To test this hypothesis, we observed the HW coloration in *aaNAT* RNAi adults. In all of the 17 RNAi resulting individuals, the anal lobe region of the HW became melanized (Fig. 3.8D2), whereas the black pigmentation of the FW was not affected (Fig. 3.8D1). These observations indicate that *aaNAT* was involved in suppression of melanin formation in the colorless anal lobe region of the HW. However there was no indication that this role was required for proper pigmentation of the FW. In summary, the *Oncopeltus* FW and HW seem to utilize distinct mechanisms to generate non-black subregions: the NBAD branch is applied to suppress melanization in the orange areas of the FW, whereas the HW employs the NADA branch to generate the colorless anal lobe.

In addition to the melanin suppressing factors *ebony*, *black*, and *aaNAT*, we tested the function of the melanin promoting factors *yellow* and *tan* in the black subregions of *Oncopeltus* wings. In *yellow* RNAi adults there was a significant reduction of black intensity in both pairs of wings (Fig. 3.8E1&E2; Fig. 3.6; $P < 0.05$ in FW and $P \ll 0.05$ in HW). This effect was much greater in the HW (average brightness increased by 89%) than the FW (19%) (Fig. 3.6). In contrast, the depletion of *tan* did not generate any noticeable effect on the black patterns of either the FW or HW (Fig. 3.8F1&F2) nor significant reduction in their black intensity (Fig. 3.6; $P > 0.05$), indicating that this gene was not essential for wing melanin patterns. These observations suggest that the roles in wing melanization are distinct between different melanin promoting

factors: *yellow* is required for the proper intensity of black melanin in the wings, especially the HW, whereas *tan* may not be involved at all in wing pigmentation in *Oncopeltus*.



Fig. 3.8. Functions of *ebony*, *black*, *aaNAT*, *yellow*, and *tan* in the FW and HW of *Oncopeltus* adults. (A1-A2) Pigmentation patterns of wild-type wings. The *ebony* RNAi adults show an expansion of black pigmentation into the orange subregion of the FW (B1), while the HW remains unaffected (B2). (C1&C2) The *black* RNAi adult wings show a similar phenotype to the *ebony* RNAi adults as described above. The *aaNAT* RNAi adult phenotypes show no effect on the FW (D1), while melanization expands into the anal region of the HW (asterisk in D2). The *yellow* RNAi adult wing phenotype shows a reduction of black pigment on the FW (E1) and the HW (E2). The *tan* RNAi adult phenotype shows no noticeable pigmentation effect in the FW and HW. Abbreviations: FW, forewing; HW, hindwing. Scale bars: 1mm.

Differential involvement of pigmentation genes between FW and HW correlates with their expression patterns

Previous studies in the wings of *Drosophila* and *Heliconius* have shown strong correlations between melanin patterns and the expression patterns of melanin genes (Ferguson et al., 2011b; Gompel et al., 2005; Hines et al., 2012; Wittkopp et al., 2002). In particular, such correlations have been seen in the *Drosophila melanogaster* abdomen (Camino et al., 2015; Rebeiz et al., 2009) and FW (Gompel et al., 2005) and occur in diverse *Drosophila* species with divergent patterns of melanic pigmentation (Arnoult et al., 2013; Camino et al., 2015; Ordway et al., 2014; Werner et al., 2010), indicating that these correlations are functionally meaningful. Thus, we hypothesized that the difference in mechanisms regulating non-black patterns between FW (NBAD branch) and HW (NADA branch) comprise differential expression of the relevant core genes. To test this hypothesis, we utilized *in situ* hybridization to detect in developing wing pads of *Oncopeltus* the expression patterns of *ebony* and *aaNAT*, the two essential genes in the NBAD and NADA branches. Note that because the formation of the cuticle precludes the expression analysis later in development (see Materials and Methods), we can only study early stages during which initial patterns are beginning to be laid out and do not fully correspond to the final patterns. As shown in Fig. 3.9A1, *ebony* expression was observed in three distinct patches on the FW: two are located on the anterior and posterior edges of the proximal portion, the other in the middle of the anterior edge. These locations correspond with the anterior and posterior margins of orange subregions on the FW (Fig. 3.8A1). The expression of *ebony* on the HW, however, was not detectable (Fig. 3.9A1), consistent with the fact that *ebony* RNAi displayed no phenotype. On the other hand, *aaNAT* expression was not observed in the FW but was present in the anal lobe region of the HW (Fig. 3.9B1). This expression

pattern of *aaNAT* was strongly correlated with its RNAi phenotype, where the colorless anal lobe region of the HW became melanized (Fig. 3.8A2). Hence, the expression patterns of *ebony* and *aaNAT* correlated with their functions in generating the non-black patches on the FW and HW.

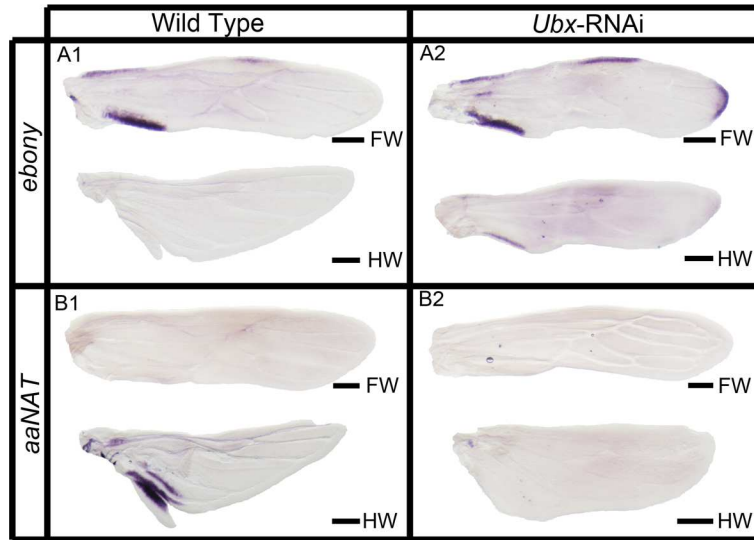


Fig. 3.9. *in situ* hybridization of *ebony* and *aaNAT* in developing wild-type and *Ubx* RNAi *Oncopeltus* wings. (A1) In wild-type wings, *ebony* is expressed exclusively in the FW. (A2) In *Ubx* RNAi wings, the HW exhibits expression of *ebony*. (B1) In wild-type wings, *aaNAT* is expressed only in the HW. (B2) In *Ubx* RNAi wings, *aaNAT* is no longer expressed in the HW. Abbreviations: FW, forewing; HW, hindwing. Scale bars: 200 μ m.

These differences in RNAi phenotypes between FW and HW pigmentation may be explained by the differential activations of *ebony* and *aaNAT*. If so, this regional regulation of melanin genes would require specific selector genes (Wittkopp and Beldade, 2009; Wittkopp et al., 2003). In the butterfly *Junonia coenia*, the Hox gene *Ultrabithorax* (*Ubx*) plays such a role by differential regulation of HW and FW color patterns (Weatherbee et al., 1999). Recently, *Ubx* was shown to also control the identity of HW in *Oncopeltus* (Medved et al., 2015) allowing us to test the generality of the selector genes role in regional regulation. Therefore, upon the depletion of *Ubx*, we

would expect *ebony* to be expressed in the developing HW whereas *aaNAT* should be absent. As shown in Fig. 3.9A2, the HW expresses *ebony* at the proximal margins, which resembles the patterns observed in the wild type FW. However, the expression of *aaNAT* is lost in the HW, even in a moderate phenotype showing an intermediate shape transformation (Fig. 3.9B2). These findings indicate that *Ubx* governs the differential activation of melanin genes between the wings. This further suggests that the different pigmentation roles of melanin genes across different *Oncopeltus* body regions, as shown by the present RNAi analyses, may be due to the functions of other region-specific regulatory genes.

The expression patterns of *black*, *yellow*, and *tan*, however, could not be detected using *in situ* hybridization. Note that the wing tissue is amenable to this procedure only during the middle part of 5th nymphal stage (see Materials and Methods) when these three genes may not be active. To test this possibility, we examined the expression of *black*, *yellow*, and *tan* during the entire 5th nymphal stage (Fig. 3.10). As predicted, expression of these genes was noticeable only during the later half of the stage (Fig. 3.10). These observations suggest that during the development of *Oncopeltus* wings, enzymes such as Ebony and AANAT, which utilize dopamine as direct substrates (Fig. 1.1), perform their patterning roles at early-mid 5th nymphal stage. In contrast, Black, Yellow and Tan are turned on at a later stage.

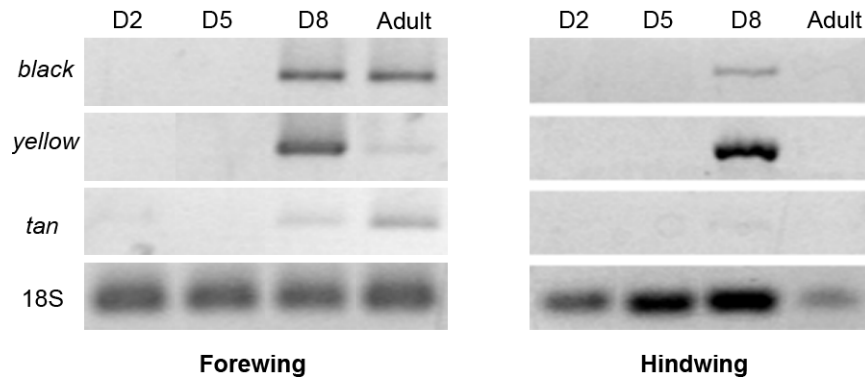


Fig. 3.10. RT-PCR analyses of *black*, *yellow*, and *tan* mRNA in the developing wings of *Oncopeltus* throughout the entire 5th nymphal stage. The chosen time points are: Day2 (initialization of adult melanin cycle), Day5 (formation of wing tissue), Day8 (localization of melanin enzymes), and freshly molted adults (initialization of melanin process). The expression levels of the targeted mRNA are dynamic among these four time points. At Day2 and Day5, none of these three genes were detectable in the wings. Starting by Day8, the expression of *black*, *yellow* and *tan* showed up with different patterns. *black* was expressed in both Day8 and adult forewings. However, its expression in the hindwing was only observed at Day8. The expression of *yellow* was observed in both wings at Day8, which were significantly reduced in the adults. *tan* expression was very low on day 8 in both wings. The expression in the forewing later reached its peak in adult, whereas the hindwing expression was not detected at adult stage.

Discussion

Pigmentation functions of melanin genes in *Oncopeltus*

In this study we performed a comprehensive functional analysis of the putative core melanin genes using RNAi. Although there has been limited success in RNAi silencing by direct body cavity injection in *Drosophila*, this approach has proven to be highly effective in other insects (Li et al., 2015). This is especially the case in *Oncopeltus*, which is characterized by a strong systemic gene depletion upon RNAi treatment (Angelini and Kaufman, 2005; Liu and Kaufman, 2004a, b, 2005). The recent RNAi analysis of the essential enzymes for the production of black melanin in this species also showed a systemic reduction in coloration encompassing the entire body (Liu et al 2014). In the present study, the whole-body RNAi response is documented by

RT-PCR results showing similar reduction in the amount of transcript across different body regions in *black* RNAi individuals (Fig. 3.4). Hence, the observed region-specific effects of RNAi against melanin genes are likely true phenotypes resulting from systemic responses, rather than low penetrance phenotypes. These results suggest distinct regional utilization of melanin genes.

The NBAD branch of the melanin pathway has been reported to be essential for melanin patterning in *Drosophila* (Wittkopp et al., 2002; Wright, 1987). In this pathway, both *black* and *ebony* can suppress melanin formation via the production of β -alanine and NBAD, respectively (Fig. 1.1). In *Oncopeltus*, RNAi knockdown of these two genes causes the non-black subregions to become black in the head (Fig. 3.5B2&C2), thorax (Fig. 3.5B3&C3), and FW (Fig. 3.5B1&C1), whereas a majority of the non-black patches in the HW (Fig. 3.8B2&C2) and abdomen (Figs. 3.5B4-B5 and C4-C5) are not affected. These findings suggest that the melanin suppressing role of *ebony* and *black* is crucial in the head, thorax, and FW, but not necessary for proper coloration in the HW and abdomen. This is in contrast with findings in *Drosophila* and *Tribolium*, where loss of function of either *ebony* or *black* results in an overall darkening of body pigmentation (Arakane et al., 2009; Tomoyasu et al., 2009; Wittkopp et al., 2002; Wright, 1987).

Another gene of the NBAD branch, *tan*, counteracts the function of *ebony* and promotes black pigmentation by converting NBAD back to dopamine (Jeong et al., 2008; True et al., 2005; Wright, 1987). *tan* RNAi phenotypes in *Oncopeltus* indicate that it is essential for the black patterns present in the abdomen (Fig. 3.5D4-D5) but is not a significant player in forming the melanin patterning in the head (Fig. 3.5D2), thorax (Fig. 3.5D3), and wings (Fig. 3.8F1&F2). Again, these results are different from *Drosophila*,

where *tan* mutants display a reduction in melanization spanning the entire body (Jeong et al., 2008; True et al., 2005).

Despite the fact that the reactions catalyzed by *tan* and *ebony* appear as a circuit from the biochemical perspective (Fig. 1.1), in *Oncopeltus* they are employed differently in distinct body regions. It is possible that in hemimetabolous insects, only half of this circuit is essential for melanization in one specific body region, whereas the other half might be active but not required for pigmentation. Instead, they might be involved in other biological processes such as behavior (Wittkopp and Beldade, 2009). Subsequently, in more derived groups such as dipterans, the entire *tan-ebony* circuit (both reactions) are fully involved in melanization (True et al., 2005). Extending future studies of *tan* to additional hemimetabolous species may show how the NBAD branch of the melanin pathway has changed during insect evolution.

Finally, the NADA branch can also suppress melanin production by transforming dopamine to NADA, thus creating colorless tissue (Wright, 1987). The key gene in this pathway is *aaNAT* (Brodbeck et al., 1998; Hintermann et al., 1995; Wright, 1987). Here, we observed that the role of *aaNAT* is restricted to the anal lobe region of the HW (Fig. 3.8D2), which correlates with its expression profile (Fig. 3.9B1). This observation is in contrast to the depletion of *aaNAT* in the silk worm *Bombyx*, which causes a global darkening of the adult body (Osanai-Futahashi et al., 2012; Zhan et al., 2010). Thus, *Oncopeltus* appears to preferentially activate *aaNAT* expression in wings to create the colorless tissue in the anal lobe region. It is worth noting that *aaNAT* may not be the only gene used in this region because the anterior portion of the proximal half of the HW remains colorless when *aaNAT* is depleted by RNAi (Fig. 3.8D2). Future studies will

need to assess whether other members of the AANAT family are involved in generating colorless patches in this region (Long et al., 2015; Mehere et al., 2011).

The pigmented phenotypes of *yellow* have been reported in both *Drosophila* and *Tribolium*, with distinct results. Loss of *yellow* causes global reduction of melanin in *Drosophila* (Wittkopp et al., 2002), whereas only the HW is affected in *Tribolium* (Arakane et al., 2010; Tomoyasu et al., 2009). In *Oncopeltus*, *yellow* RNAi adults display a mix of features previously observed in *Drosophila* and *Tribolium*: black coloration in the abdomen and HW are greatly reduced but other body regions are only moderately affected (Fig. 3.6). Therefore, the restriction of *yellow* function appears to have changed during insect evolution. At present, we cannot rule out the possibility that in regions where *yellow* RNAi was observed to have a moderate effect, other *yellow* family members might play additional roles in melanization (Han et al., 2002). However, currently the functional roles of most of the *yellow* family genes are yet to be determined. Even for the *yellow* gene itself, despite the fact that it is known to be required for melanization in *Drosophila* and *Tribolium* (Arakane et al., 2010; Bray et al., 2014; Jeong et al., 2008; Tomoyasu et al., 2009; Wittkopp et al., 2002; Wright, 1987), its enzymatic activity has not yet been established. In terms of the position of *yellow* in the melanin pathway, two different hypotheses have been proposed (Fig. 1.1): it may be essential for the production of either DOPA melanin (Walter et al., 1996; Wright, 1987) or dopamine melanin (Wittkopp et al., 2003; Wittkopp et al., 2002). Our present results and another recent report (Liu et al., 2014) show that black pigment in the HW is dopamine melanin, suggesting that *yellow* may be involved only in dopamine melanin production.

Overall, our results show that the pigmentation functions of the five genes under study are regionalized in *Oncopeltus*. This is in contrast with previous studies in *Drosophila*, *Tribolium* and *Bombyx*, where the depletion of *ebony*, *black*, *tan*, *aaNAT*, or *yellow* resulted in alteration of melanin patches throughout the body (Arakane et al., 2009; Gibert et al., 2007; Jeong et al., 2008; Osanai-Futahashi et al., 2012; Tomoyasu et al., 2009; True et al., 2005; Walter et al., 1996; Wittkopp et al., 2002; Wright, 1987; Zhan et al., 2010). Hence, the insight from *Oncopeltus* is that the entire melanin pathway can be split into different sections that are utilized in different body regions.

In the present study, the regional patterns of melanin genes are observed from analyses at a whole-body scale. To obtain a deeper comprehension of how complex melanin patterns are generated will require analyzing pigmentation genes at a finer morphological scale (such as a subregion of a segment). Classical studies in *Drosophila* have shown that selector genes involved in a general anterior-posterior axis determination, such as *hedgehog* (*hh*), *engrailed* (*en*), and *optomotor-blind* (*omb*), also regulate melanin patterning in the abdominal segments (Kopp and Duncan, 1997; Kopp et al., 1997). It is tempting to speculate that similar mechanisms may account for the presence of centrally positioned black rectangles on A3 and A4 segments in *Oncopeltus*. Also, other axis determination mechanisms, especially medial-lateral, may also be involved in generating the black spots located on the lateral edges of each abdominal segment (Fig. 3.5A5). Furthermore, it is interesting to note that *hh* and *en* regulate melanin genes in a cell-autonomous manner in *Drosophila* (Kopp et al., 1997). In contrast, melanin genes themselves can function non-autonomously, semi-autonomously, or autonomously in different body regions (Borycz et al., 2002; Hanna,

1953; Hotta and Benzer, 1970; True et al., 2005; Wittkopp et al., 2002). At present, we do not know if such region-specific cell autonomy of melanin genes may also account for production of regional color patterns observed in *Oncopeltus*. Extending future studies in this direction will be required to gain a better understanding of the regulatory mechanisms that generate species-specific melanin patterns in insects in general.

Region-specific employment of melanin genes

To better understand the regional utilization of melanin genes, we provide a summary of the general principles that appear to guide melanin patterning (Fig. 3.11). In this summary we refer to a putative case as the “preliminary background”, in which only the basic enzymes required for melanin production, such as TH and DDC, would be active. In other words, none of the melanin promoting or suppressing factors function in such a background. Under the first scenario, the “painting” mode would be utilized in a body region that lacks melanin patterns, such as the *Oncopeltus* abdomen that is predominantly orange. The preliminary background in this case would be non-melanin, as most of the abdomen may not be capable of producing black pigments. The dark melanin is “painted” onto specific areas of this background, which requires melanin promoting factors (*tan* and *yellow*) to ensure the proper boundary and intensity of black patterns. Under a second scenario, the “erasing” mode would apply to a body region where dark melanin is the predominant pigment (as observed in the head, thorax, and FW in *Oncopeltus*, as well as the body and wings of *Periplaneta*). In this instance, the preliminary background would be fully melanized and the melanin suppressors such as *ebony*, *black* and *aaNAT* are utilized for “erasing” melanin production in a specific area or for lowering the overall melanin intensity. In addition to situations where one of these

two modes is utilized exclusively, there are also regions in which the melanin promoting factors and suppressors can both play active roles, such as the HW in *Oncopeltus* where melanin and non-melanin subregions are equally distributed. Under this scenario, the preliminary background is defined as a region undergoing melanization but lacking a proper level of intensity. Finalizing the melanin patterns requires both the melanin-suppressing factor (*aaNAT*), which generates the non-melanin patches, and the melanin-promoting factor (*yellow*), which intensifies the dark color within melanin patches.

In terms of their generality, these three scenarios can account for most of the functional results in the previously studied species. The painting mode may be evidenced in the dark-colored pterostigma on the HW of *Tribolium*. In that study, this specific black pattern becomes lighter in *yellow* RNAi individuals, whereas *ebony* RNAi has no effect on the flanking non-black subregions (Arakane et al., 2010; Tomoyasu et al., 2009). The erasing mode may be evidenced in the butterfly *Papilio*, where the default fully melanized FW was observed in *ebony* mutant adults (Koch et al., 2000). Another example is the depletion of *ebony* or *black* in *Tribolium*, which results in the general blackening of the whole body (Arakane et al., 2009; Tomoyasu et al., 2009). In addition to present results in *Oncopeltus*, the mixed mode has only been fully confirmed in *Drosophila melanogaster*, where functional analyses revealed that *ebony* and *yellow* contribute equally to both wing and body pigmentation (Gompel et al., 2005; Wittkopp et al., 2002). In general, our summary of the principles of melanin patterning can serve as a practical framework explaining the diversity in melanin coloration observed in previously reported insects. A broader taxonomic sampling in basal groups, from which

we can infer the ancestral melanin patterning, will be required to examine if this framework can be applied to a wider range of insect species.

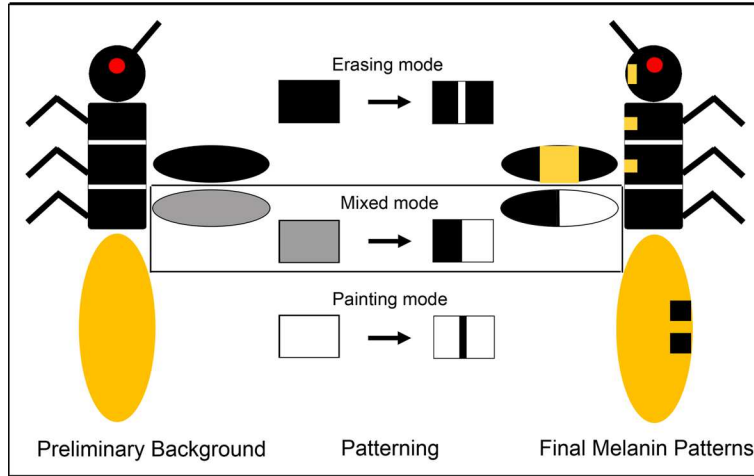


Fig. 3.11. Three proposed modes of insect melanin patterning, as illustrated by pigmentation in *Oncopeltus*. The final melanin patterns (right) are generated from the preliminary background (left) via different modes of melanin patterning. In the head, thorax, and forewing, where the background is fully black, the non-melanin patches are generated by “erasing” the background. In the abdomen where the background is non-black, the melanin patches are “painted” onto the background. A mixture of these two modes may be used in the hindwing, in which black is intensified in the melanin subregions, whereas melanin is suppressed in the non-black subregions.

Acknowledgment

We thank Victor Medved for help with cloning gene fragments in *Oncopeltus*. We also thank Mark VanBerkum, Patricia Wittkopp, William Branford, and two anonymous reviewers for helpful comments that greatly improved this manuscript. This work was supported in part by NIH grant GM071927 to A.P. and WSU Rumble Fellowship to J. L. J.H.M.’s participation was facilitated by NSF grants IOS-0950416 and IOS-1354667 and a HITS grant from the Huck Institutes of the Life Sciences.

CHAPTER 4 PIGMENTATION PATHWAYS UNDERLYING ORANGE COLORATION IN INSECTS

Introduction

Pigmentation is one of the most variable traits of insect morphology, and is frequently involved in establishing the species-specific differences. As such, studies of pigmentation have provided important insights into diverse biological processes, including sexual selection, photoprotection and predator avoidance (Wittkopp and Beldade, 2009). While there are many different types of pigments, the three that are most common are melanin, ommochrome, and pteridine (Kato et al., 2006). Among these three, melanin is the best studied and is responsible in generating black and brown colorations (Arakane et al., 2009; Arakane et al., 2005; Liu et al., 2014; Tomoyasu et al., 2009; True et al., 1999; Walter et al., 1996; Wittkopp et al., 2002; Wright, 1987; Zhan et al., 2010). Mechanistically, melanin is processed by incorporating pigment molecules into the cuticle overlying the epidermal cells (Wittkopp and Beldade, 2009). In contrast, the ommochrome and pteridine pigments are deposited in granules that are stored in specific cells (Ziegler, 1961). While these two pigments have been mainly associated with eye coloration in *Drosophila* (Ewart and Howells, 1998; Linzen, 1974; Summers et al., 1982; Ziegler and Harmsen, 1970), their presence have also been detected in other body tissues and organs by biochemical detection and expression studies (Futahashi et al., 2012; Gao et al., 2013; Kato et al., 2006; Morehouse et al., 2007; Nijhout, 1997; Reed and Nagy, 2005). Currently, though, no functional studies have established the pigmentation roles of either of these pathways at a whole body scale level. Furthermore, pigmentation studies in model systems have focused primarily on variation in a single pigmentation pathway. With a

large number of species displaying a combination of various color patterns, comprehensive studies featuring multiple pathways are essential to further understand mechanisms generating the great diversity in pigmentation that is observed in nature.

Here, we performed the functional analyses on both the ommochrome and pteridine pathways in the hemipteran *Oncopeltus fasciatus* to examine their functions in overall pigmentation. This species is ideally suited for such a study due to its striking orange aposematic coloration that model species such as *Drosophila* or *Tribolium* are lacking. By depleting the functions of the core genes in the ommochrome (*vermillion*, *cinnabar*, and *scarlet*; Fig. 1.2) (Reed and Nagy, 2005) and pteridine pathways (*Punch*, *purple*, *white*, and *brown*; Fig. 1.2)(Ewart and Howells, 1998; Kim et al., 2013), we found that each pathway is utilized in different body regions at different developmental stages. The ommochrome pathway is functioning exclusive in the eye coloration during post-embryonic development. In contrast, pteridine pathway is essential for both eye and body coloration starting from the embryonic stage, with a subsequent recruitment in the forewings. The establishment of pteridine coloration occurs immediately after the melanization of cuticle, which overlies the pteridine pigments to form the final orange/black color patterns of *Oncopeltus*. These findings highlight the fundamental principles of coordinating multiple pigmentation mechanisms in a single species: stepwise formation of multi-layer colorations. This insight can be generally applied to a wide range of species, providing a better understanding on the extraordinary diversity in insect color patterns observed in nature.

Materials and Methods

Cloning and Sequence Analysis of cDNA Fragments

Total RNA was extracted from mixed stages of *Oncopeltus fasciatus* embryos. This procedure, as well as the following cDNA generation, nested RT-PCR and cloning were performed regarding to Liu et al. (2016). One or two reactions of PCR were performed to amplify the gene fragments. The primers used for PCR cloning, as well as the lengths of the resulting cDNA fragments, are listed in Table 4.1. The orthologies of these fragments were confirmed by phylogenetic analysis (Fig. 4.1).

RNA interference (RNAi)

Preparation and injection of dsRNA were carried out following Liu et al (2016). For *Punch*, dsRNA was injected into early 5th nymphs due to the fact that injection carried out before this stage is causes failure in molting. For *vermilion*, *cinnabar*, *scarlet*, *purple*, *white*, *brown* and *eya*, dsRNA was injected consecutively in both 4th and 5th nymphal stages. For *vermilion* RNAi, 35 nymphs were injected and 22 successfully molted into adults. For *cinnabar* RNAi, 40 nymphs were injected and 30 molted to adults. For *scarlet* RNAi, 40 nymphs were injected and 30 molted to adults. For *Punch* RNAi, 45 nymphs were injected and 33 molted to adults. For *purple* RNAi, 40 nymphs were injected and 34 molted to adults. For *white* RNAi. 35 nymphs were injected and 30 molted into adults. For *brown* RNAi. 25 nymphs were injected and all molted to adults. For *eya* RNAi, 20 nymphs were injected and 13 molted into adults.

Maternal RNAi was carried out following Chesebro et al. (2009). Double-stranded RNA of *Punch* and *vermilion* was injected into the abdomen of adult *Oncopeltus* females. These females were reared in separate containers with a single male. Eggs clutches were collected on a daily basis and allowed to develop at room

temperature. In total, 643 *vermillion* RNAi 1st nymphs and 791 *Punch* RNAi embryos were observed.

	Primers for PCR cloning	Primers for RT-PCR	Length of fragment
<i>Of-vermillion</i>	Forward: 5' GCAGATCTTCCGAGATCCAG 3' Reverse: 5' CCTGATGAACCTCTGTCC 3'	Forward: 5' TGAGCGACAACTCTGGATG 3' Reverse: 5' GGCACCTTGAAATGCTTTGT 3'	967 bp
<i>Of-cinnabar</i>	Forward: 5' GCCCAGAGGTCACCTTATGC 3' Reverse: 5' CAAAACCGAGTCTTGCCATT 3'	Forward: 5' TGAGAAGACAGGAACCGTTGT 3' Reverse: 5' GGCAGCCAATATTGTGGAAT 3'	616 bp
<i>Of-scarlet</i>	Forward: 5' TCTGGCTCAACTTCAGGAT 3' Reverse: 5' CCACAAGCTGATGAAACCAA 3'	Forward: 5' AGGTGCAGTGGAAATCAGGAC 3' Reverse: 5' TGGAAAATGCAAACACGGTA 3'	1516 bp
<i>Of-Punch</i>	Forward: 5' GGGCACTCCTAAGACCCCTA 3' 5' TCCAGGGAGTCAAATGGAG 3' Reverse: 5' TCCCTTGTCTTTGGGTCATC 3' 5' CTGAAGACCCCAAGCATTGT 3'	Forward: 5' TCCAGGGAGTCAAATGGAG 3' Reverse: 5' CTGAAGACCCCAAGCATTGT 3'	628 bp
<i>Of-purple</i>	Forward: 5' TCCTTACCTATTGCATACCTCCA 3' Reverse: 5' TAAAGCAAGCTTGGGTCCTC 3'	Forward: 5' CATAGCCCTCATTGGGAGA 3' Reverse: 5' CTGTGGTGCTCACAAATCC 3'	356 bp
<i>Of-white</i>	Forward: 5' GGCAAACCACTACTGAA 3' Reverse: 5' AGGGCTTCATCCCGTACTT 3'	Forward: 5' GCCAACATCTGGATTGGACT 3' Reverse: 5' TGTCAGTCCGGTACATTCCA 3'	1470 bp
<i>Of-brown</i>	Forward: 5' TGTGATGAGCCTACGACAGG 3' 5' CACCAGCCAACCTCAGGAAT 3' Reverse: 5' GCCAGCCAAGAAGATCATA 3' 5' TCAAAGCGTTCATCACAAGG 3'	Forward: 5' CACCAGCCAACCTCAGGAAT 3' Reverse: 5' TCAAAGCGTTCATCACAAGG 3'	1082 bp
<i>Of-eya</i>	Forward: 5' AGCTTGCTCACTGGCTCCTA 3' Reverse: 5' TGTGAAGAGACTCGCCAGAA 3'	Forward: 5' CCAGGTGCACATAGATGACG 3' Reverse: 5' ACGGGAAATTCATCTGCTTG 3'	704 bp

Table 4.1. Primers for RT-PCR and the lengths of the obtained cDNA fragments of *Oncopeltus* genes. Abbreviations: *Of*, *Oncopeltus fasciatus*.

Method: Neighbor Joining; Bootstrap (500 reps); tie breaking = Systematic
 Distance: Poisson-correction
 Gaps distributed proportionally

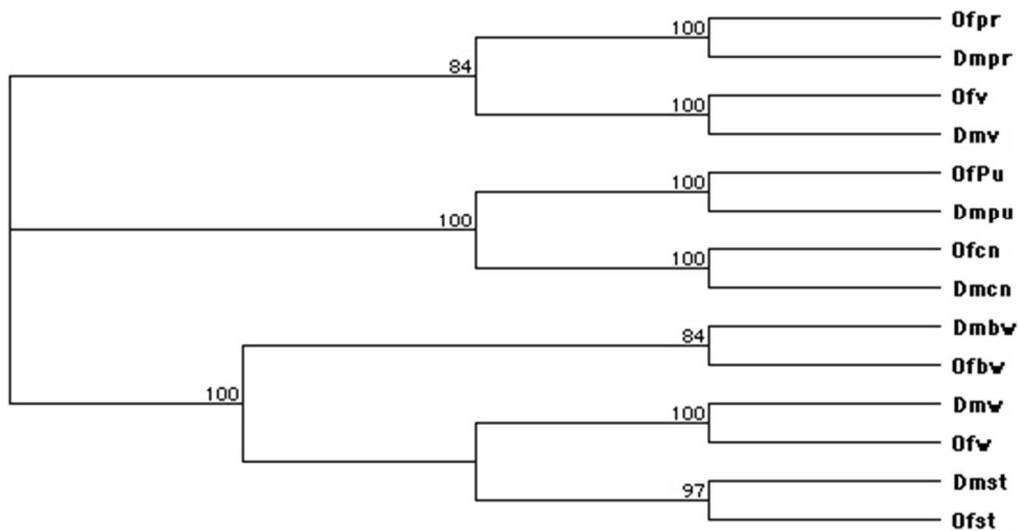


Fig. 4.1. Phylogenetic analysis of ommochrome and pteridine pathway genes in *Drosophila melanogaster* and *Oncopeltus fasciatus*. Phylogeny carried out using the Neighbor-Joining method based on amino acid sequences. Abbreviations: *Of*, *Oncopeltus fasciatus*; *Dm*, *Drosophila melanogaster*; *v*, *vermillion*; *cn*, *cinnabar*; *st*, *scarlet*; *Pu*, *Punch*; *pr*, *purple*; *w*, *white*; *bw*, *brown*.

Image Processing

Microscopy images were taken with SZX16 Microscope (Olympus) and DP72 camera (Olympus). To minimize the possible variation in the captured images, all of the microscope and camera settings were standardized: the images under a particular magnification were taken under the same light condition, aperture, exposure time, and white balance.

RT-PCR Analysis

Independent RT-PCR analyses on *vermillion*, *cinnabar*, *scarlet*, *punch*, *purple*, *white*, *brown* and *eya* were performed to determine the efficiency of our RNAi approach (Fig. 4.2). Preparation of total RNA and cDNA were following Liu et al (2016). Primers used for RT-PCR are listed in Table 4.1. In addition, complementary RT-PCR analyses

on *Punch* and *vermillion* were performed on embryos from mixed stages (Fig. 4.3), which was carried out following Chesebro et al. (2009).

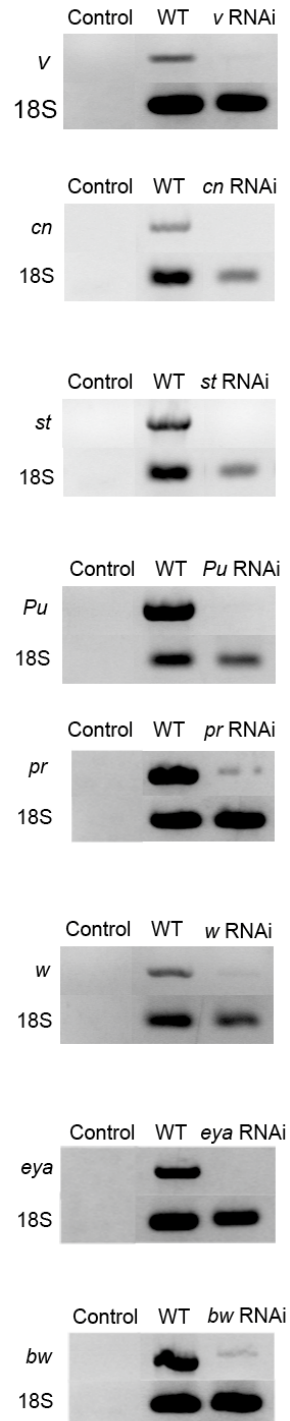


Fig. 4.2. RT-PCR analysis of RNAi depletion of targeted genes in 5th nymphs of *Oncopeltus*. In all instances, the transcription levels of targeted genes are significantly reduced when compared to wild types.

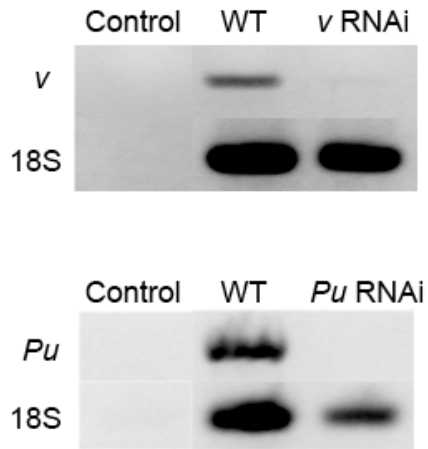


Fig. 4.3. RT-PCR analysis of embryonic RNAi against *vermillion* (*v*) and *Punch* (*Pu*) in *Oncopeltus*.

Results

Pigmentation functions of ommochrome genes in the eyes of adult *Oncopeltus*

Unlike holometabolous insects such as *Drosophila* and *Tribolium*, where the adult eyes develop from imaginal discs during the pupal stage, hemimetabolous species such as *Oncopeltus* exhibit a gradual eye development. The compound eyes are first formed in the first instar nymphs and are much smaller compared to the adult eyes. At each subsequent nymphal stage, newly formed ommatidia are added into the medial margin of the old eye, which, in turn, increases the overall size of the eyes progressively. Therefore, the adult compound eyes are composed of old ommatidia (formed prior to the last nymphal stage) together with the newly formed ommatidia (Fig. 4.4A). This phenomenon has been reported previously in the grasshopper, *Schistocerca americana*, which showed that the depletion of eye genes causes defects only in the newly formed ommatidia located at the medial margin of the eyes (Dong and

Friedrich, 2005, 2010). Based upon this insight, if a gene is required for eye coloration in *Oncopeltus* adults, knocking down its function in the last nymphal stage would result in color changes in the newly formed medial region of the consequent adult eyes.

The ommochrome pathway is best known for its role in the eye coloration (Beard et al., 1995; Dong and Friedrich, 2005; Dustmann, 1968; Lorenzen et al., 2002; Moraes et al., 2005; Quan et al., 2002; Sethuraman and O'Brochta, 2005; Summers et al., 1982). Functional analyses have shown that the depletion of essential ommochrome genes results in loss or reduction of eye coloration (Dong and Friedrich, 2005; Grubbs et al., 2015; Lorenzen et al., 2002; Summers et al., 1982). To determine if and to what degree this pathway is involved in the dark red color in *Oncopeltus* eyes, we performed RNAi analyses targeting three principle genes in the ommochrome pathway: *vermilion*, *cinnabar*, and *scarlet* (Summers et al., 1982). As illustrated in Fig. 4.4, the resulting *vermilion*, *cinnabar* and *scarlet* RNAi adults all display similar phenotypes. The coloration of the newly formed ommatidia showed a significant reduction in coloration, which turned into bright red (Figs 4.4C~4.4E, compare to 4.4B). Such change in color observed in the freshly molted adults (Figs. 4.4C1, D1&E1), still persist after 24 hours, when these adults became fully melanized (Figs. 4.4C2, D2&E2). The observed changes in coloration are consistent with the observations in *Drosophila* eyes with mutation in ommochrome genes (Summers et al., 1982), indicating that the role of ommochrome pathway in eye coloration is consistent between *Drosophila* and *Oncopeltus*.

Pigmentation functions of pteridine genes in the eyes of adult *Oncopeltus*

In the RNAi assays described above, the depletion of ommochrome pathway could not eliminate the coloration in the newly formed ommatidia, suggesting that other pathways are also involved in eye coloration of *Oncopeltus*. The top candidate mechanism is the pteridine pathway, which also contributes to eye pigmentation in *Drosophila* (Summers et al., 1982; Ziegler and Harmsen, 1970). More specifically, the pteridine pathway produces red pigments, which co-exist with the brown pigments produced by the ommochrome pathway thus forming the normal dark red eye coloration in flies (Summers et al., 1982; Ziegler and Harmsen, 1970). Although classical *Oncopeltus* studies from 50 years ago suggested that both ommochrome and pteridine pathways contribute to eye coloration (Lawrence, 1970), this hypothesis has never been formally tested. This was likely due to the fact that majority of the pteridine pathway is still unknown, with the exception of few essential genes, including *Punch*, *purple*, *brown*, and *white* (Ewart and Howells, 1998; Kim et al., 2013). The former two genes govern the initial reactions of this pathway whereas the latter two are required for the assembly of pteridine granules (Ewart and Howells, 1998; Kim et al., 2013). To determine the roles of pteridine pathway in the eye coloration of *Oncopeltus*, we performed RNAi analyses targeting these four putative genes and observed their adult phenotypes. As illustrated in Fig. 4.4, in *Punch* and *purple* RNAi adults, no significant color change can be observed in the eyes (Figs 4.4F1&F2, 4.4G1&G2). These results indicate that the genes governing the initial reactions of the pteridine pathway, such as *Punch* and *purple*, are not required for adult eye pigmentation. Similar phenotype was also observed in *brown* RNAi adults (Fig. 4.5). In contrast, with the depletion of *white*, the newly formed eye region showed reduction in color, which turns light brown in the fresh

adults (Fig. 4.4H1). While this brown colored region became darker after melanization, it did not reach the same intensity observed in *Punch* and *purple* RNAi individuals (compare Fig. 4.4H2 to F2 or G2). Such reduction in color is consistent with previous observations in *Oncopeltus* mutants with the loss of pteridine pigments (Lawrence, 1970). Taken together, our findings indicate that in *Oncopeltus* adults, proper establishment of eye coloration only requires the low hierarchical portion of the pteridine pathway.

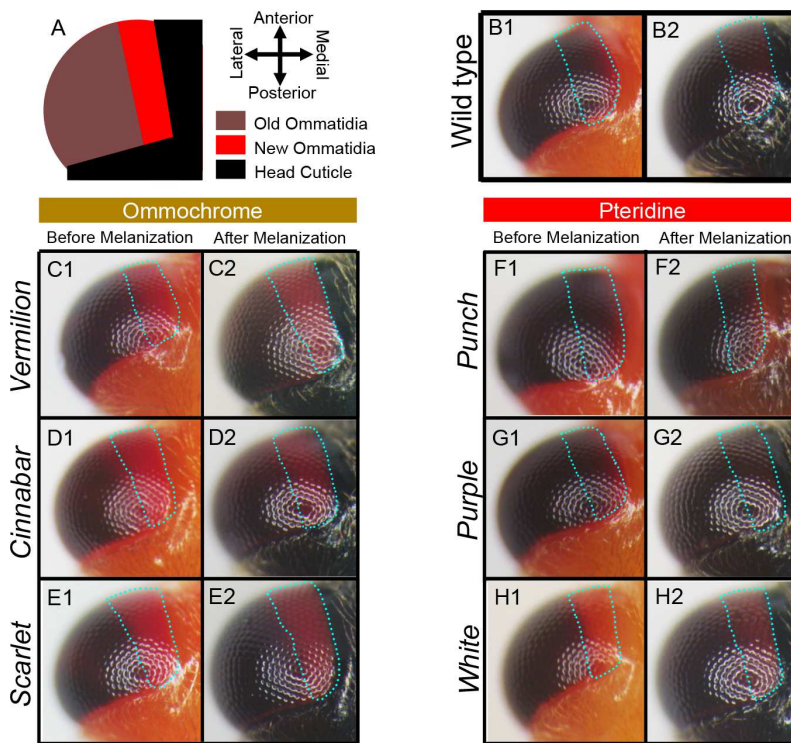


Fig. 4.4. Functions of ommochrome and pteridine genes in the coloration of adult eyes in *Oncopeltus*. (A) The adult eyes of *Oncopeltus* are composed of old ommatidia formed prior to 5th nymphs (dark red), and newly formed ommatidia developed during the 5th nymphal stage (bright red). (B1-B2) Wild type *Oncopeltus* adult eyes shown as before melanization (B1) and after melanization (B2). Newly formed ommatidia are outlined. (C1-C2) *vermillion* RNAi adults establish bright red in the newly formed eye region. (D1-D2) *cinnabar* RNAi adults showed similar red color phenotype in the newly formed ommatidia. (E1-E2) *scarlet* RNAi adults also showed red color phenotype in the newly formed eye region. (F1-F2) Eye coloration in *Punch* RNAi adults was similar to wild type. (G1-G2) In *purple* RNAi adults, coloration of the newly formed ommatidia appear to be wild type. (H1-H2) In *white* RNAi adults, the newly formed ommatidia was

changed to brown. The brown coloration is bright in the pre-melanization eyes (H1), which became dark in the fully melanized adults (H2).

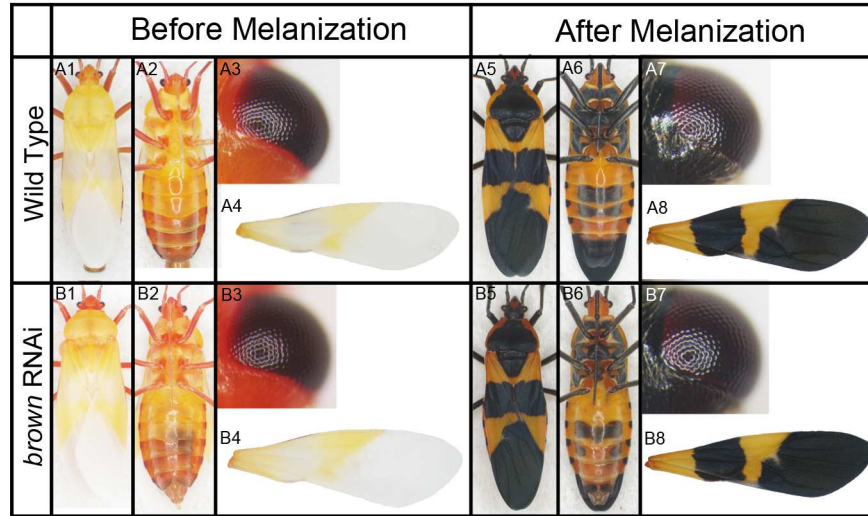


Fig. 4.5. *brown* RNAi does not reduce the eye coloration or the orange coloration in the body and forewing. The wild type coloration is shown as before melanization (A1-A4) and after melanization (A5-A8). Upon depletion of *brown*, the eye and body orange colorations appear identical to those in wild type (B1-B8).

Pigmentation functions of ommochrome and pteridine genes in the forewings of adult *Oncopeltus*

The orange warning coloration in *Oncopeltus* is formed before melanization occurs (Figs. 4.6A1). This is most apparent in the forewing (FW) featuring two orange patches: one in the proximal region and another in the middle of the wing (Fig. 4.6A1). These patches darken throughout the melanization process, reaching their full intensity of orange coloration only upon the completion of melanization (Fig. 4.6A2).

If the ommochrome and pteridine pathways are involved in these orange pigments, we expect to observe a reduction in orange coloration in the relevant RNAi adults. As illustrated in Fig 4.6, in adults with depleted ommochrome genes, the orange patches on the FW remain identical to those in wild type, both before and after melanization (Figs. 4.6B~D, 4.7). These findings establish that ommochrome pathway

does not contribute to the orange coloration in FW of *Oncopeltus*. In contrast, in adults with RNAi against pteridine genes including *Punch*, *purple* and *white*, we observe a severe reduction in orange coloration in the pre-melanization FWs (Fig. 4.6E1, F1&G1). This result indicates that these orange patches are produced via the pteridine pathway. However, this phenomenon was not observed in *brown* RNAi adults, suggesting that *brown* might not be involved in pteridine coloration in *Oncopeltus* (Fig. 4.5, 4.7). After melanization, the RNAi of pteridine genes resulted in different coloration effects. In *Punch* RNAi FW, in addition to the reduction of orange coloration, we also observed a great reduction in black coloration, indicating that *Punch* is also required for proper melanization (Fig. 4.6E2). This is likely due to the fact that *Punch* is critical for the production of an essential cofactor of tyrosine hydroxylase (TH), the initializing enzyme of the melanin pathway (Chen et al., 2015; Kato et al., 2006). Similar defects were not observed in *purple* and *white* RNAi adults. Instead, the black melanin regions in the FWs of these adults were similar to wild type (Figs. 4.6F2&G2), suggesting that *purple* and *white* are not essential for melanization. At the same time, the orange patches in these FWs became light yellowish, displaying significantly lighter coloration than wild type (Figs. 4.6F2&G2, 4.7). Such reduction in color intensity may be due to the absence of pteridine pigments, as shown by the pre-melanized wings (Figs. 4.6F1&G1). Under such circumstances, the remaining light yellow pigments, which are established after melanization process, are likely to be produced by the melanin pathway as was suggested by previous observations in *Oncopeltus* (Liu et al., 2014). This further corroborates the idea that orange coloration in *Oncopeltus* FW requires input from two distinct pigmentation mechanisms: the pteridine pathway and melanin pathway.

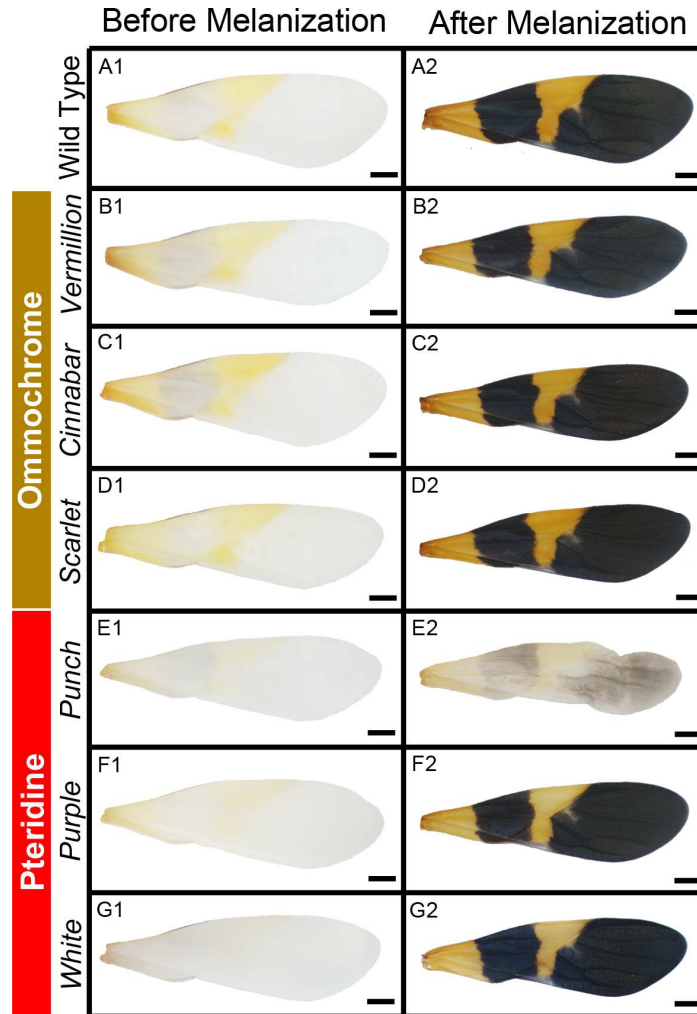


Fig. 4.6. Functions of ommochrome and pteridine genes in the orange coloration of adult forewings (FW). (A1) Orange patterns are visible in the FW. (A2) After melanization, the orange coloration becomes darker. (B1-B2) The orange coloration in *vermillion* RNAi FW was similar to the wild type. (C1-C2) The FW coloration in *cinnabar* RNAi appeared identical to wild type. (D1-D2) The orange coloration in *scarlet* RNAi FW did not establish noticeable difference from those in wild type adults. (E1-E2) The orange coloration was significantly reduced in *Punch* RNAi FW. Also, the melanization is reduced in these wings as well (E2). (F1) The initial orange coloration in the pre-melanization FW is significantly reduced upon depletion of *purple*. (F2) The orange patches in the FW became yellowish in the fully melanized *purple* RNAi adults. (G1) The orange coloration were significantly reduced in *white* RNAi FW prior to melanization. (G2) In fully melanized *white* RNAi adults, the FW orange coloration became light yellow.

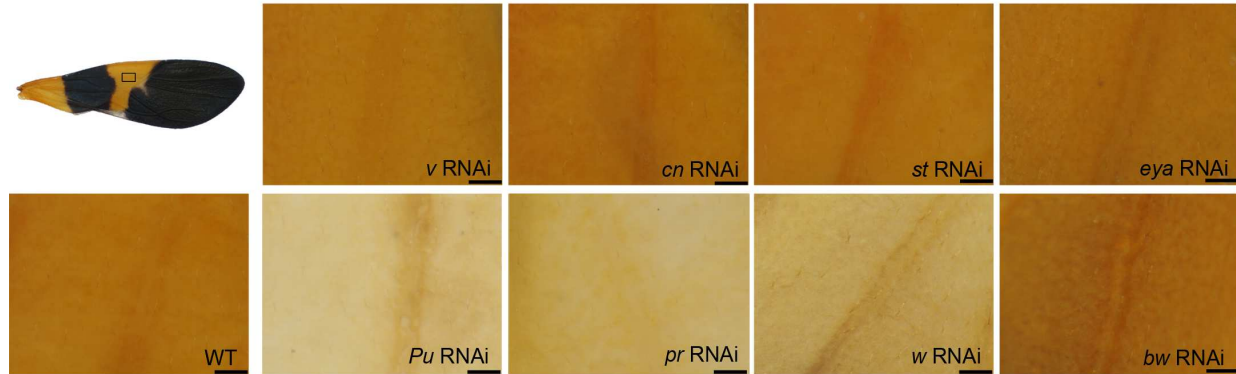


Fig. 4.7. The magnified views of the orange subregions surrounding the medial veins of the forewing. Only the depletion of *Punch*, *purple* and *white* caused a significant reduction in orange coloration.

***eya* is not a candidate gene for controlling fore wing pigmentation**

Our previous assays have already shown that the pteridine pigment is present in both eyes and wings in *Oncopeltus*. It is possible that the wing orange patches are regulated by the co-option of eye development network, which was proposed to have occurred in lepidopterans (Monteiro, 2012). This hypothesis postulates that, at least one of the retinal determination (RD) genes (*eyeless*, *twin of eyeless*, *eyes absent*, *sine oculis*, *dachsous* and *optix*; Fig. 4.8) would also be expressed in the developing wings. By analyzing a recently published wing transcriptome of *Oncopeltus* (Medved et al., 2015), the gene at the top hierarchical position of the RD network that we could find is *eyes absent* (*eya*), whereas the transcripts of *eyeless*, *twin of eyeless*, *sine oculis* and *optix* were not detected. In addition, recent studies have found that *eya* is also required for the development of pigment cells containing pigment granules (Karandikar et al., 2014; Takagi et al., 2012). Taken together, it is tempting to speculate that the establishment of pteridine coloration in the FW of *Oncopeltus* might be regulated by the *eya*. To test this hypothesis, we knocked down *eya* using RNAi. The resulting adults had severe defects in their eyes and also reduction in their two dorsal ocelli (Figs.

4.8C1&C2, 4.8D1&D2). However, the orange patterns in the FW remained identical to wild type (Figs. 4.8C3&D3, 4.7). These results clearly show that while *eya* is essential for eye development in *Oncopeltus*, it is not involved in wing coloration despite its elevated expression in the FW. This in turn, suggests that the orange wing coloration in *Oncopeltus* is not due to the co-option of eye network, but instead is a wing-specific process.

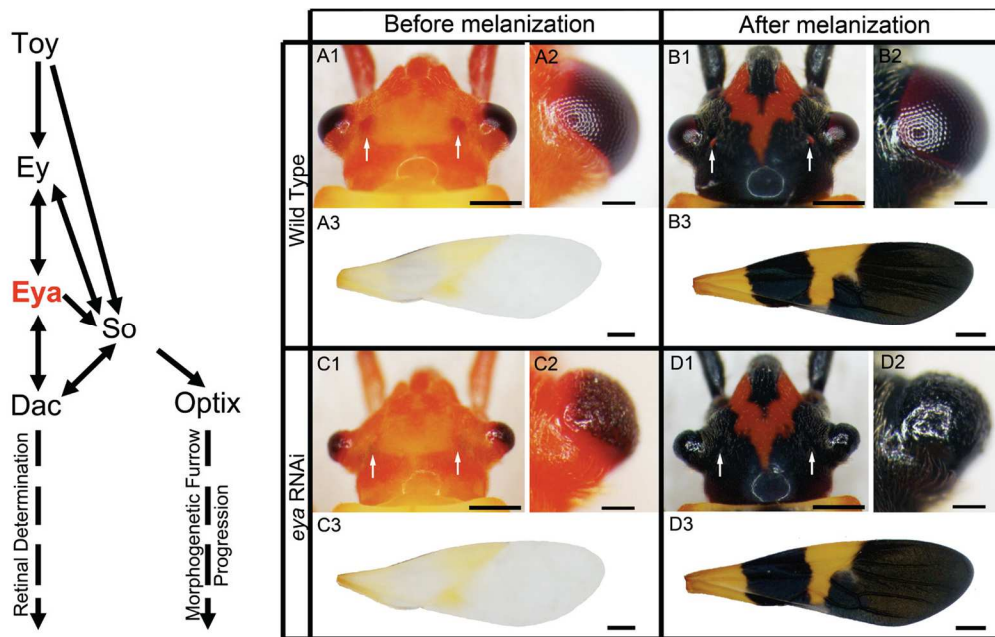


Fig. 4.8. Effects of RNAi against *eya* in the eyes and forewings of *Oncopeltus* adults. (Left) The classical eye regulatory network, redrawn based upon (Li et al., 2013). (A1-A3) The eye and forewing (FW) coloration in the pre-melanized wild type adults. The dorsal ocelli were shown from the dorsal view of the head (arrows in A1). (B1-B3) The eye and FW coloration in the fully melanized adults. (C1-C3) The *eya* RNAi adults establish a reduction of dorsal ocelli (arrows in C1), a severe defect in the eyes (C2), whereas the FW coloration was normal (C3). (D1-D3) Such phenotype persists in the fully melanized *eya* RNAi adults. The dorsal ocelli were not visible (arrows in D1), the eyes were defected (D2), however the FW coloration was similar to wild type (D3)

Despite the fact that we did not observe noticeable changes in the FW of *eya* RNAi adults, we cannot rule out the possible contributions to wing morphology by this gene. A previous study in *Tribolium* found that *eya* is involved in the development of a wide range of morphological traits, including the elytra (Yang et al., 2009). These

functions of *eya* are processed during early-mid post-embryonic stages. Currently, however, RNAi performed at the equivalent stages in *Oncopeltus* is lethal (Chesebro et al., 2009). Future studies with improved functional approaches would be required to validate the exact functions of *eya* in the wings in this species.

Pigmentation functions of ommochrome and pteridine genes in the body of adult *Oncopeltus*

In addition to the FW, orange coloration also exists throughout the body of *Oncopeltus* adults and nymphs (Fig. 4.9A1~A4). The body orange coloration can be observed in the freshly molted adults (Fig. 4.9A1&A2), which becomes darker after melanization (Fig. 4.9A3&A4). To determine the involvement of the ommochrome and pteridine pathways in the body orange coloration, we observed the analyzed gene's RNAi adults. In individuals with depletion of ommochrome genes, no noticeable reduction was observed in the body orange coloration, either before or after melanization (Figs. 4.9B~D). This result shows that ommochrome pathway is not involved in body orange coloration of *Oncopeltus* adults.

In contrast, RNAi targeting different pteridine genes resulted in a range of effects in body orange coloration. In the freshly molted *Punch* RNAi adults, no reduction in the body orange coloration was observed (Fig. 4.9E1&E2). Later on, though, the black coloration is significantly reduced in these individuals (Fig. 4.9E3&E4). Such reductions in melanin coloration indicate that *Punch* is required for proper body melanization in *Oncopeltus* adults. This lack of input from melanization resulted in an overall bright orange color in these individuals, similar to that in the pre-melanized adults (Figs. 4.9E3&E4, compared to 4.9E1&E2). Unlike the *Punch* RNAi, the resulting adults from

purple RNAi were similar to wild types, showing no noticeable effect in orange or melanin coloration in their bodies, similar to the wild type (Figs. 4.9F1~F4). In *white* RNAi adults, we observed a significant reduction in body orange coloration before (Figs. 4.9G1&G2) and after melanization (Figs. 4.9G3&G4), whereas the melanin coloration was generally unaltered (Figs. 4.9G3&G4). Therefore, the overall brighter orange coloration in these individuals are likely due to the lack of pteridine pigments, indicating that *white* is essential for establishing pteridine coloration in the bodies of *Oncopeltus* adults. Hence, unlike the situation in the FW, where the entire pathway is required, the body coloration relies primarily on the genes at low hierarchical positions of the pathway, especially *white*.

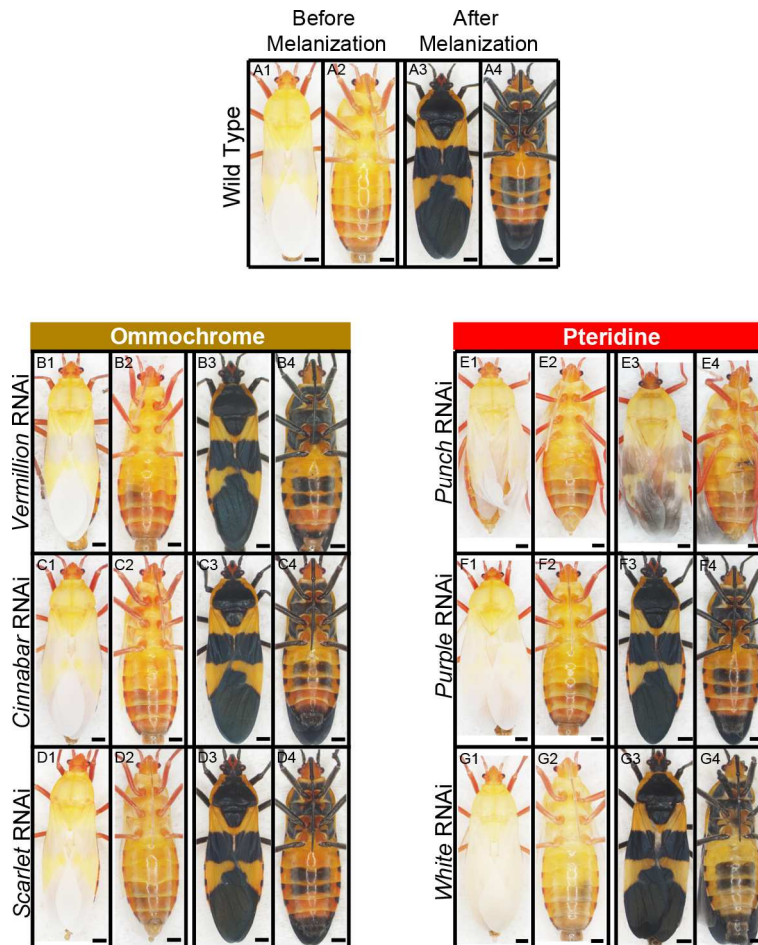


Fig. 4.9. Functions of ommochrome and pteridine genes in the orange body coloration of *Oncopeltus* adults. (A1-A2) The orange coloration has been established prior to melanization, as shown on both dorsal (A1) and ventral (A2) sides. (A3-A4) The overall orange coloration becomes darker in the fully melanized adults. (B1-B4) *vermilion* RNAi adults showed normal orange coloration in the bodies of adults. (C1-C4) *cinnabar* RNAi adults established wild type orange body coloration. (D1-D4) Body orange coloration in *scarlet* RNAi adults was similar to wild type. (E1-E4) The coloration of *Punch* RNAi adults. Note that these individuals were not able to completely shed their exoskeleton, therefore the wings could not extend completely. The remaining exoskeleton was then manually removed to show the coloration of the molted adults. (E1-E2) The orange coloration in the body of pre-melanized *Punch* RNAi adults appeared to be wild type. (E3-E4) The melanization was significantly reduced in *Punch* RNAi adults. (F1-F4) *purple* RNAi adults established normal body orange coloration. The wing orange coloration became light yellowish in the fully melanized adults (F3). (G1-G2) The overall body coloration in the pre-melanized *white* RNAi adults was changed to light yellow. (G3-G4) The orange coloration in the body of *white* RNAi became yellowish.

Pigmentation roles of ommochrome and pteridine pathways in the 1st nymphs of *Oncopeltus*

In all of the previously described post-embryonic RNAi assays, we could not completely deplete the ommochrome or pteridine coloration in the eyes or body. It is worth noting that between adjacent stages, only the melanin patterns are shed together with the exoskeleton (Fig. 4.10). In contrast, the eye and body colorations are all retained into the next developmental stage. In other words, a large portion of the eye and body coloration is actually “inherited” from the previous nymphal stages. In fact, the red color in the eyes and the orange coloration in the body can be observed in the earliest developmental stages. As illustrated by Fig. 4.11A1, in the embryos that are 5 days old, the body is already orange/red in color, becoming darker as these embryos turn into the 1st nymphs (Fig. 4.11A2). Similar phenomenon is observed in the eyes of the embryos (Fig. 4.11A1') and 1st nymphs as well (Fig. 4.11A2'). To test whether the ommochrome and pteridine pathways are involved in embryonic and early nymphal coloration, we performed maternal RNAi to deplete these two pathways. To ensure that

the entire pathways are completely turned off, we targeted the genes that are the main “switches” initializing each pathway: *vermilion* and *Punch* (refer to Fig. 1.2).

Upon depletion of *vermilion*, the body and eye colorations of 5-day embryos were similar to that of the wild type (Figs. 4.11B1&B1'). Similarly, the resulting 1st nymphs appeared to be wild type as well (Figs. 4.11B2&B2'). These results indicate that *vermilion* is not required for eye or body coloration in the early developmental stages of *Oncopeltus*. Therefore, the ommochrome coloration does not contribute to coloration at this early stage.



Fig. 4.10. The remaining exoskeleton of the 5th nymphs after molting into adults. Only black patterns are shed away with the exoskeleton.

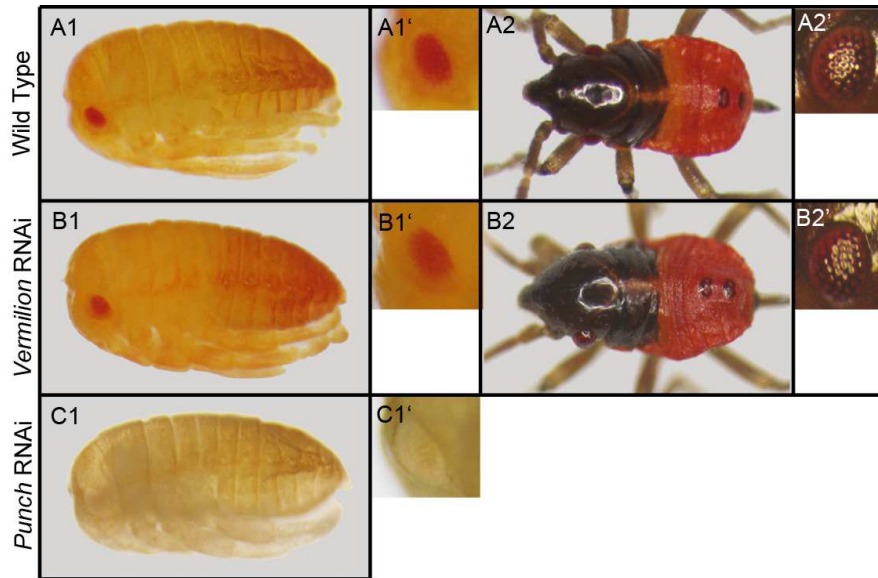


Fig. 4.11. Functions of *vermilion* and *Punch* in the eye and body coloration during early developmental stages. (A1) Eye coloration and body orange coloration are visible in 5 days old embryos. (A1') Zoom-in view of the eye, showing partial establishment of the eye coloration. (A2) The body coloration in wild type 1st nymphs, with (A2') showing the lateral view of the compound eyes. (B1&B1') The eye and body coloration of 5 day old *vermilion* RNAi embryos were similar to the wild type. (B2&B2') *vermilion* RNAi 1st nymphs showed normal coloration in body (B2) and eye (B2'). (C1&C1') 5 days old *Punch* RNAi embryos established a severe reduction in body coloration, also the eye coloration is barely visible.

In contrast, the 5-day *Punch* RNAi embryos display a severe loss of body coloration, which turned into light yellowish (Fig. 4.11C1). In addition, we also observed a significant reduction in the red eye coloration, which is barely visible (Fig. 4.11C1'). Unfortunately, as these individuals can not complete the embryogenesis, we could not extend the phenotypic analysis into the 1st nymphs. Despite this, our observations are sufficient to demonstrate that pteridine coloration is essential for both eye and body coloration during *Oncopeltus* embryogenesis. Furthermore, the establishment of orange coloration requires the activation of the entire pathway starting from its initialization step that is catalyzed by *Punch*, similar to the findings in the FW of the adults.

Discussion

The functions of ommochrome in the coloration of *Oncopeltus*

In this study, we performed the first comprehensive functional analysis on the core genes within both the ommochrome and pteridine pathways using RNAi. This approach has been confirmed to be very effective, consistently resulting in a systemic response that allows one to analyze the contributions of relevant genes across the whole body (Liu et al., 2016). Here we document the presence of diverse phenotypes in eyes, wings, and the bodies, indicating that the ommochrome and pteridine genes are utilized differently in different body regions.

Ommochrome is primarily known as the brown pigment that is exclusively found in the eyes of *Drosophila* and *Tribolium* (Lorenzen et al., 2002; Summers et al., 1982). More recent studies have also shown the presence of ommochrome in the wings of several lepidopteran species, whereas its existence in the eyes remains to be verified (Nijhout, 1997; Reed and Nagy, 2005). Combined together, none of these studies have clarified whether or not in one single individual, the ommochrome pathway is capable of functioning in the pigmentation of both eyes and wings, or whether it can extend to other body regions. In the present study on *Oncopeltus*, we show that the depletion of both the synthesis (*vermillion* and *cinnabar*) and transporter (*scarlet*) genes, results in bright red color change in the newly formed ommatidia in the adult eyes (Fig. 4.4). However, no effect on the orange coloration of the wings or body was observed in any of these three instances (Fig. 4.6&4.9). These results show that the pigmentation function of the ommochrome pathway is restricted to the eyes during post-embryonic development. In addition, our embryonic RNAi against *vermillion* had no effect in eye coloration (Fig.

4.11), suggesting that the ommochrome pathway does not contribute to the eye pigmentation at this earliest developmental stage. Taken together, we can infer that while ommochrome is an eye exclusive pigment in *Oncopeltus*, its function is restricted solely to post-embryonic development.

The functions of pteridine genes in the coloration of *Oncopeltus*

In contrast to ommochrome, pteridine is required for eye coloration early during embryonic development in *Oncopeltus*. The depletion of pteridine pathway resulted in a severe reduction in eye color in embryos (Fig. 4.11), which shows that this pathway plays a critical role in initialization of eye pigmentation. In the post-embryonic RNAi assays, depletions of pteridine synthesis (*Punch* and *purple*) and transporter (*white*) genes caused different alterations in pigmentation among different body regions. In the newly formed ommatidia, only *white* RNAi adults showed a reduction in color (Fig. 4.4). In summary, while the eye coloration during embryonic development requires the entire pteridine pathway, only its lower hierarchical portion is required in adults. Similar differences in utilization of pteridine pathway are observed in regard to body coloration as well. *white* RNAi showed a significant reduction in orange coloration in the adult body, whereas such effects are not detected in *Punch* and *purple* RNAi individuals (Fig. 4.9). In contrast, embryonic knockdown of *Punch* is sufficient to deplete the orange body coloration (Fig. 4.11).

Unlike the above observations, the orange patches of the FW require both pteridine synthesis and transporter genes. The pre-melanized FWs showed similar reduction under the depletion of *Punch*, *purple* and *white* (Fig. 4.6). These observations

suggest that the entire pteridine pathway must be active to produce the orange patterns of the FW.

Based on these findings, the pteridine pathway may be utilized in two different fashions in *Oncopeltus*. Under the first scenario, if the orange/red coloration is initialized from a colorless background (such as in the embryos or FW), the pteridine pathway has to be turned on from the beginning. In contrast, in the second scenario (as was observed in the newly eclosed adults), the previously produced pteridine pigments are still retained in the eyes and body. Therefore, the establishment of adult eye and adult body coloration is more of a process of maintenance and expansion. Under such circumstances, the pteridine pathway does not have to be turned on from the beginning. Instead, starting from an intermediate step might be sufficient for proper coloration of the body and the eyes. At present, though, we can not identify the exact step that is turned on in the latter scenario due to the general lack of knowledge of the pteridine pathway. A better characterization of this pathway will be critical for better understanding of its role in insect coloration during embryonic and post-embryonic development.

The changes in the roles of ABC transporters in eye coloration

Previous studies have reported that three ABC transporters (Scarlet, White, and Brown), are essential for eye coloration in *Drosophila* (Ewart and Howells, 1998). More specifically, Scarlet and White work jointly in ommochrome coloration, whereas White and Brown are both required for pteridine coloration (Ewart and Howells, 1998)(Fig. 1.2). However, in the present study we observed that only Scarlet is essential for ommochrome coloration, while White serves exclusively in the pteridine pathway (Fig.

4.4). These findings suggest that in *Oncopeltus*, Scarlet and White work as the sole transporters for ommochrome and pteridine pathways, respectively. The observed lack of contribution of Brown in *Oncopeltus* pigmentation is consistent with previous reports in *Tribolium* (Grubbs et al., 2015), suggesting that its recruitment in this process may have occurred only in later derived groups such as flies.

The wing and body color patterns in *Oncopeltus* require both pteridine and melanin pathways

Present RNAi study in *Oncopeltus* shows that melanization in the body and FW is severely reduced under the knockdown of the pteridine initializing gene, *Punch* (Figs 4.6&4.9). This finding is consistent with a previous report that *Punch* is required to produce co-factors for the melanin pathway (Kato et al., 2006). Moreover, in the wings with depletion of pteridine pigments, melanin pathway is able to generate bright yellow coloration in the non-black patches (Fig. 4.6&4.7). This yellow pigment is likely to be produced by the NBAD branch of the melanin pathway (Liu et al., 2016; Wittkopp et al., 2002; Wright, 1987). Such insight furthers the hypothesis that melanin pathway functions as a secondary contributor to the orange pigmentation in *Oncopeltus* (Liu et al., 2014). It is worth noting that even when melanin and pteridine pigments are both present in the same orange region, they are deposited in different layers. The melanin products are directly incorporated into the non-cellular cuticle, whereas pteridine coloration is stored in the underlying cells (Wittkopp and Beldade, 2009; Ziegler and Harmsen, 1970). Therefore, the color patterns in *Oncopeltus* FW is generated by the products from one pathway overlying those from another: melanin in the cuticle, and pteridine in the underneath tissue. Such “overlay” is also present in the body of

Oncopeltus. The orange pteridine coloration is visible throughout the head, thorax, and abdomen during eclosion (Fig. 4.9). Later on, black patterns are produced, overlying the majority of the orange regions in the head and thorax, and to a much lesser degree in the abdomen (Fig. 4.9).

Summary of adult coloration in *Oncopeltus*

We have identified and characterized three pathways underlying the coloration in *Oncopeltus* adults: pteridine, melanin, and ommochrome. The contributions of these pathways are illustrated in Fig. 4.12. In freshly molted adults, the initial orange coloration is produced by the pteridine pathway, which also partially contributes to the eye coloration (Fig. 4.12A). At the same time, individual substrates produced by the pteridine pathway (such as tetrahydrobiopterin, BH4) also act as essential co-factors for the TH (Kato et al., 2006). This, in turn, activates the melanin pathway and initializes melanization. During this process (Fig. 4.12B), the melanin pathway produces black patches, yellow sclerotin that overlies the pteridine colorations, and colorless sclerotin that covers the proximal half of the hindwing. Hence, the body and wing color patterns are finalized by the cooperation of the pteridine and melanin pathways. Throughout the adult coloration process, the pigmentation function of the ommochrome pathway is restricted in the eyes, which appears to be independent of the other two pathways (Fig. 4.12A). Overall, the coloration process in *Oncopeltus* adults is a stepwise, multi-layer system that requires the inputs from three distinct pathways. This finding reveals a general principle of how complex color patterns, commonly observed across a wide range of species in nature, are produced in insects.

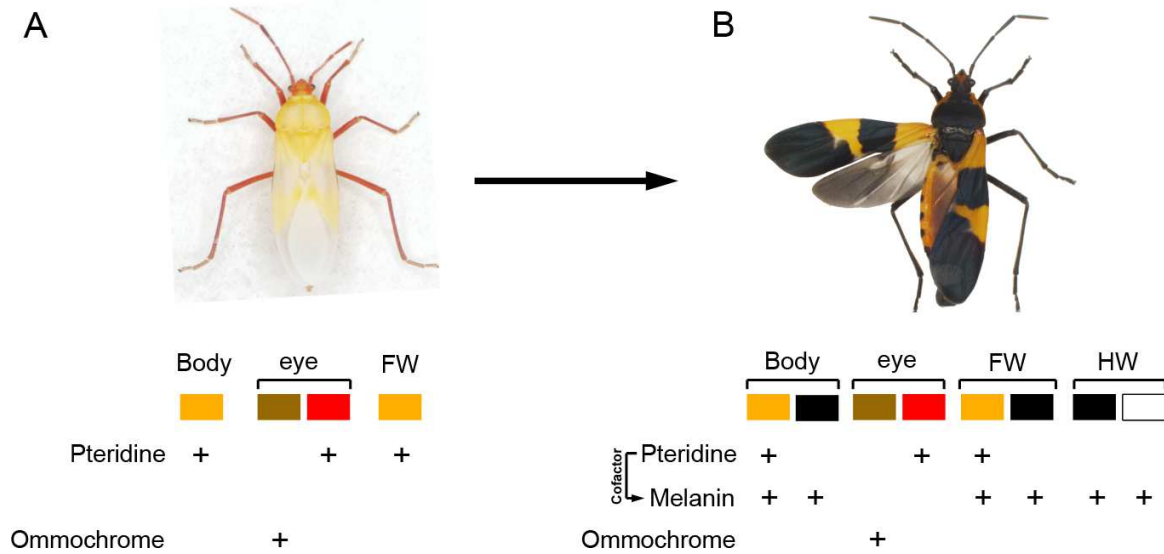


Fig. 4.12 Summary of the contributions by the pteridine, melanin, and ommochrome pathways to the adult color patterns of *Oncopeltus*. The color blocks represent the components in the patterns with specific body regions of freshly molted (A) and fully melanized adults (B). The underneath “+” indicates input from a specific pathway.

Coloring insects: decoration and glazing

To better demonstrate the stepwise coloration of insects featuring multiple pathways, here we propose the two-layer model that utilizes porcelain painting as a reference (Fig. 4.13). First step, the “decorating”, takes place prior to cuticle sclerotization, during which coloration is established in a particular tissue. This is followed by the second step, “glazing”, when the cuticle is formed to provide a overlying protective layer, with possible incorporation of other pigments such as melanin. Depending on the choice of a color and its character (whether it is incorporated into the cuticle or not), the contributions of decoration and glaze would vary among different species. Based upon how these two steps are utilized to establish final coloration, we propose that the insect pigmentation process can be categorized into three different types (Fig. 4.13). In the first case, the “underglaze” mode, color patterns are well established within the decorating step, whereas the overlying glaze is mainly colorless

and transparent. In contrast, in the second “inglaze” mode, colorations are generated primarily by the glaze, whereas little to no decoration is applied under the glaze. Alternatively, these two strategies can be combined in the third “overlay” mode. These three modes can be easily distinguished from one another by observing their colorations during eclosion. If the coloration of an insect is completed by eclosion, with little to no change later (such as in pea aphids and green katydids), this specie would undergo the “underglaze” mode. In contrast, if an insect is generally colorless by eclosion, and becomes pigmented after cuticle sclerotization (such as American cockroaches and two spotted field crickets), it belongs to the “inglaze” category. In addition, the “overlay” insects such as *Oncopeltus* and ladybugs display partial coloration upon eclosion, which is finalized following cuticle sclerotization. Precise identification of each mode will provide essential information for understanding the coloration of a species, including when the color is produced, whether the coloration is single- or multi-layered, as well as in which layer a specific color is present. This insight will be especially useful for pigmentation studies focusing on regulatory mechanisms, since one specific mechanism can regulate the decorating (body tissue coloration), or the glazing (cuticular coloration), or both steps in a tandem. Such multi-layer concept will in turn enable the comprehensive understanding of the extraordinary diversity in insect coloration that is observed in nature.

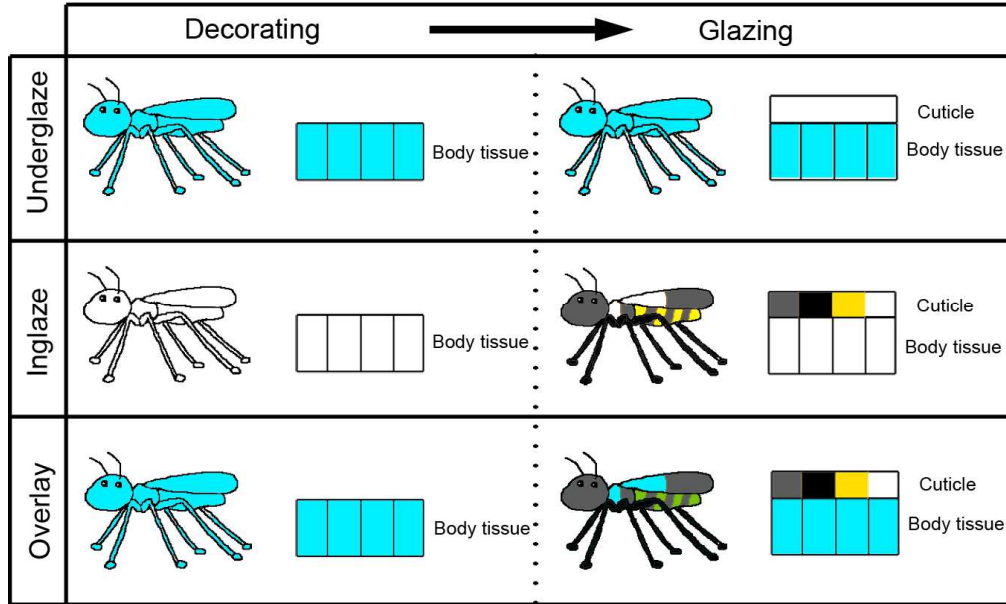
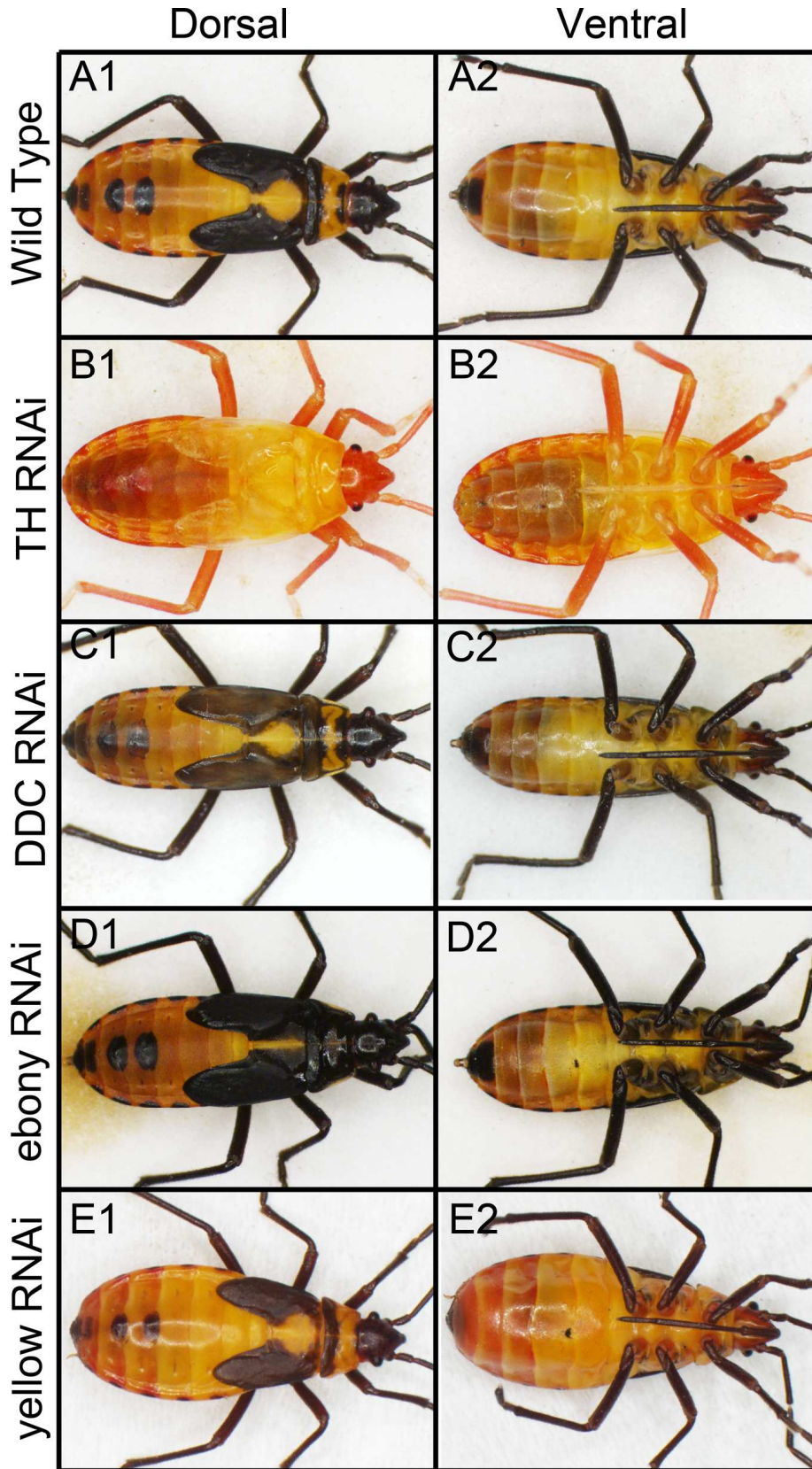


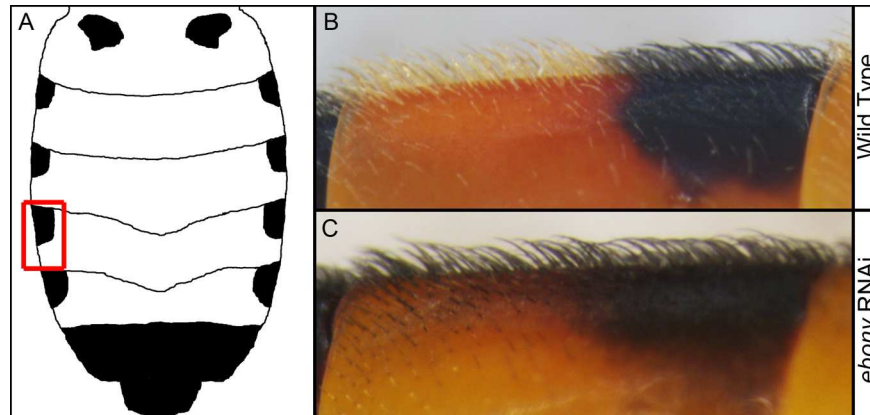
Fig. 4.13. The three proposed types of insect coloration. The “decorating” of body tissue is processed first (Left), followed by the “glazing” provided by the overlying cuticle (Right). The coloration of “underglaze” type insects is primarily generated during decorating. The “inglaze” type insects establish their coloration by glazing. In the third type, “overlay”, the final coloration requires contributions from both decorating and glazing.

APPENDIX

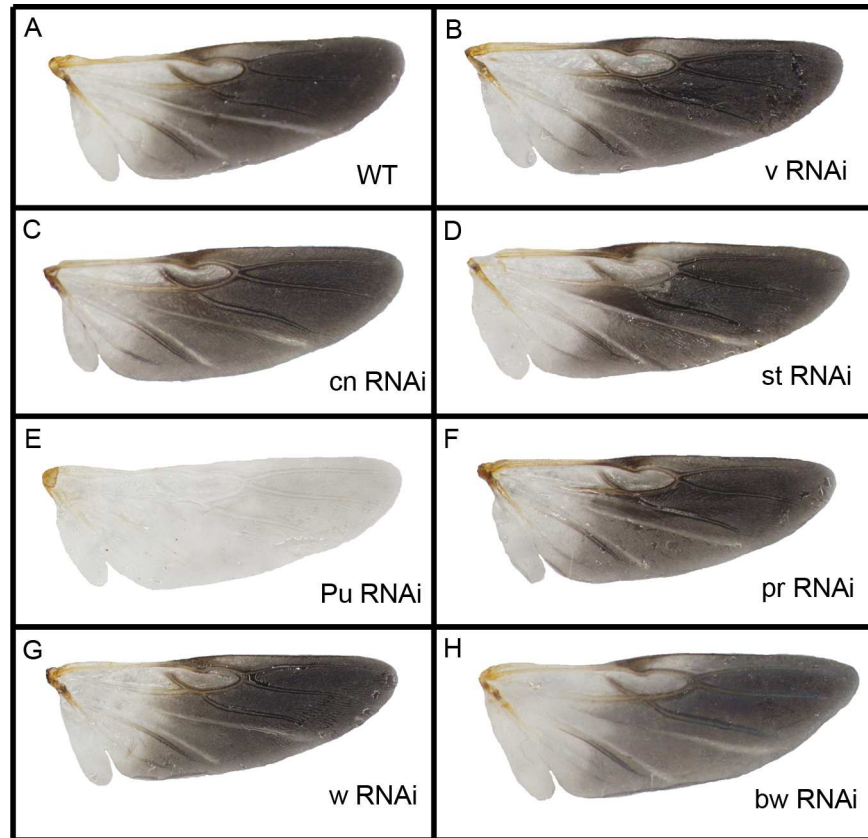
APPENDIX A. *TH*, *DDC*, *ebony* and *yellow* contribute to the black color patterns in 5th nymphs of *Oncopeltus*. (A1&A2) Wild type 5th nymphs of *Oncopeltus*. (B1&B2) *TH* RNAi causes loss of black coloration. (C1&C2) *DDC* RNAi causes a reduction in black coloration. (D1&D2) *ebony* RNAi resulted in expansion of black coloration in the thorax, but not in the abdomen. (E1&E2) *yellow* RNAi reduced the overall intensity of black patches, and reduced the sizes of black spot on the dorsal abdomen (E1).



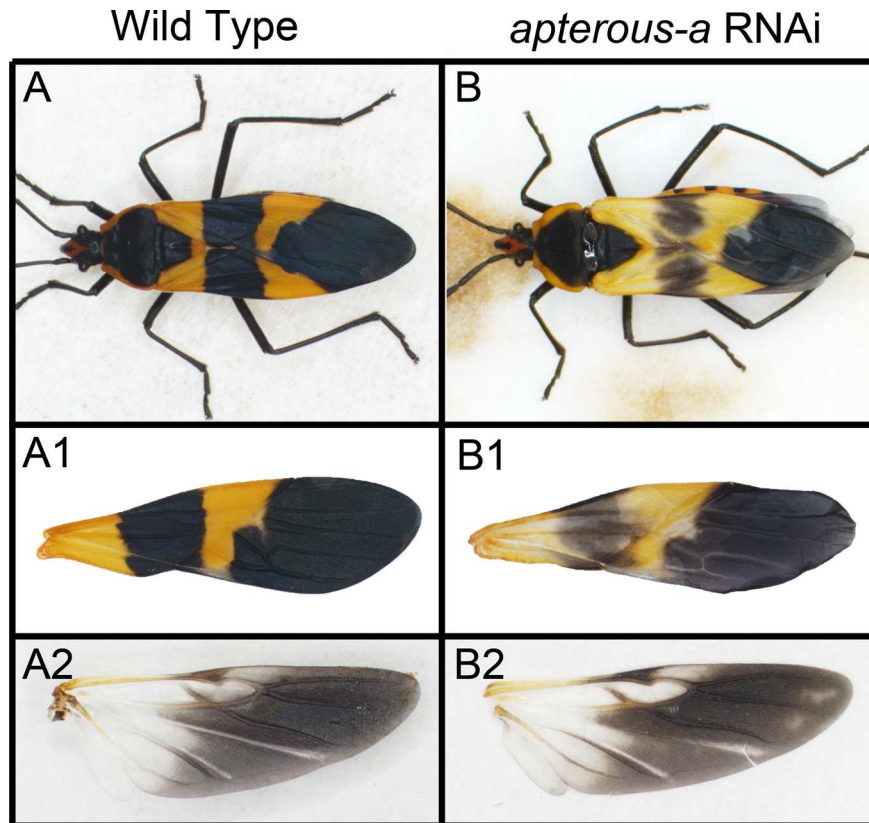
APPENDIX B. *ebony* RNAi altered the color patterns of the lateral bristles the abdominal segments of *Oncopeltus* adults. (A) The black patterns on the dorsal side of the abdomen. (B) The magnified view of lateral black patches of dorsal A4 segment. (C) In *ebony* RNAi adults, the transparent bristles become black colored.



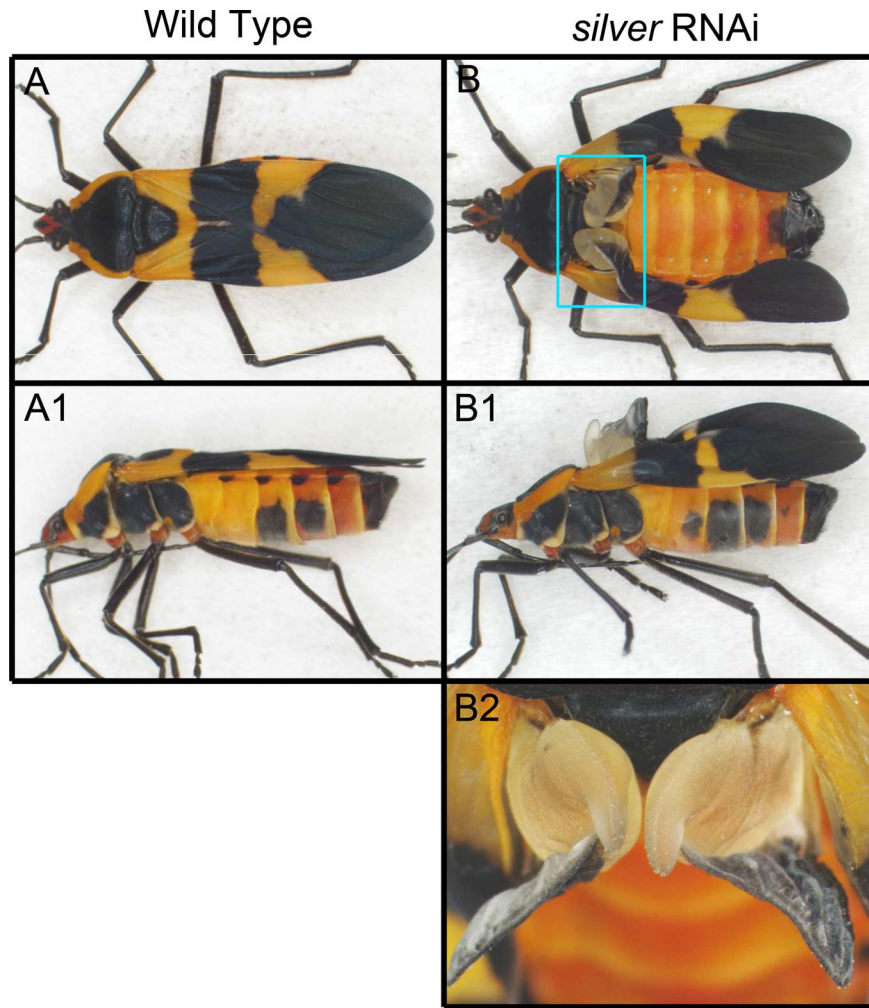
APPENDIX C. Among the ommochrome and pteridine genes, only *Punch* affects the color patterns of the hindwings. The hindwings of *vermilion* (B), *cinnabar* (C), *scarlet* (D), *Punch* (E), *purple* (F), *white* (G), *brown* (H) RNAi adults are shown. Only the depletion of *Punch* significantly reduced the black coloration of the hindwing due to the lack of input from melanization (E).



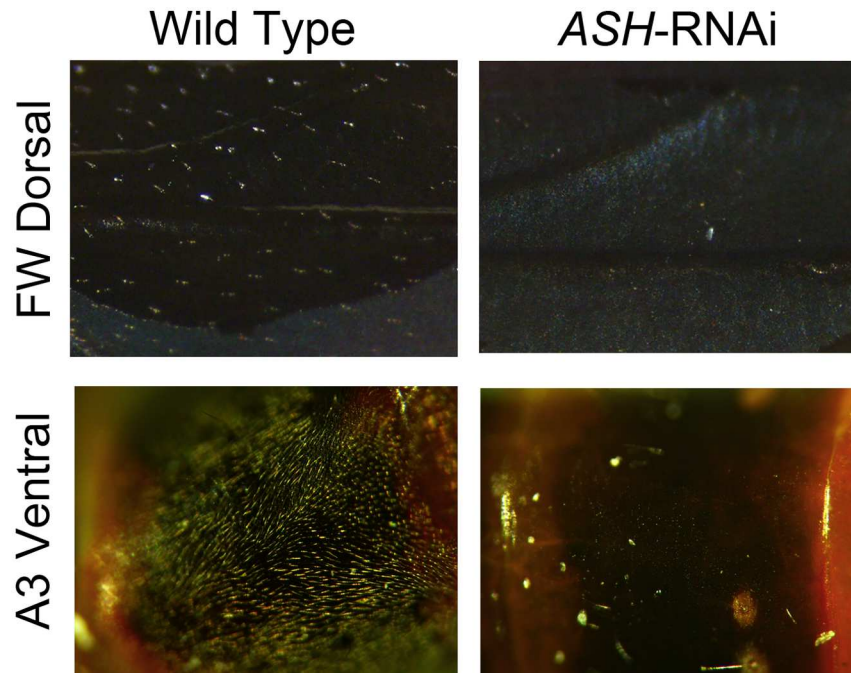
APPENDIX D. *apterous-a* (*ap-a*) RNAi caused defects in the forewings of *Oncopeltus* adults. (A-A2) The wild type *Oncopeltus* adults, shown as the whole bug (A), forewing (A1) and hindwing (A2). (B-B2) *ap-a* RNAi adults possess thinner and overall brighter forewings (B1), whereas hindwings appear similar to wild type (B2).



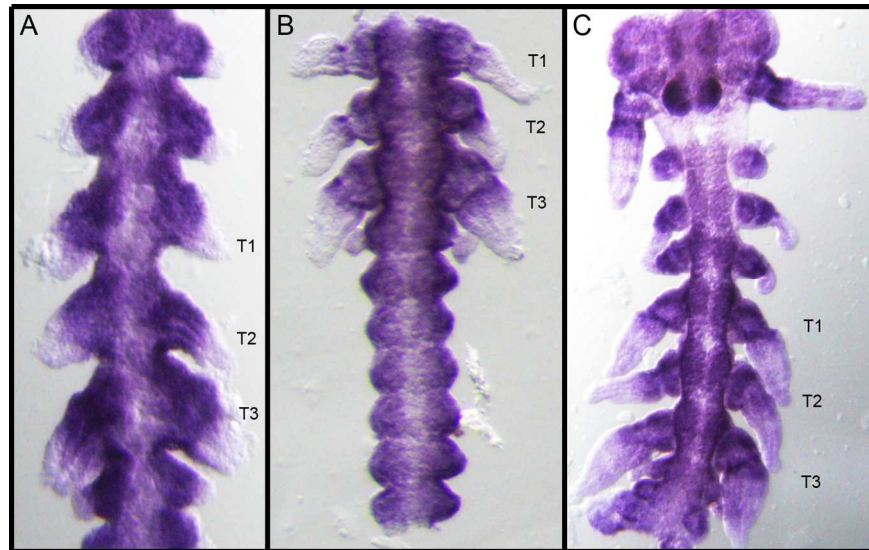
APPENDIX E. *silver* (*svr*) RNAi resulted inflated wings in *Oncopeltus* adults. (A-A1) The dorsal and lateral views of wild type *Oncopeltus* adults. (B-B1) Depletion of *silver* causes failure in expansion of hindwings and inflation of the proximal half of both the forewings and hindwings. (B2) Magnified view of the blue rectangle in (B), showing the inflation of hindwings.



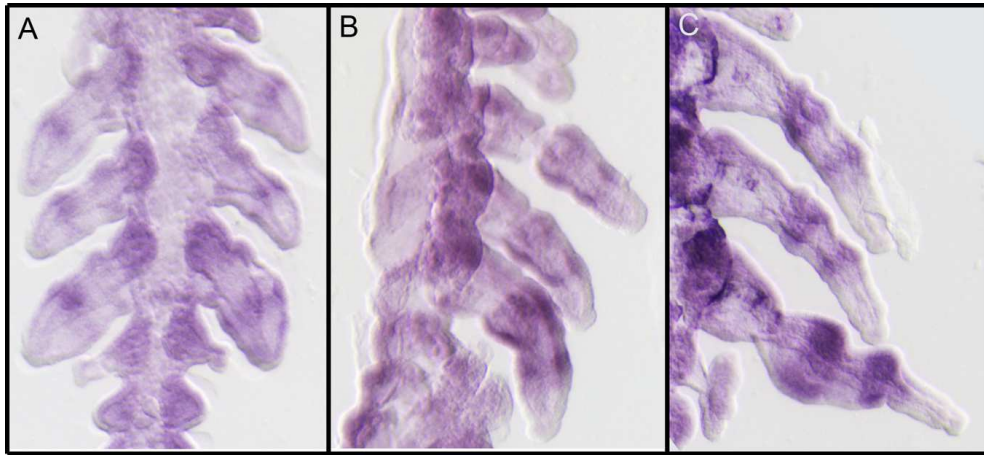
APPENDIX F. *achaete-scute homolog (ASH)* is responsible for bristle development of *Oncopeltus* adults. *ASH* RNAi causes loss of bristles, as shown in the dorsal surface of the forewings and ventral surface of the abdomen.



APPENDIX G. *homothorax* (*hth*) is expressed in the body and proximal regions of the appendages in *Gryllus bimaculatus* embryos. As illustrated by *in situ* hybridization, *hth* transcripts are detected throughout the body. In the developing leg buds, the expression of *hth* is restricted to the proximal region, which remains consistent throughout stage 8 (A), stage 9 (B), and stage 10 (C).



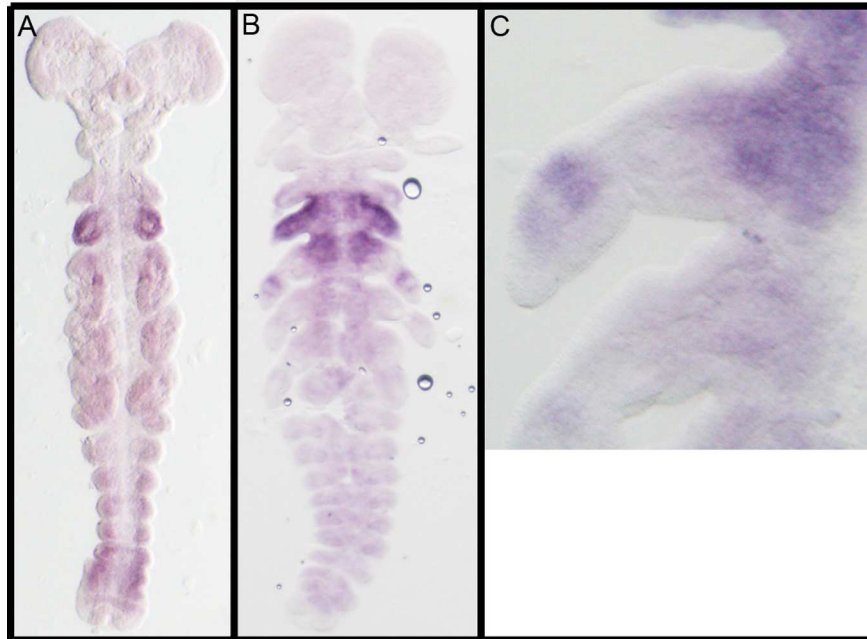
APPENDIX H. *dachshund* (*dac*) is primarily expressed in the middle regions of the developing legs in *Gryllus bimaculatus* embryos. All panels show the results of *in situ* hybridization using *dac* probe. (A) At stage 8, *dac* is expressed as an anterior patch in the middle region of the developing leg buds. (B) At stage 10, the expression of *dac* becomes rings surrounding the middle portions of the leg buds. In addition, the expression in T3 leg is higher in T3 leg compared to T1 and T2 counterparts. (C) At stage 11, the *dac* expression domain breaks into two separated rings, which are located in the putative femur and tibia segments of the leg buds.



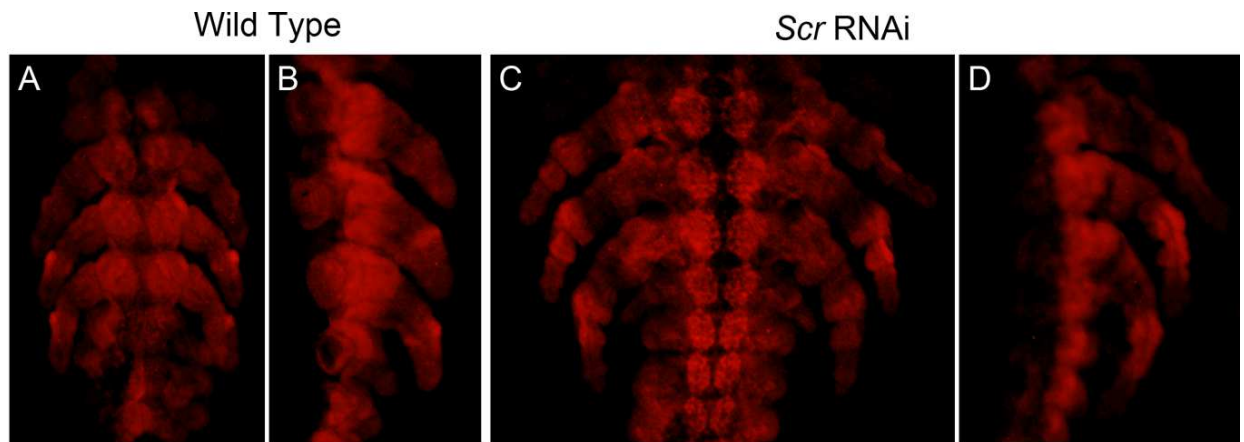
APPENDIX I. *Delta (Dl)* is expressed at boundaries between segments of appendages in *Gryllus bimaculatus* embryos. All panels show the results of *in situ* hybridization using *Dl* probe. (A) At stage 8, *Dl* is expressed in three patches in the developing leg buds. Also, in the developing antennae, *Dl* expression is detected as three rings marking the boundaries between putative segments. (B&C) At stage 10, the expression of *Dl* is detected as rings that separate the putative leg segments.



APPENDIX J. *Sex comb reduced (Scr)* is expressed in the labial and T1 segments of *Tenodera sinensis* embryos. All panels show the results of in situ hybridization using *Tenodera Scr* probe. (A) In early embryos, *Scr* is expressed in the developing buds of the labial segment. (B) Later at early-mid stage, *Scr* expression is detected throughout the labial segment, which also expands into the body of the T1 segment. The T1 leg bud is magnified in (C), showing two anterior patches of *Scr* expression in the middle-distal region of the developing T1 leg.



APPENDIX K. Depletion of *Scr* did not alter the expression pattern of Antennapedia (*Antp*) in *Periplaneta americana* embryos. All panels show the results of antibody staining of Antp protein. (A&B) Wild type embryos at day 7 show the expression of Antp as anterior patches located in the middle of the developing T2 and T3 legs, but not in T1 leg counterparts. (C&D) In day 8 embryos of *Scr* RNAi embryos, Antp is highly expressed in the putative femur and tibia segments in T2 and T3 legs, while the level of expression is much lower in T1 legs.



REFERENCES

- Andersen, S.O., 2010. Insect cuticular sclerotization: a review. *Insect Biochem Mol Biol* 40, 166-178.
- Angelini, D.R., Kaufman, T.C., 2005. Functional analyses in the milkweed bug *Oncopeltus fasciatus* (Hemiptera) support a role for Wnt signaling in body segmentation but not appendage development. *Dev Biol* 283, 409-423.
- Arakane, Y., Dittmer, N.T., Tomoyasu, Y., Kramer, K.J., Muthukrishnan, S., Beeman, R.W., Kanost, M.R., 2010. Identification, mRNA expression and functional analysis of several yellow family genes in *Tribolium castaneum*. *Insect Biochem Mol Biol* 40, 259-266.
- Arakane, Y., Lomakin, J., Beeman, R.W., Muthukrishnan, S., Gehrke, S.H., Kanost, M.R., Kramer, K.J., 2009. Molecular and functional analyses of amino acid decarboxylases involved in cuticle tanning in *Tribolium castaneum*. *J Biol Chem* 284, 16584-16594.
- Arakane, Y., Muthukrishnan, S., Beeman, R.W., Kanost, M.R., Kramer, K.J., 2005. Laccase 2 is the phenoloxidase gene required for beetle cuticle tanning. *Proc Natl Acad Sci U S A* 102, 11337-11342.
- Arnoult, L., Su, K.F., Manoel, D., Minervino, C., Magrina, J., Gompel, N., Prud'homme, B., 2013. Emergence and diversification of fly pigmentation through evolution of a gene regulatory module. *Science* 339, 1423-1426.
- Barbera, M., Mengual, B., Collantes-Alegre, J.M., Cortes, T., Gonzalez, A., Martinez-Torres, D., 2013. Identification, characterization and analysis of expression of

- genes encoding arylalkylamine N-acetyltransferases in the pea aphid *Acyrtosiphon pisum*. *Insect Mol Biol* 22, 623-634.
- Beard, C.B., Benedict, M.Q., Primus, J.P., Finnerty, V., Collins, F.H., 1995. Eye pigments in wild-type and eye-color mutant strains of the African malaria vector *Anopheles gambiae*. *J Hered* 86, 375-380.
- Berenbaum, M.R., Miliczky, E., 1984. Mantids and milkweed bugs: efficacy of aposematic coloration against invertebrate predators. *The American Midland Naturalist* 111, 64-68.
- Borycz, J., Borycz, J.A., Loubani, M., Meinertzhagen, I.A., 2002. tan and ebony genes regulate a novel pathway for transmitter metabolism at fly photoreceptor terminals. *J Neurosci* 22, 10549-10557.
- Bray, M.J., Werner, T., Dyer, K.A., 2014. Two genomic regions together cause dark abdominal pigmentation in *Drosophila tenebrosa*. *Heredity (Edinb)* 112, 454-462.
- Bridges, C.B., Morgan, T.H., 1923. The third-chromosome group of mutant characters of *Drosophila melanogaster*. Carnegie Institution of Washington, Washington,.
- Brodbeck, D., Amherd, R., Callaerts, P., Hintermann, E., Meyer, U.A., Affolter, M., 1998. Molecular and biochemical characterization of the aaNAT1 (Dat) locus in *Drosophila melanogaster*: differential expression of two gene products. *DNA Cell Biol* 17, 621-633.
- Camino, E.M., Butts, J.C., Ordway, A., Vellky, J.E., Rebeiz, M., Williams, T.M., 2015. The evolutionary origination and diversification of a dimorphic gene regulatory network through parallel innovations in cis and trans. *PLoS Genet* 11, e1005136.

- Chen, P., Wang, J., Li, H., Li, Y., Li, T., Chen, X., Xiao, J., Zhang, L., 2015. Role of GTP-CHI links PAH and TH in melanin synthesis in silkworm, *Bombyx mori*. *Gene* 567, 138-145.
- Chesebro, J., Hrycaj, S., Mahfooz, N., Popadic, A., 2009. Diverging functions of Scr between embryonic and post-embryonic development in a hemimetabolous insect, *Oncopeltus fasciatus*. *Dev Biol* 329, 142-151.
- Dong, Y., Friedrich, M., 2005. Nymphal RNAi: systemic RNAi mediated gene knockdown in juvenile grasshopper. *BMC Biotechnol* 5, 25.
- Dong, Y., Friedrich, M., 2010. Enforcing biphasic eye development in a directly developing insect by transient knockdown of single eye selector genes. *J Exp Zool B Mol Dev Evol* 314, 104-114.
- Dreesen, T.D., Johnson, D.H., Henikoff, S., 1988. The brown protein of *Drosophila melanogaster* is similar to the white protein and to components of active transport complexes. *Mol Cell Biol* 8, 5206-5215.
- Dustmann, J.H., 1968. Pigment studies on several eye-colour mutants of the honey bee, *Apis mellifera*. *Nature* 219, 950-952.
- Elias-Neto, M., Soares, M.P., Simoes, Z.L., Hartfelder, K., Bitondi, M.M., 2010. Developmental characterization, function and regulation of a Laccase2 encoding gene in the honey bee, *Apis mellifera* (Hymenoptera, Apinae). *Insect Biochem Mol Biol* 40, 241-251.
- Ewart, G.D., Cannell, D., Cox, G.B., Howells, A.J., 1994. Mutational analysis of the traffic ATPase (ABC) transporters involved in uptake of eye pigment precursors

- in *Drosophila melanogaster*. Implications for structure-function relationships. *J Biol Chem* 269, 10370-10377.
- Ewart, G.D., Howells, A.J., 1998. ABC transporters involved in transport of eye pigment precursors in *Drosophila melanogaster*. *Methods Enzymol* 292, 213-224.
- Ferguson, L.C., Green, J., Surridge, A., Jiggins, C.D., 2011a. Evolution of the insect yellow gene family. *Mol Biol Evol* 28, 257-272.
- Ferguson, L.C., Jiggins, C.D., 2009. Shared and divergent expression domains on mimetic *Heliconius* wings. *Evol Dev* 11, 498-512.
- Ferguson, L.C., Maroja, L., Jiggins, C.D., 2011b. Convergent, modular expression of ebony and tan in the mimetic wing patterns of *Heliconius* butterflies. *Dev Genes Evol* 221, 297-308.
- Futahashi, R., Banno, Y., Fujiwara, H., 2010. Caterpillar color patterns are determined by a two-phase melanin gene prepatterning process: new evidence from tan and laccase2. *Evol Dev* 12, 157-167.
- Futahashi, R., Fujiwara, H., 2005. Melanin-synthesis enzymes coregulate stage-specific larval cuticular markings in the swallowtail butterfly, *Papilio xuthus*. *Dev Genes Evol* 215, 519-529.
- Futahashi, R., Kurita, R., Mano, H., Fukatsu, T., 2012. Redox alters yellow dragonflies into red. *Proc Natl Acad Sci U S A* 109, 12626-12631.
- Futahashi, R., Tanaka, K., Matsuura, Y., Tanahashi, M., Kikuchi, Y., Fukatsu, T., 2011. Laccase2 is required for cuticular pigmentation in stinkbugs. *Insect Biochem Mol Biol* 41, 191-196.

- Galant, R., Skeath, J.B., Paddock, S., Lewis, D.L., Carroll, S.B., 1998. Expression pattern of a butterfly achaete-scute homolog reveals the homology of butterfly wing scales and insect sensory bristles. *Curr Biol* 8, 807-813.
- Gao, J., Wang, J., Wang, W., Liu, C., Meng, Y., 2013. Isolation, purification, and identification of an important pigment, sepiapterin, from integument of the lemon mutant of the silkworm, *Bombyx mori*. *J Insect Sci* 13, 118.
- Gibert, J.M., Peronnet, F., Schlotterer, C., 2007. Phenotypic plasticity in *Drosophila* pigmentation caused by temperature sensitivity of a chromatin regulator network. *PLoS Genet* 3, e30.
- Gompel, N., Prud'homme, B., Wittkopp, P.J., Kassner, V.A., Carroll, S.B., 2005. Chance caught on the wing: cis-regulatory evolution and the origin of pigment patterns in *Drosophila*. *Nature* 433, 481-487.
- Gorman, M.J., Arakane, Y., 2010. Tyrosine hydroxylase is required for cuticle sclerotization and pigmentation in *Tribolium castaneum*. *Insect Biochem Mol Biol* 40, 267-273.
- Grubbs, N., Haas, S., Beeman, R.W., Lorenzen, M.D., 2015. The ABCs of Eye Color in *Tribolium castaneum*: Orthologs of the *Drosophila* white, scarlet, and brown Genes. *Genetics*.
- Han, Q., Fang, J., Ding, H., Johnson, J.K., Christensen, B.M., Li, J., 2002. Identification of *Drosophila melanogaster* yellow-f and yellow-f2 proteins as dopachrome-conversion enzymes. *Biochem J* 368, 333-340.
- Hanna, A., 1953. Non-autonomy of *yellow* in gynandromorphs of *Drosophila melanogaster*. *J. Exp. Zool.* 123, 523-560.

- Hines, H.M., Papa, R., Ruiz, M., Papanicolaou, A., Wang, C., Nijhout, H.F., McMillan, W.O., Reed, R.D., 2012. Transcriptome analysis reveals novel patterning and pigmentation genes underlying *Heliconius* butterfly wing pattern variation. *BMC Genomics* 13, 288.
- Hintermann, E., Jenó, P., Meyer, U.A., 1995. Isolation and characterization of an arylalkylamine N-acetyltransferase from *Drosophila melanogaster*. *FEBS Lett* 375, 148-150.
- Hodgetts, R.B., Konopka, R.J., 1973. Tyrosine and catecholamine metabolism in wild-type *Drosophila melanogaster* and a mutant, *ebony*. *J Insect Physiol* 19, 1211-1220.
- Hotta, Y., Benzer, S., 1970. Genetic dissection of the *Drosophila* nervous system by means of mosaics. *Proc Natl Acad Sci U S A* 67, 1156-1163.
- Jacobs, M.E., Brubaker, K.K., 1963. Beta-Alanine Utilization of *Ebony* and Non-*ebony* *Drosophila melanogaster*. *Science* 139, 1282-1283.
- Janssen, J.M., Monteiro, A., Brakefield, P.M., 2001. Correlations between scale structure and pigmentation in butterfly wings. *Evol Dev* 3, 415-423.
- Jeong, S., Rebeiz, M., Andolfatto, P., Werner, T., True, J., Carroll, S.B., 2008. The evolution of gene regulation underlies a morphological difference between two *Drosophila* sister species. *Cell* 132, 783-793.
- Karandikar, U.C., Jin, M., Jusiak, B., Kwak, S., Chen, R., Mardon, G., 2014. *Drosophila* eyes absent is required for normal cone and pigment cell development. *PLoS One* 9, e102143.

- Kato, T., Sawada, H., Yamamoto, T., Mase, K., Nakagoshi, M., 2006. Pigment pattern formation in the quail mutant of the silkworm, *Bombyx mori*: parallel increase of pteridine biosynthesis and pigmentation of melanin and ommochromes. *Pigment Cell Res* 19, 337-345.
- Kim, H., Kim, K., Yim, J., 2013. Biosynthesis of drospterins, the red eye pigments of *Drosophila melanogaster*. *IUBMB Life* 65, 334-340.
- Koch, P.B., Behnecke, B., ffrench-Constant, R.H., 2000. The molecular basis of melanism and mimicry in a swallowtail butterfly. *Curr Biol* 10, 591-594.
- Koch, P.B., Nijhout, H.F., 2002. The role of wing veins in colour pattern development in the butterfly
- Papilio xuthus* (Lepidoptera: Papilionidae). *Eur. J. Entomol.* 99, 67-72.
- Kopp, A., Duncan, I., 1997. Control of cell fate and polarity in the adult abdominal segments of *Drosophila* by optomotor-blind. *Development* 124, 3715-3726.
- Kopp, A., Muskavitch, M.A., Duncan, I., 1997. The roles of hedgehog and engrailed in patterning adult abdominal segments of *Drosophila*. *Development* 124, 3703-3714.
- Kronforst, M.R., Barsh, G.S., Kopp, A., Mallet, J., Monteiro, A., Mullen, S.P., Protas, M., Rosenblum, E.B., Schneider, C.J., Hoekstra, H.E., 2012. Unraveling the thread of nature's tapestry: the genetics of diversity and convergence in animal pigmentation. *Pigment Cell Melanoma Res* 25, 411-433.
- Lawrence, P.A., 1970. Some new mutants of the Large Milkweed Bug *Oncopeltus fasciatus* Dall. *Genet. Res.* 15, 347-350.

- Li, H., Popadic, A., 2004. Analysis of nubbin expression patterns in insects. *Evol Dev* 6, 310-324.
- Li, Y., Jiang, Y., Chen, Y., Karandikar, U., Hoffman, K., Chattopadhyay, A., Mardon, G., Chen, R., 2013. optix functions as a link between the retinal determination network and the dpp pathway to control morphogenetic furrow progression in *Drosophila*. *Dev Biol* 381, 50-61.
- Li, Z., Zeng, B., Ling, L., Xu, J., You, L., Aslam, A.F., Tan, A., Huang, Y., 2015. Enhancement of larval RNAi efficiency by over-expressing Argonaute2 in *Bombyx mori*. *Int J Biol Sci* 11, 176-185.
- Linzen, B., 1974. The Tryptophan → Omnochrome Pathway in Insects. *Advances in Insect Physiology* 10, 117-246.
- Liu, J., Lemonds, T.R., Marden, J.H., Popadic, A., 2016. A Pathway Analysis of Melanin Patterning in a Hemimetabolous Insect. *Genetics* 203, 403-413.
- Liu, J., Lemonds, T.R., Popadic, A., 2014. The genetic control of aposematic black pigmentation in hemimetabolous insects: insights from *Oncopeltus fasciatus*. *Evol Dev* 16, 270-277.
- Liu, P., Kaufman, T.C., 2009. Morphology and husbandry of the large milkweed bug, *Oncopeltus fasciatus*. *Cold Spring Harb Protoc* 2009, pdb emo127.
- Liu, P.Z., Kaufman, T.C., 2004a. hunchback is required for suppression of abdominal identity, and for proper germband growth and segmentation in the intermediate germband insect *Oncopeltus fasciatus*. *Development* 131, 1515-1527.

- Liu, P.Z., Kaufman, T.C., 2004b. Kruppel is a gap gene in the intermediate germband insect *Oncopeltus fasciatus* and is required for development of both blastoderm and germband-derived segments. *Development* 131, 4567-4579.
- Liu, P.Z., Kaufman, T.C., 2005. even-skipped is not a pair-rule gene but has segmental and gap-like functions in *Oncopeltus fasciatus*, an intermediate germband insect. *Development* 132, 2081-2092.
- Long, Y., Li, J., Zhao, T., Li, G., Zhu, Y., 2015. A new arylalkylamine N-acetyltransferase in silkworm (*Bombyx mori*) affects integument pigmentation. *Appl Biochem Biotechnol* 175, 3447-3457.
- Lorenzen, M.D., Brown, S.J., Denell, R.E., Beeman, R.W., 2002. Cloning and characterization of the *Tribolium castaneum* eye-color genes encoding tryptophan oxygenase and kynurenine 3-monooxygenase. *Genetics* 160, 225-234.
- Massey, J.H., Wittkopp, P.J., 2016. The Genetic Basis of Pigmentation Differences Within and Between *Drosophila* Species. *Curr Top Dev Biol* 119, 27-61.
- Medved, V., Marden, J.H., Fescemyer, H.W., Der, J.P., Liu, J., Mahfooz, N., Popadic, A., 2015. Origin and diversification of wings: Insights from a neopteran insect. *Proc Natl Acad Sci U S A* 112, 15946–15951.
- Meher, P., Han, Q., Christensen, B.M., Li, J., 2011. Identification and characterization of two arylalkylamine N-acetyltransferases in the yellow fever mosquito, *Aedes aegypti*. *Insect Biochem Mol Biol* 41, 707-714.

- Monteiro, A., 2012. Gene regulatory networks reused to build novel traits: co-option of an eye-related gene regulatory network in eye-like organs and red wing patches on insect wings is suggested by *optix* expression. *Bioessays* 34, 181-186.
- Moraes, A.S., Pimentel, E.R., Rodrigues, V.L., Mello, M.L., 2005. Eye pigments of the blood-sucking insect, *Triatoma infestans* Klug (Hemiptera, Reduviidae). *Braz J Biol* 65, 477-481.
- Moran, N.A., Jarvik, T., 2010. Lateral transfer of genes from fungi underlies carotenoid production in aphids. *Science* 328, 624-627.
- Morehouse, N.I., Vukusic, P., Rutowski, R., 2007. Pterin pigment granules are responsible for both broadband light scattering and wavelength selective absorption in the wing scales of pierid butterflies. *Proc Biol Sci* 274, 359-366.
- Nijhout, H.F., 1991. *The Development and Evolution of Butterfly Wing Patterns*. Smithsonian Institution Press, Washington DC.
- Nijhout, H.F., 1997. Ommochrome pigmentation of the *linea* and *rosa* seasonal forms of *Precis coenia* (Lepidoptera: Nymphalidae). *Arch Insect Biochem* 36, 215-222.
- Niu, B.L., Shen, W.F., Liu, Y., Weng, H.B., He, L.H., Mu, J.J., Wu, Z.L., Jiang, P., Tao, Y.Z., Meng, Z.Q., 2008. Cloning and RNAi-mediated functional characterization of *MaLac2* of the pine sawyer, *Monochamus alternatus*. *Insect Mol Biol* 17, 303-312.
- Novakova, E., Moran, N.A., 2012. Diversification of genes for carotenoid biosynthesis in aphids following an ancient transfer from a fungus. *Mol Biol Evol* 29, 313-323.
- Ordway, A.J., Hancuch, K.N., Johnson, W., Williams, T.M., Rebeiz, M., 2014. The expansion of body coloration involves coordinated evolution in *cis* and *trans*

- within the pigmentation regulatory network of *Drosophila prostipennis*. *Dev Biol* 392, 431–440.
- Osanai-Futahashi, M., Ohde, T., Hirata, J., Uchino, K., Futahashi, R., Tamura, T., Niimi, T., Sezutsu, H., 2012. A visible dominant marker for insect transgenesis. *Nat Commun* 3, 1295.
- Poulton, E.B., 1890. *The colours of animals*. D. Appleton and company, New York,.
- Quan, G.X., Kim, I., Komoto, N., Sezutsu, H., Ote, M., Shimada, T., Kanda, T., Mita, K., Kobayashi, M., Tamura, T., 2002. Characterization of the kynurenine 3-monooxygenase gene corresponding to the white egg 1 mutant in the silkworm *Bombyx mori*. *Mol Genet Genomics* 267, 1-9.
- Rebeiz, M., Pool, J.E., Kassner, V.A., Aquadro, C.F., Carroll, S.B., 2009. Stepwise modification of a modular enhancer underlies adaptation in a *Drosophila* population. *Science* 326, 1663-1667.
- Reed, R.D., Gilbert, L.E., 2004. Wing venation and Distal-less expression in *Heliconius* butterfly wing pattern development. *Dev Genes Evol* 214, 628-634.
- Reed, R.D., Nagy, L.M., 2005. Evolutionary redeployment of a biosynthetic module: expression of eye pigment genes vermilion, cinnabar, and white in butterfly wing development. *Evol Dev* 7, 301-311.
- Riedel, F., Vorkel, D., Eaton, S., 2011. Megalin-dependent yellow endocytosis restricts melanization in the *Drosophila* cuticle. *Development* 138, 149-158.
- Roseland, C.R.K., K.J. Hopkins, T.L. , 1987. Cuticular strength and pigmentation of rust-red and black strains of *Tribolium castaneum*. Correlation with catecholamine and β -alanine content *Insect Biochemistry* 17, 21-28.

- Sethuraman, N., O'Brochta, D.A., 2005. The *Drosophila melanogaster* cinnabar gene is a cell autonomous genetic marker in *Aedes aegypti* (Diptera: Culicidae). *J Med Entomol* 42, 716-718.
- Sexton, O.J., Hoger, C., Ortleb, E., 1966. *Anolis carolinensis*: Effects of Feeding on Reaction to Aposematic Prey. *Science* 153, 1140.
- Shirataki, H., Futahashi, R., Fujiwara, H., 2010. Species-specific coordinated gene expression and trans-regulation of larval color pattern in three swallowtail butterflies. *Evol Dev* 12, 305-314.
- Summers, K.M., Howells, A.J., Pylotis, N.A., 1982. Biology of Eye Pigmentation in Insects. *Advances in Insect Physiology* 16, 119-166.
- Takagi, A., Kurita, K., Terasawa, T., Nakamura, T., Bando, T., Moriyama, Y., Mito, T., Noji, S., Ohuchi, H., 2012. Functional analysis of the role of eyes absent and sine oculis in the developing eye of the cricket *Gryllus bimaculatus*. *Dev Growth Differ* 54, 227-240.
- Takahashi, A., Takahashi, K., Ueda, R., Takano-Shimizu, T., 2007. Natural variation of ebony gene controlling thoracic pigmentation in *Drosophila melanogaster*. *Genetics* 177, 1233-1237.
- Tomoyasu, Y., Arakane, Y., Kramer, K.J., Denell, R.E., 2009. Repeated co-options of exoskeleton formation during wing-to-elytron evolution in beetles. *Curr Biol* 19, 2057-2065.
- True, J.R., Edwards, K.A., Yamamoto, D., Carroll, S.B., 1999. *Drosophila* wing melanin patterns form by vein-dependent elaboration of enzymatic prepatterns. *Curr Biol* 9, 1382-1391.

- True, J.R., Yeh, S.D., Hovemann, B.T., Kemme, T., Meinertzhagen, I.A., Edwards, T.N., Liou, S.R., Han, Q., Li, J., 2005. *Drosophila tan* encodes a novel hydrolase required in pigmentation and vision. *PLoS Genet* 1, e63.
- Walter, M.F., Black, B.C., Afshar, G., Kermabon, A.Y., Wright, T.R., Biessmann, H., 1991. Temporal and spatial expression of the yellow gene in correlation with cuticle formation and dopa decarboxylase activity in *Drosophila* development. *Dev Biol* 147, 32-45.
- Walter, M.F., Zeineh, L.L., Black, B.C., McIvor, W.E., Wright, T.R., Biessmann, H., 1996. Catecholamine metabolism and in vitro induction of premature cuticle melanization in wild type and pigmentation mutants of *Drosophila melanogaster*. *Arch Insect Biochem Physiol* 31, 219-233.
- Weatherbee, S.D., Nijhout, H.F., Grunert, L.W., Halder, G., Galant, R., Selegue, J., Carroll, S., 1999. Ultrabithorax function in butterfly wings and the evolution of insect wing patterns. *Curr Biol* 9, 109-115.
- Werner, T., Koshikawa, S., Williams, T.M., Carroll, S.B., 2010. Generation of a novel wing colour pattern by the Wingless morphogen. *Nature* 464, 1143-1148.
- Wittkopp, P.J., Beldade, P., 2009. Development and evolution of insect pigmentation: genetic mechanisms and the potential consequences of pleiotropy. *Semin Cell Dev Biol* 20, 65-71.
- Wittkopp, P.J., Carroll, S.B., Kopp, A., 2003. Evolution in black and white: genetic control of pigment patterns in *Drosophila*. *Trends Genet* 19, 495-504.

- Wittkopp, P.J., True, J.R., Carroll, S.B., 2002. Reciprocal functions of the *Drosophila* yellow and ebony proteins in the development and evolution of pigment patterns. *Development* 129, 1849-1858.
- Wright, T.R., 1987. The genetics of biogenic amine metabolism, sclerotization, and melanization in *Drosophila melanogaster*. *Adv Genet* 24, 127-222.
- Yang, X., Zarinkamar, N., Bao, R., Friedrich, M., 2009. Probing the *Drosophila* retinal determination gene network in *Tribolium* (I): The early retinal genes *dachshund*, *eyes absent* and *sine oculis*. *Dev Biol* 333, 202-214.
- Yu, H.S., Shen, Y.H., Yuan, G.X., Hu, Y.G., Xu, H.E., Xiang, Z.H., Zhang, Z., 2011. Evidence of selection at melanin synthesis pathway loci during silkworm domestication. *Mol Biol Evol* 28, 1785-1799.
- Zhan, S., Guo, Q., Li, M., Li, J., Miao, X., Huang, Y., 2010. Disruption of an N-acetyltransferase gene in the silkworm reveals a novel role in pigmentation. *Development* 137, 4083-4090.
- Ziegler, I., 1961. Genetic Aspects of Ommochrome and Pterin Pigments. *Adv Genet* 10, 349-&.
- Ziegler, I., Harmsen, R., 1970. The biology of pteridines in insects. *Adv. Insect Physiol.* 6, 139–203.

ABSTRACT**UNRAVELING THE MOLECULAR MECHANISMS OF APOSEMATIC
PIGMENTATION IN ONCOPELTUS FASCIATUS**

by

JIN LIU**August 2016****Advisor:** Dr. Aleksandar Popadić**Major:** Biological Sciences**Degree:** Doctor of Philosophy

Insects display the extraordinary amount of morphological variation, particularly in regard to their colorations. This diversity in coloration exists both in terms of the array of colors as well as the patterning of pigments. Previous studies have revealed that melanin, ommochrome, and pteridine are the most common pigments constituting insect color patterns. Among these three, the melanin pathway has been best studied so far and presents the foundation of the current understanding of insect coloration. At the same time, though, most of this insight relied on work performed in model systems such as *Drosophila* and *Tribolium*, which have significant limitations in their color palettes. Our knowledge on the roles of the melanin pathway in aposematic coloration, which is possessed by a wide variety of non-model insects, remains extremely limited. Other than the melanin pathway, functional studies on ommochrome and pteridine pathways have primarily focused on the eyes, whereas their roles in overall body coloration are much less understood. Furthermore, because these three pigmentation mechanisms have traditionally been studied separately from each other, it is still unknown how they are coordinated in a single species. Presently, there are significant

gaps within single pigmentation pathways, between different pathways, as well as between model and non-model insects, all of which limits our general understanding of evolution and diversity of coloration in insects.

To address such lack of knowledge, in this dissertation we performed a comprehensive analysis involving all three major pigment pathways in *Oncopeltus fasciatus* (milkweed bug), a hemimetabolous insect featuring distinct orange/black aposematic color patterns. We first analyzed the pigmentation roles of the core melanin genes (*TH*, *DDC*, *lac2*, *ebony*, *tan*, *yellow*, *black*, and *aaNAT*) using RNAi. We found that although the melanin pathway is generally conserved in *Oncopeltus*, the pathway is employed differently between body regions. Based upon these findings, we proposed that melanin coloration can be processed in two distinct modes, “painting” and “erasing”, depending on the overall coverage of dark coloration in a specific body region. These principles of melanin patterning can be generally applied to most of the previously studied species, which in turn provides a practical framework for future studies on a wider range of insects. In addition to the melanin pathway, we also determined the roles of core ommochrome (*vermilion*, *cinnabar*, and *scarlet*), and pteridine genes (*Punch*, *purple*, and *white*) in the coloration of *Oncopeltus*. Our results show that the pigmentation roles of ommochrome pathway is restricted to the nymphal and adult eyes, whereas the contributions of pteridine pathway extend into the forewings and the body. Our latter results are especially interesting, indicating that the pteridine pathway can be utilized differently between embryonic and postembryonic stages. In addition, we found that the overall orange/black color patterns of *Oncopeltus* are formed by a two-component overlay: pteridine pigments in the body tissue and melanin coloration in the

cuticle. Such multi-layer concept provides a novel insight into the coloration of insects with complex color patterns that are commonly observed in nature. Overall, our work has now established *Oncopeltus* as a new system for pigmentation studies, and laid out the foundation for future studies focusing on the regulatory mechanisms.

AUTOBIOGRAPHICAL STATEMENT

JIN LIU

I completed my Bachelor of Science (B.S.) degree at the University of Science and Technology of China. After my graduation I decided to enhance my experience in biological research in the U. S. and entered the Ph.D. program at the Department of Biological Sciences at Wayne State University. During my first year, I took the Evo-Devo course taught by Dr. Popadić, which lured my interest towards the evolution of insect morphology. After I joined the Popadić lab, my initial projects were focusing on the roles of selector genes in the appendages of *Periplaneta americana* and *Gryllus bimaculatus*. These experiences provided me with in depth understanding of insect morphology, which, in turn, allowed me to write an invited review chapter in the book “Cricket as a Model Organism: Development, Regeneration, and Behavior”. In my dissertation research, I focused on the mechanisms underlying the aposematic orange/black color patterns in *Oncopeltus fasciatus*. As a result, I successfully characterized multiple pigmentation pathways in this species, and built it into a practical system for future pigmentation studies.

In addition to my dissertation, I also conducted and supervised several side research projects for undergraduate and master students. Meanwhile I have been serving as a GTA for Anatomy and Physiology over 16 semesters. These experiences have significantly improved my skills in teaching and mentoring. Furthermore, there are also transferrable skills that I have obtained from my Ph.D. studies, which, together with teaching and research skills, prepared me well enough to face the upcoming challenges in my future career.